Chapter 3

SYNTHESIS AND CHARACTERISATION OF CONJUGATED MOLECULES AND ITS APPLICATIONS

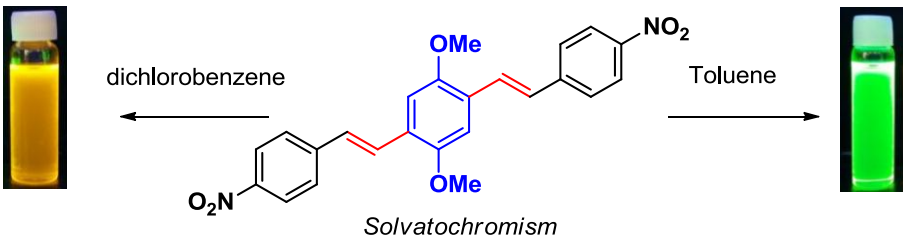

Solvatochromism

3.1. *Introduction*

Conjugated molecules are important class of compounds due to their varied applications in different fields which has already been discussed in the introduction part as well as in chapter 2 where we have presented one-pot methodologies for the synthesis of conjugated molecules. This chapter mainly describes the synthesis and the applications of different conjugated molecules as acid sensing compounds and compounds with mesomorphic properties. This chapter is further divided into three sections.

3.2 *Result and Discussion*

3.2.1 Application of one-pot Wittig-Heck methodology towards synthesis of OPVs and PPV

As described in the previous chapter one-pot multistep synthesis is found to be a method for the synthesis of wide variety of conjugated molecules. Amongst the number of one-pot synthetic methodologies developed so far, our group has previously reported a variant of olefination reaction involving *in situ* generation of styrene by either one-pot dehydrohalogenation–Heck or one-pot multicomponent Wittig–Heck reaction.[1]

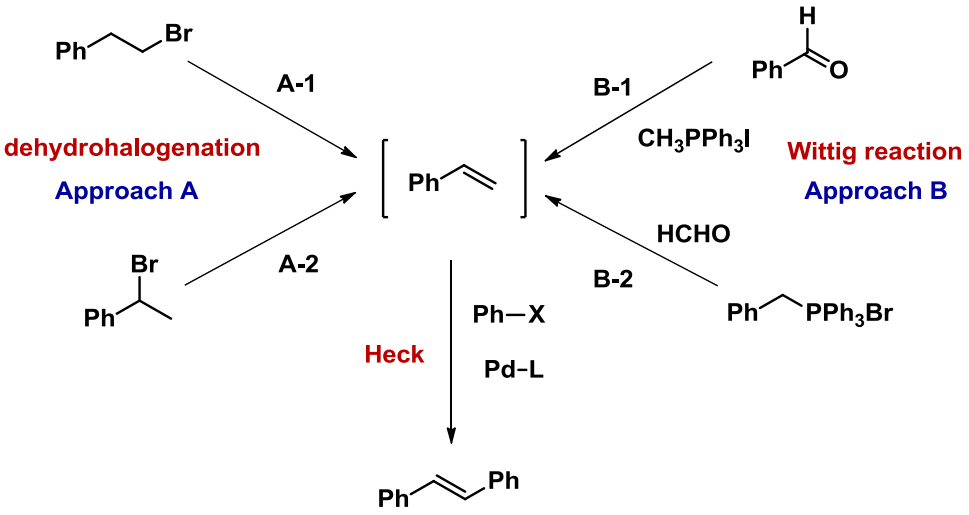

Scheme 1: One-pot dehydrohalogenation-Heck and Wittig-Heck reaction

In this reaction sequence, the Mizoroki-Heck reaction is carried out with Pd-catalyst and a suitable base. The required olefin is prepared either by dehydrohalogenation of suitable alkyl halide [Approach A] or alternatively from Wittig reaction of aldehyde [Approach B], both being carried out in the basic medium. The two approaches are outlined in [**Scheme-1**] while taking the example of the *in situ* synthesis of styrene and then subjected to Mizoroki-Heck conditions to form stilbene.[1]

We have used this one-pot Wittig-Heck methodology for the synthesis of oligo-p-phenylenevinylenes (OPVs) which correspond to the model compounds of PPV that have been extensively studied for years due to their good stability, high luminescence. It exhibits absorption and fluorescence in the UV-Vis region, which can be widely tuned by chemical functionalization and external control. OPVs find wide applications in organic electronics and molecular devices but are less studied as chromic compounds. Following OPV (**1-12**) derivatives were synthesized by one-pot method [**Chart 1**].

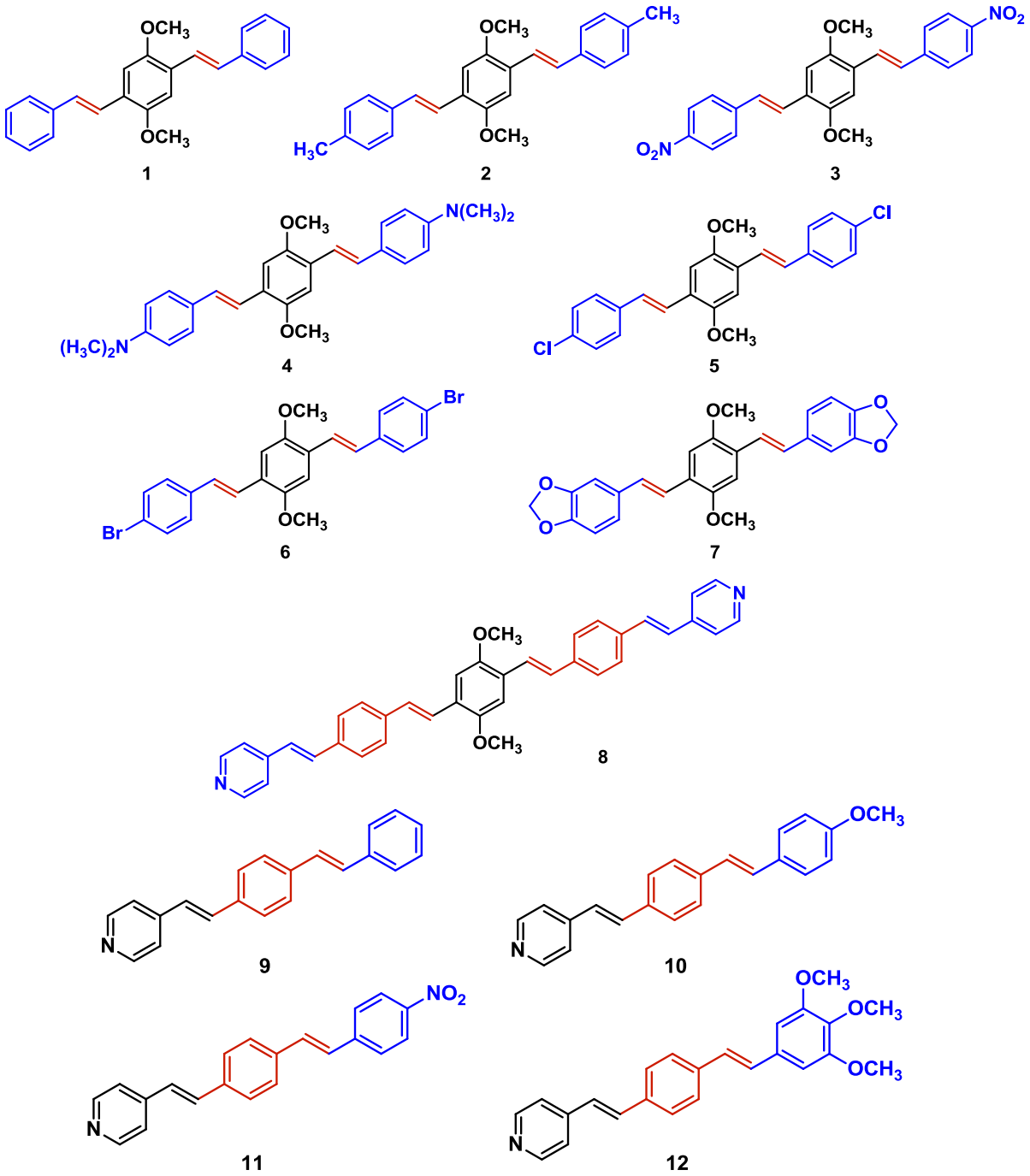

Chart 1: Synthesized Oligo-(phenylene vinylene)s

Synthesis of OPVs by One-pot Wittig-Heck methodology

OPVs **1** to **7** were synthesized by carrying out Wittig reaction of *p*-substituted benzaldehyde **13a-13f** and **14** with methyl triphenyl phosphine iodide **15** to give *in situ* generation of *p*-substituted styrene which will subsequently undergo Mizoroki-Heck reaction with 1,4-diiodo-2,5-dimethoxybenzene in the same pot to give final products (OPV **1** to **7**) [**Scheme 2**].

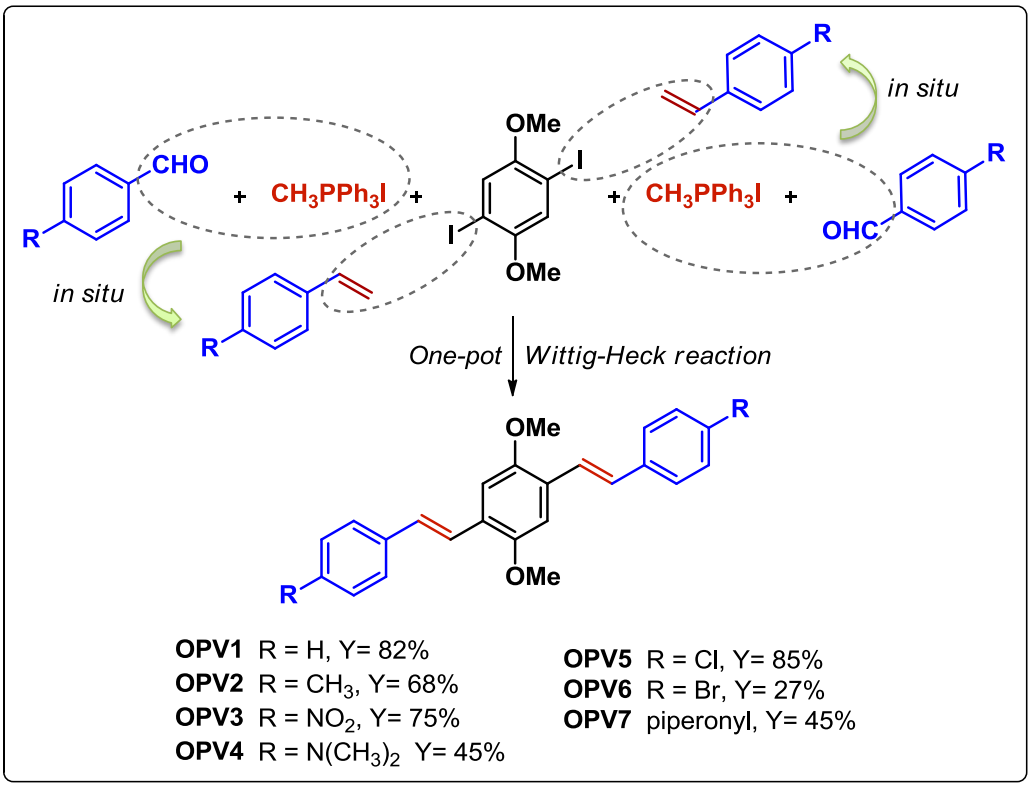

Aldehydes: R=H (**13a**), CH_3(**13b**), NO_2(**13c**), $N(CH_3)_2$(**13d**), Cl (**13e**), Br (**13f**), piperonal (**14**)

Scheme 2: Synthesis of **OPV 1** to **7**

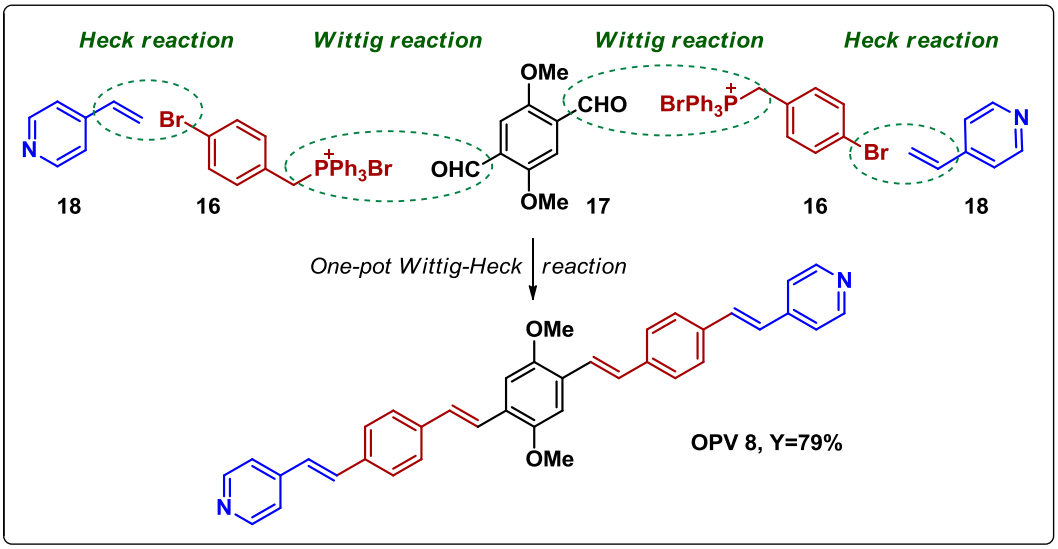

Scheme 3: Synthetic scheme for **OPV 8**

In the similar manner **OPV 8** was synthesized using 4-bromo benzyl triphenyl phosphine bromide salt **16** which will undergo Wittig reaction with 2,5-dimethoxyterephthalaldehyde **17** and Heck reaction with 4-vinyl pyridine **18** to give final product [**Scheme 3**]. OPVs **9**, **10**, **11** and **12** were synthesized from 4-bromobenzyl triphenyl phosphine bromide **16** which undergoes Wittig reaction with substituted aldehydes (**13a**, **13c**, **19**, **20**) followed by Heck reaction with vinyl pyridine **18** to give pyridine terminated OPVs [**Scheme 4**].

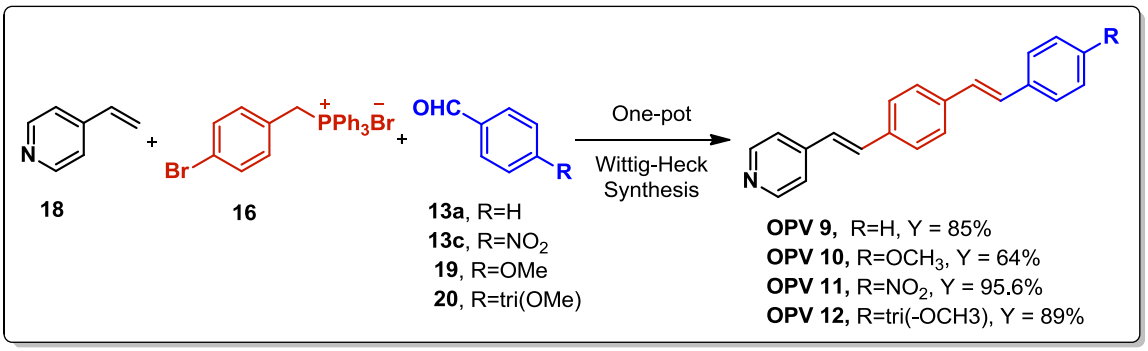

Scheme 4: Synthetic scheme for **OPV 9** to **12**

Photophysical Properties of OPVs

All the synthesized derivatives of OPVs were highly florescent in solid state as well as in diluted solution. **Figure 1** shows all the synthesized OPVs in solid state as well as in solution as viewed under UV light.

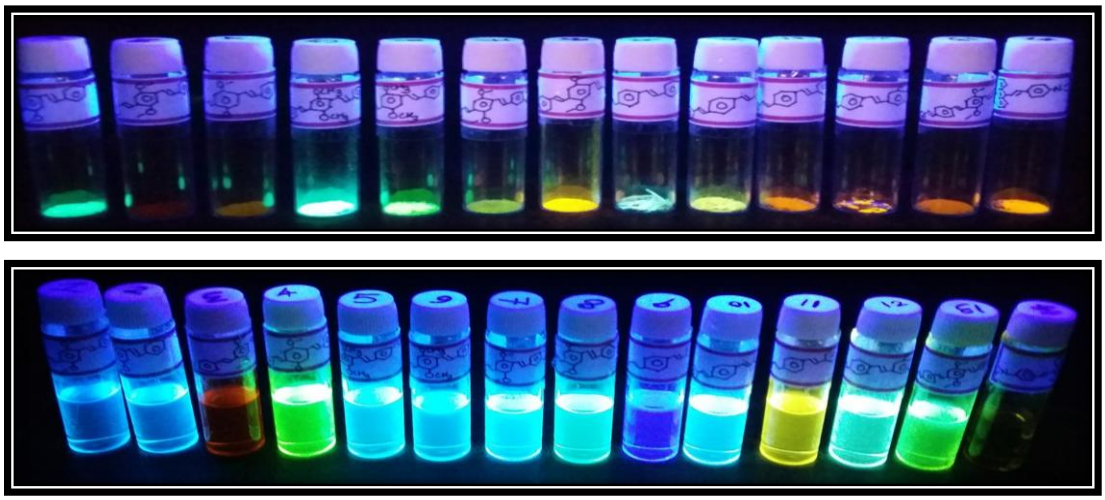

Figure 1: OPV 1 to 12 as viewed under UV light in solid state and in solution

Photophysical properties of OPV 1-7

Firstly we have studied **OPVs 1-7** by UV-visible spectroscopy and fluorescence spectroscopy as they are structurally similar with two methoxy substituents at 2 and 5 position of the central ring. The only difference is the terminal functional group which

shows distinct variation in its optical properties. It is established that OPVs can have *cis-cis*, *cis-trans* and *trans-trans* forms contributing to distinctly different optical and physical properties.[2] We have determined that all the OPV in our study are of *trans-trans* configuration, established by ^{1}H-NMR analysis. We have studied the UV-Visible absorbance and fluorescence emission of solution of **OPV 1** to **7** in toluene and it was found that there were two characteristic broad absorption peaks in the UV-Visible spectra of all the compounds depicting different electronic transitions. All the compounds showed higher energy band around 330 nm, whereas **OPV5** with electronegative nitro end group showed it at 350 nm. Another absorption band i.e. lower energy band varied from around 390 nm for most **OPVs**, whereas 420 nm for **OPV6** with $-N(CH_3)_2$ end group and 431nm for **OPV5**. Hence it was observed that just the end group modification of **OPVs** showed the variation in λ_{max} over the range of 41 nm. The emission spectra for all these compounds in toluene also showed distinct variation with the change in end group functionality. These changes are due to dipole-dipole interactions between solvent and solute as well as aggregation effects. It was observed that all the **OPVs** except the one with $-NO_2$ end group showed vibronic features (due to distinct transitions associated with a typical C-C stretching motion strongly coupled to the electronic system) suggesting the dominance of single molecule species. Also the absence of such vibronic features in **NO_2-OPV** indicates the presence of highly aggregated species in solution.[3]

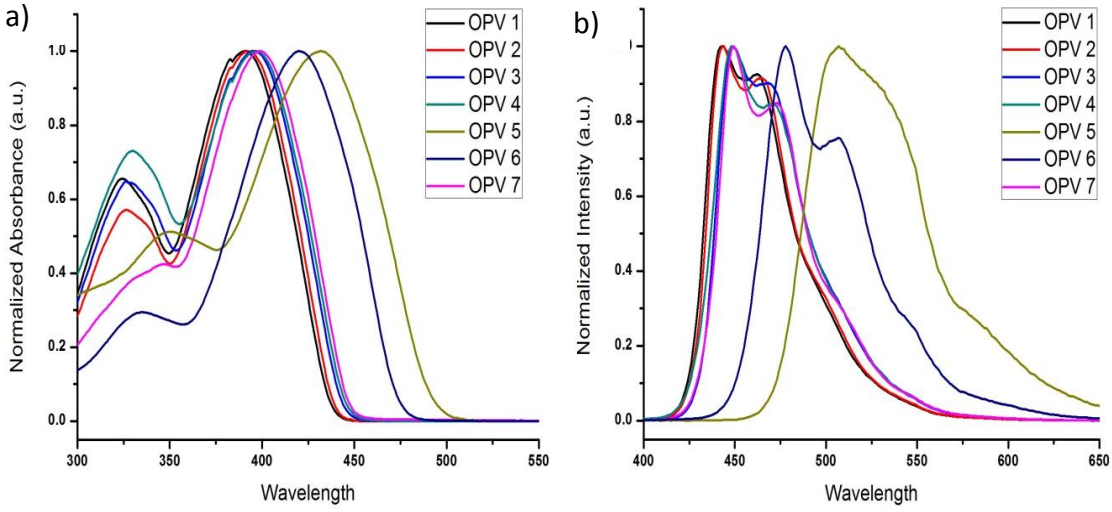

Figure 2: a) UV-Visible spectra for **OPV 1-7**. b) PL spectra for **OPV 1-7**

The λ_{em} for **OPV1-7** varied in the range of 64 nm i.e. from 442 to 506 nm. The Stoke shifts for most OPVs were around 52 nm whereas the **NO_2-OPV** showed distinctly high λ_{em} at 506 nm with the Stoke shift of 75 nm. Another important observation about the **NO_2-OPV** was its solvatochromism. **NO_2-OPV** was dissolved in different solvents such

as toluene, chloroform, tetrahydrofuran, dichlorobenzene, acetonitrile, dimethylsulphoxide and absorption as well as emission of those were measured. The absorption peak varied over 42 nm i.e. starting from 390 to 432 nm for different solvents. But in case of emission, the role of solvent was prominent as the emission span ranged over 218 nm i.e. from 432 nm in methanol to 650 nm in acetonitrile and DMSO [**Figure 3**]. Such strong solvatochromism can be attributed to combination of electrostatic OPV-solvent interactions, intramolecular charge transfer and aggregate formation in solution.[3] Solvent stabilization of intramolecular charge transfer in the excited state also leads to such high solvatochromism.

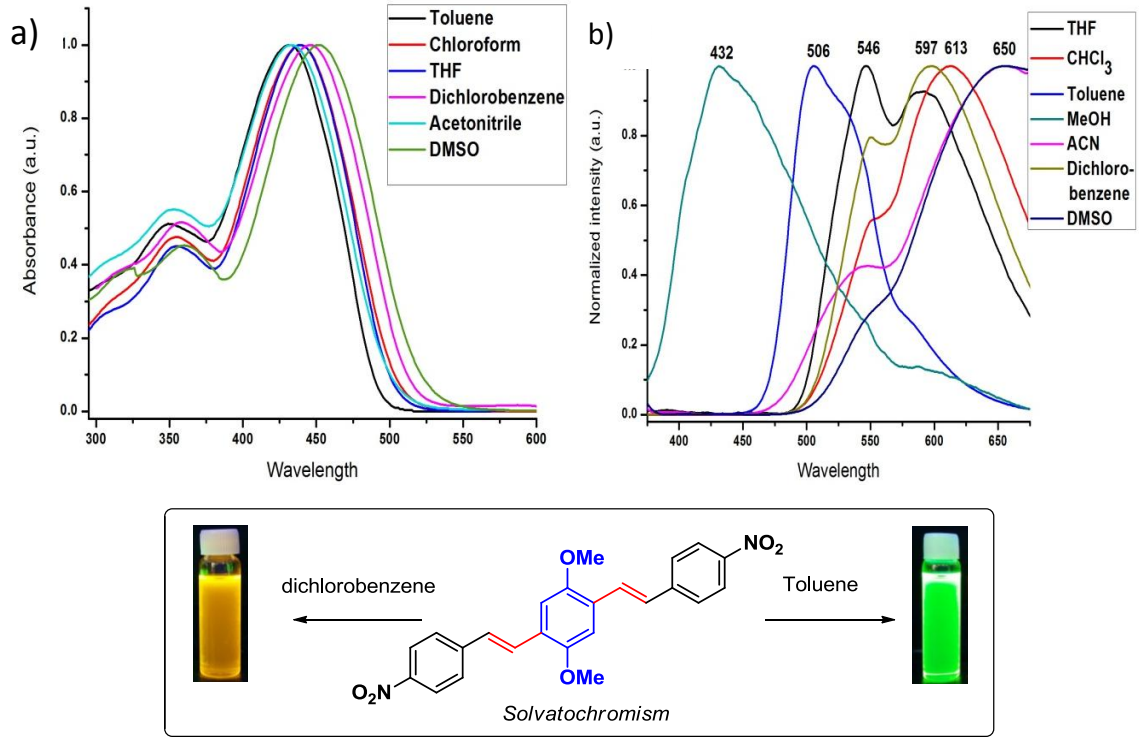

Figure 3: a) UV-Visible and b) PL spectra of **NO_2-OPV** in different solvents

Photophysical properties of OPV 8-11

The presence of terminal pyridine group in **OPVs 8-11** was explored as, nitrogen of pyridine ring can prove to be an active site for the protonation and hence can drastically alter the absorption and emission of the compound. The pyridine terminated **OPVs 8-11** were studied for its protonation behavior spectroscopically. All the pyridine terminated compounds were easily soluble in organic solvents. They were highly fluorescent in diluted solutions and display a spectral sensitivity to pH in absorption spectra as well as in fluorescence spectra at the low concentration range of 0.01mM. All the compounds exhibit highly pH-dependent absorption and emission. The absorption spectrum of pyridine terminated OPVs showed a strong absorption in the range of 300-400 nm. The

absorption near 300 nm can be assigned to π-π* electronic transitions while the absorption band near 400 nm can be due to n-π* transition. In order to compare the effect of conjugation length of **OPV 8**, we have also synthesized **OPV 21** with two terminal pyridyl ring i.e. 4,4'-((1*E*,1'*E*)-(2,5-dimethoxy-1,4-phenylene)bis(ethene-2,1-diyl))dipyridine (with three ring system) by Heck reaction of iodobenzene and vinyl pyridine. In case of **OPV 21** upon addition of diluted HCl, the absorption band at 329 nm and 402 nm shifts to 359 nm and 456 nm respectively. The UV titration for **OPV 21** in methanol with diluted methanolic HCl is shown in the **Figure 4**. This acid-induced change is clearly visible whereas the emission of **OPV 21** changed from blue to orange. The absorption and emission change is highly reversible, as the blue emission can be fully recovered upon the addition of ammonia. The pH-dependent change can be readily attributed to the protonation-deprotonation process of the terminal pyridine groups, which allows the reversible inter-conversion between the cationic and neutral forms of OPV. The quinonoid form formed due to the protonation of pyridine nitrogen, absorbs at higher wavelength as compared to the benzonoid form as shown in mechanism below.

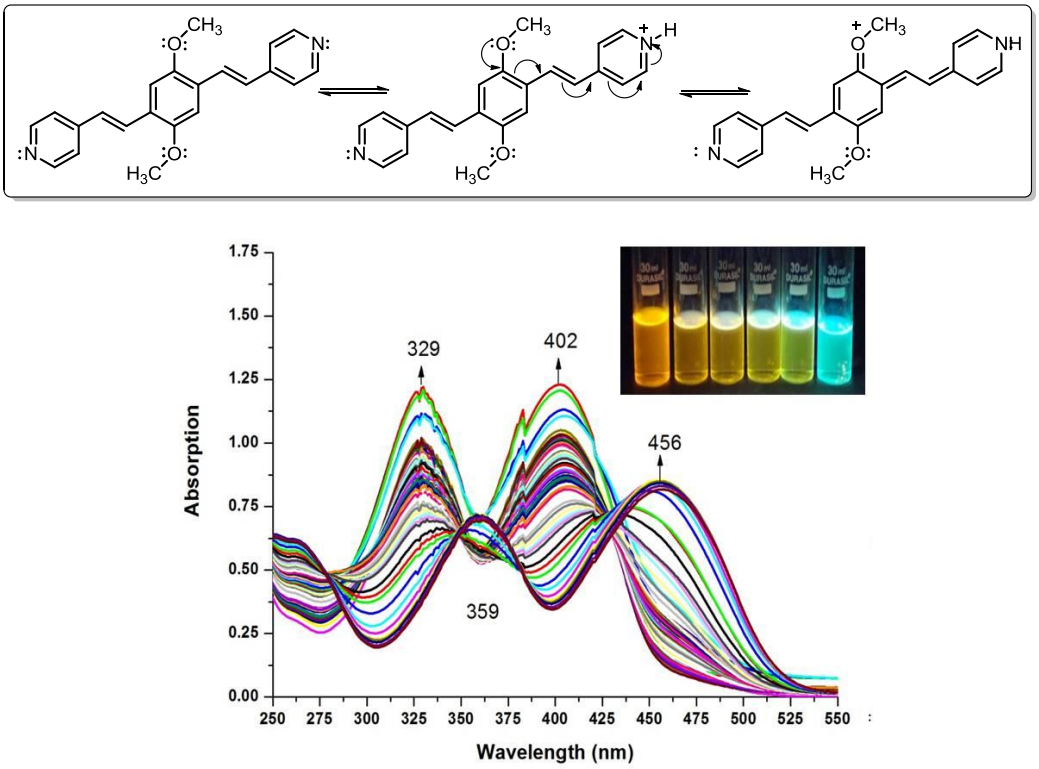

Figure 4

The changes of these compounds occur in the visible range, making it suitable for visually sensing material. The **OPV 8** showed absorptions at 352 and 408 nm which shows red shift compared to **OPV 21** due to extended conjugation. On acidification of

OPV 8 with dilute HCl the absorption band shifts to a broad peak at 427 nm. Further in order to study the substituent effect we have systematically studied **OPV 9-11** with electron releasing and electron withdrawing substituents. The **OPV 9** (R=H) showed absorption at 318 and 332 nm which after protonation shifts to 368 nm. **OPV 10** (R= OMe) functional group absorbed at 364 nm whereas **OPV 11** with chromophoric $–NO_2$ group showed absorption peaks at 316 and 366 nm. Upon protonation in **OPV 10** the absorption peak at 364 nm shifted to 417 nm and such a high bathochromic shift can be attributed to the presence of electron releasing –OMe group which can stabilize the pyridyl nitrogen after protonation. In case of **11** ($R=NO_2$) protonation leads to a small bathochromic shift i.e. from 366 to 376 nm due to the presence of electron withdrawing $–NO_2$ group. Also the emission spectra of all the pyridine terminated **OPVs** showed emission peak in the visible region of electromagnetic spectrum and showed a bathochromic shift after protonation. The **OPV 8** exhibited a clear emission band at 480 nm which quickly disappeared on protonation with methanolic HCl and a new band appeared at 618 nm. Such a large bathochromic shift can be attributed to the long conjugation of π-bond across the pyridine nitrogen and the electron donating -OMe group. The OPVs **9**, **10** and **11** showed an emission band at 421, 455 and 508 nm respectively and after protonation new band appears at 496, 604 and 517 nm correspondingly. It is observed that there is 75 nm bathochromic shift in **OPV 9** whereas 149 nm bathochromic shift was observed in case of **OPV 10** with -OMe substitution where the positive charge of protonated pyridine will be stabilized by the push-pull mechanism. On the other hand the **OPV 11** showed only 9 nm shift due to the presence of electron withdrawing $-NO_2$ group. Florescence spectrum for **OPV 9**, **10** and **11** are shown in **Figure 5**. The absorption and emission wavelengths are summarized in **Table 1**.

Table 1: Absorption and Emission values for pyridine terminated OPVs

Compound	Absorption (λmax) nm	Absorption after protonation	Emission nm	Emission after protonation	Shift in Emission peak (nm)
8	352, 408	427	480	618	138
9	318, 332	368	421	496	75
10	364	417	455	604	149
11	316, 366	376	508	517	9

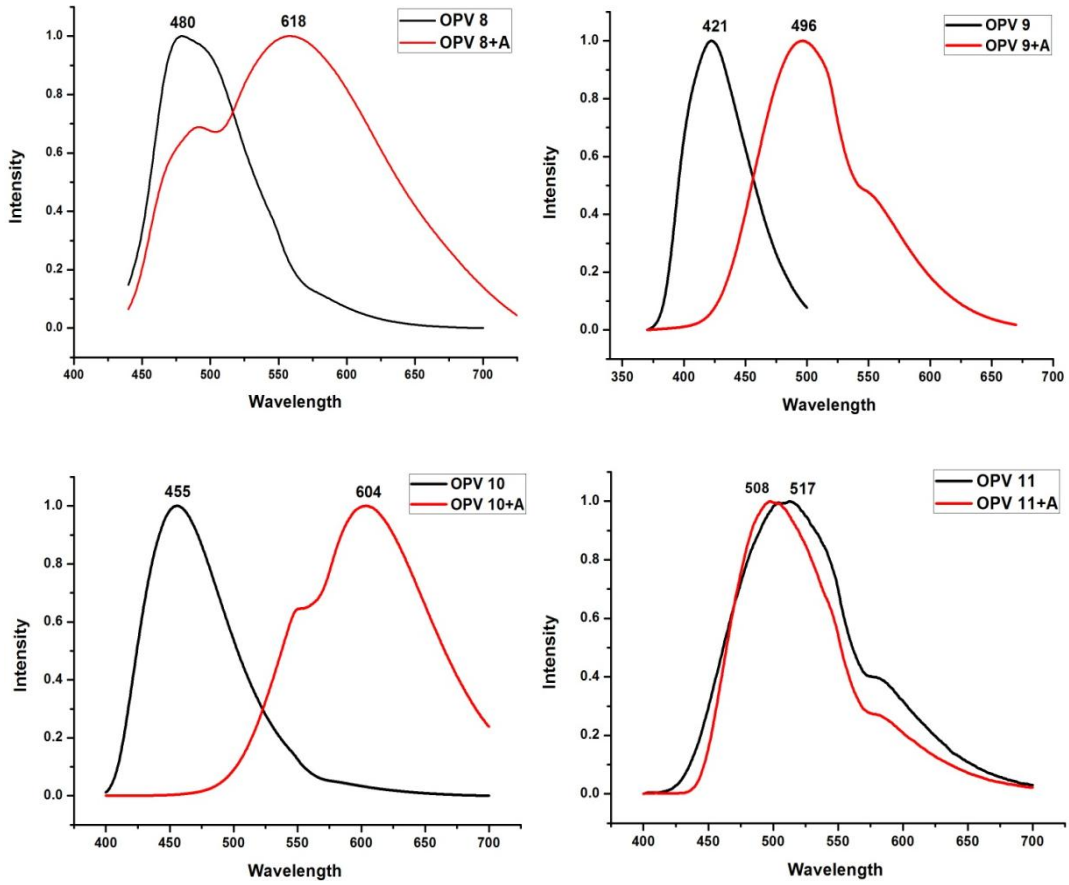

Figure 5: Emission spectra for **OPV 8, 9, 10** and **11**

Synthesis and characterization of PPV

Having synthesized different derivatives of OPVs, we have also synthesized poly(phenylenevinylene). Typically PPV and its numerous derivatives are prepared by palladium catalyzed Mizoroki-Heck reaction of corresponding olefins and aryl halides. For the preparation of such derivatives the availability of styrene and divinyl benzene is a cumbersome and difficult process due to its unstable nature. Hence we present the synthesis of PPV **22** by more efficient one-pot methodology. The synthesis of PPV is presented in **Scheme 5**, where we begin the synthesis with p-bromobenzaldehyde **23** having two functionalities i.e. a halide and an aldehyde. Aldehyde functional group will undergo Wittig reaction with methyl triphenyl phosphine iodide **15** to generate p-bromo styrene which will subsequently undergo intramolecular Heck reaction with the bromo part of the same molecule leading to oligomerisation or polymerization. Yellow insoluble material so obtained was purified by soxhlet extraction using methanol and chloroform as solvents in order to remove the unreacted starting materials and the oligomers.

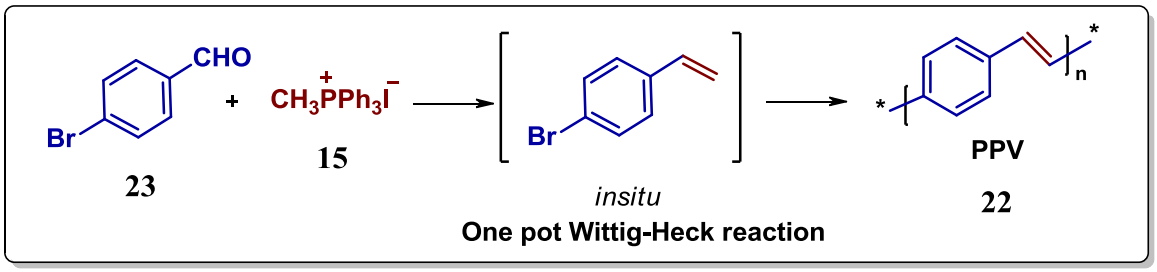

Scheme 5: Synthesis of PPV by one-pot Wittig-Heck methodology

Characterization of PPV

The material obtained from the one-pot synthesis of PPV was characterized by GPC, TGA, IR, UV-Visible and fluorescence spectroscopy. The solution of PPV was prepared in toluene due to its poor solubility in other polar solvents and it was found to be highly fluorescent as viewed under UV light. It showed absorbance (λ_{max}) at 382 nm and fluorescence emission at 450 nm which can be attributed to the absorption due to the conjugated backbone.

(a)

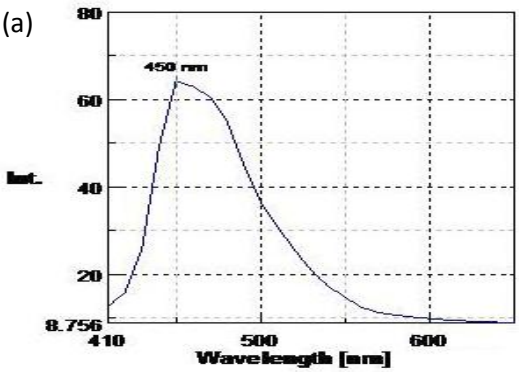

(b)

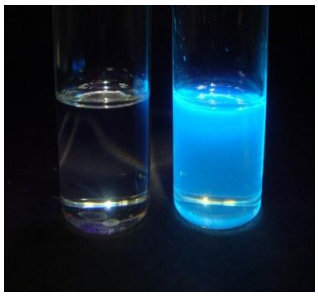

Figure 5: (a) Fluorescence spectra of PPV in toluene (b) Solution of polymer **22** as viewed under UV light

GPC analysis showed the molecular weight of the synthesized polymer **22** to be about 29420 g/mol and the polydispersity index was found to be 1.039, hence the sample is mono dispersed. Thermogravimetric analysis showed that the synthesized material was stable up to 450^{o}C with a nominal weight loss of 10% [**Figure 6]**.

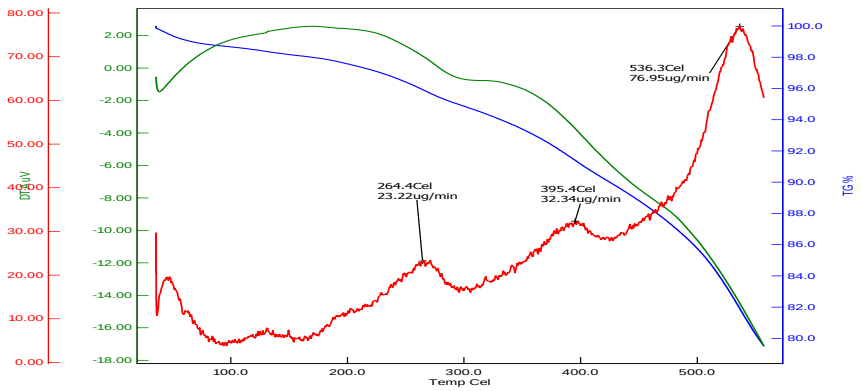

Figure 6: TG-DTA-DTG Anaylsis

IR spectra of **22** shows peaks at 835 cm^{-1} inferring C-H bending for *p*-di-substituted benzene ring, 966 cm^{-1} indicated C-H bending for di-substituted vinyl group (*trans*), 1693 cm^{-1} infers C-C bending for di-substituted alkene (*trans*), 3022 cm^{-1} infers C-H stretching for aromatic ring, supporting the structure of PPV.

Hence in conclusion in this section we have shown the application of one-pot Wittig-Heck methodology for the synthesis of oligo-(phenylenevinylene)s derivatives and poly(phenylenevinylene) PPV. All the derivatives were highly fluorescent in solid state as well as in solution and showed good absorption and emission in the UV-Visible range. Pyridine terminated OPVs showed acidochromic behavior which was systematically studied and hence can find application for development of pH sensitive probes.

Experimental Section (Section 3.2.1)

All reactions were carried out in oven-dried glassware with magnetic stirring. Purification of reaction products was carried out by column chromatography using silica gel (60-120 mesh). Thin layer chromatography was performed on TLC Silica Gel 60 F_{254} (Merck). The spots were visualized under UV light or with iodine vapour. ^{1}H-NMR spectra were recorded on Bruker Avance II 400 NMR spectrometer (400 MHz) and were run in $CDCl_3$ unless otherwise stated. Signal multiplicity is denoted as singlet (s), doublet (d), doublet of doublets (dd), triplet (t), triplet of doublets (td), quartet (q), and multiplet (m). Mass spectra were recorded on Thermo-Fischer DSQ II GCMS instrument; IR spectra were recorded on Perkin-Elmer FTIR RXI spectrometer as KBr pallets. UV-Visible absorption of all the compounds was measured as a solution in THF at room temperature on Perkin-Elmer Lambda 35 spectrometer and fluorescence was measured on Jasco FP-6300 spectro fluorometer. Melting points were recorded in Thiele's tube using paraffin oil and are uncorrected.

Solvents were dried and purified by distillation under reduced pressure and stored on molecular sieves. All chemicals were purchased from Sigma-Aldrich Chemicals Limited, SD Fine, Sisco, Qualigens, Avara Chemicals Limited etc., and used without further purification.

4,4'-((2,5-dimethoxy-1,4-phenylene)bis(ethene-2,1-diyl)dibenzene **(1)**

A two neck round bottom flask was charged with 1, 4-diiodo dimethoxy benezene (0.2 g, 0.512 mmol), methyl triphenylphosphine iodide (0.416 g,

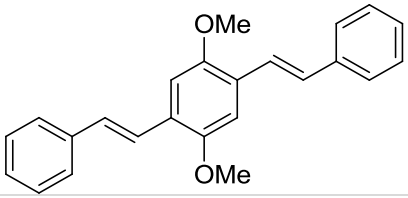

0.102mmol), benzaldehyde (0.108 g, 0.102 mmol), K_2CO_3 (0.496 g, 0.358 mmol), palladium acetate (0.0011 g, 0.00512 mmol), dppp (0.0042 g, 0.0102 mmol), TBAB (0.066 g, 0.205 mmol) in N,N-dimethyl acetamide (10 mL) and was stirred at 140 ^oC under N_2 atmosphere for 40 h. The cooled mixture was then poured in water (100 mL) and extracted with ethyl acetate (3 × 50 mL). The organic layer was washed with water (2 × 20 mL) and dried over anhydrous sodium sulfate. The solution was concentrated under reduced pressure to obtain a viscous liquid, which was purified by column chromatography on silica gel and petroleum ether-ethyl acetate mixture as eluent to give pure product.

Yield: 0.144g, 82.3 %, Pale yellow solid; Melting point: 176 ^oC (Lit.[4] 177-178 ^oC)

^{1}H-NMR ($CDCl_3$, 400 MHz) δ 7.58 (d, J = 7.2 Hz, aromatic protons of terminal benzene ring, 2H), 7.52 (d, J =16.4 Hz, *E* olefinic protons, 1H), 7.37 – 7.41 (m, aromatic protons of terminal benzene rings, 2H), 7.26 – 7.30 (m, aromatic protons of terminal benzene rings, 1H), 7.17 (s, aromatic protons of tetra substituted benzene ring, 1H), 7.15 (d, J = 16.4 Hz, *E* olefinic protons, 1H), 3.96 (s, 3H).

MS (EI) m/z : 343 (M^{+1}, 25), 342 (M^+, 100), 171 (11), 105 (35).

IR (KBr): υ 2856, 1491, 1405, 1208, 1046, 959, 748 $cm.^{-1}$

4,4'-((2,5-dimethoxy-1,4-phenylene)bis(ethene-2,1-diyl) bis(methylbenzene) **(2)**

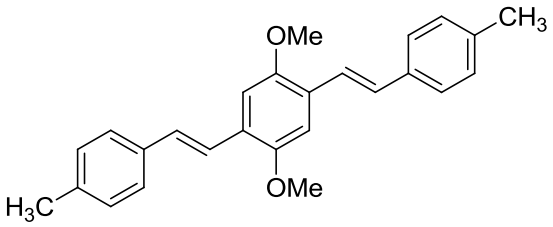

A two neck round bottom flask was charged with 1, 4-diiodo dimethoxy benezene (0.2 g, 0.512 mmol), methyl triphenylphosphine iodide (0.416 g, 0.102 mmol), 4-methylbenzaldehyde (0.123 g, 0.102 mmol), K_2CO_3 (0.496 g, 0.358 mmol), palladium acetate (0.0011 g, 0.00512 mmol), dppp (0.0042 g, 0.0102 mmol), TBAB (0.066 g, 0.205 mmol) in N,N-dimethyl acetamide (10 mL) and was stirred at 140 ^oC under N_2 atmosphere for 40 h. The cooled mixture was then poured in water (100 mL) and extracted with ethyl acetate (3 × 50 mL). The organic layer was washed with water (2 × 20 mL) and dried over anhydrous sodium sulfate. The solution was concentrated under reduced pressure to obtain a viscous liquid, which was purified by column chromatography on silica gel and petroleum ether-ethyl acetate mixture as eluent to give pure product.

Yield: 0.129 g, 68%, Yellow solid; Melting point:175 ^oC (Lit.[4] 176-178^oC)

^{1}H-NMR (400 MHz, $CDCl_3$) δ 7.47 (d, *J*=8Hz, 2H), 7.45 (d, *J*=16.4Hz, 2H), 7.18 (d, *J*=8Hz, 2H), 7.15 (s, 1H), 7.11 (d, *J*=16.4Hz, 2H), 3.94 (s, 3H), 2.38 (s, 3H).

MS (EI) m/z : 370 (M^+, 100), 369 (93).

IR (KBr): υ 2829, 1407, 1209, 1047, 967, 846 $cm.^{-1}$

4,4'-((2,5-dimethoxy-1,4-phenylene)bis(ethene-2,1-diyl)bis(nitrobenzene) **(3)**

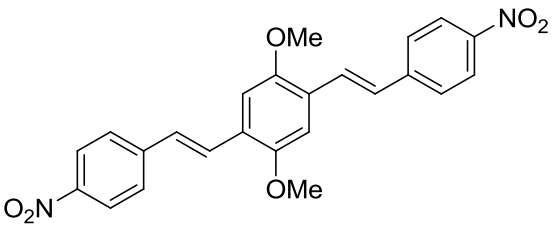

A two neck round bottom flask was charged with 1, 4-diiodo dimethoxy benezene (0.2 g, 0.512 mmol), methyl triphenylphosphine iodide (0.416 g, 0.102 mmol), 4-nitrobenzaldehyde (0.154 g, 0.102 mmol), K_2CO_3 (0.496 g, 0.358 mmol), palladium acetate (0.0011 g, 0.00512 mmol), dppp (0.0042 g, 0.0102 mmol), TBAB (0.066 g, 0.205 mmol) in N,N-dimethyl acetamide (10 mL) and was stirred at 140 ^oC under N_2 atmosphere for 40 h. The cooled mixture was then poured in water (100 mL) and extracted with ethyl acetate (3 × 50 mL). The organic layer was washed with water (2 × 20 mL) and dried over anhydrous sodium sulfate. The solution was concentrated under reduced pressure to obtain a viscous liquid, which was purified by column chromatography on silica gel and petroleum ether-ethyl acetate mixture as eluent to give pure product.

Yield: 0.166 g, 75%, Yellow solid; Melting point: 292-294 ^oC (Lit.[5] 297^oC)

^{1}H-NMR (400 MHz, $CDCl_3$) δ 8.23 (d, *J* = 8.8 Hz, 2H), 7.67 (d, *J* = 8.8 Hz, 2H), 7.65 (d, *J* = 16 Hz, 1H), 7.20 (d, *J* = 16.4 Hz, 1H), 7.15 (s, 1H), 3.96 (s, 3H).

4,4'-((2,5-dimethoxy-1,4-phenylene)bis(ethene-2,1-diyl))bis(N,N-dimethylaniline) **(4)**

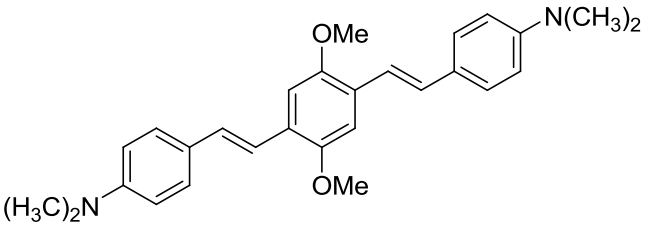

A two neck round bottom flask was charged with 1, 4-diiodo dimethoxy benezene (0.2 g, 0.512mmol), methyl triphenylphosphine iodide (0.416 g, 0.102 mmol), N,N-dimethylbenzaldehyde (0.153 g, 0.102 mmol), K_2CO_3 (0.496 g, 0.358 mmol), palladium acetate (0.0011 g, 0.00512 mmol), dppp (0.0042 g, 0.0102 mmol), TBAB (0.066 g, 0.205 mmol) in N,N-dimethyl acetamide (10 mL) and was stirred at 140 ^oC under N_2 atmosphere for 40 h. The cooled mixture was then poured in water (100 mL) and extracted with ethyl acetate (3 × 50 mL). The organic layer was washed with water (2 × 20 mL) and dried over anhydrous sodium sulfate. The solution was concentrated under

reduced pressure to obtain a viscous liquid, which was purified by column chromatography on silica gel and petroleum ether-ethyl acetate mixture as eluent to give pure product.

Yield: 0.099 g, 45.25%, Yellow solid; Melting point: 240-242 ^{o}C (Lit.[4] 238-248 ^{o}C)

^{1}H-NMR (400 MHz, $CDCl_3$) δ 7.45 (d, *J* = 8.4 Hz, 2H), 7.28 (d, *J* = 16 Hz, 1H), 7.26 (s, 1H), 7.09 (d, *J* = 16.4 Hz, 1H), 6.72 (d, *J* = 8.4 Hz, 2H), 7.15 (s, 1H), 3.96 (s, 3H), 2.99 (s, 6H).

4,4'-((2,5-dimethoxy-1,4-phenylene)bis(ethene-2,1-diyl))bis(chlorobenzene) **(5)**

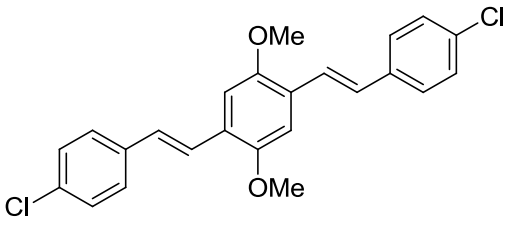

A two neck round bottom flask was charged with 1, 4-diiodo dimethoxy benezene (0.2 g, 0.512mmol), methyl triphenylphosphine iodide (0.416 g, 0.102mmol), 4-chlorobenzaldehyde (0.144 g, 0.102mmol), K_2CO_3 (0.496 g, 0.358mmol), palladium acetate (0.0011 g, 0.00512mmol), dppp (0.0042 g, 0.0102mmol), TBAB (0.066 g, 0.205mmol) in N,N-dimethyl acetamide (10 mL) and was stirred at 140 ^{o}C under N_2 atmosphere for 40 h. The cooled mixture was then poured in water (100 mL) and extracted with ethyl acetate (3 × 50 mL). The organic layer was washed with water (2 × 20 mL) and dried over anhydrous sodium sulfate. The solution was concentrated under reduced pressure to obtain a viscous liquid, which was purified by column chromatography on silica gel and petroleum ether-ethyl acetate mixture as eluent to give pure product.

Yield: 0.179 g, 85.33%, Yellow solid; Melting point: 218 ^{o}C (Lit.[4] 214-216 ^{o}C)

^{1}H-NMR ($CDCl_3$, 400 MHz) δ7.48-7.42 (m, 5H), 7.31 (d, *J*=8.4Hz, 2H), 7.11-7.05(m, 2H, a doublet with *J*=16.4Hz merged in it).

MS (EI) m/z : 412 (60), 411(25) [M^+], 410 (82), 207 (35), 139 (100).

IR (KBr): υ 2957, 2831, 1494, 1407, 1211, 1045, 969, 853 cm.$^{-1}$

4,4'-((2,5-dimethoxy-1,4-phenylene)bis(ethene-2,1-diyl))bis(bromobenzene) **(6)**

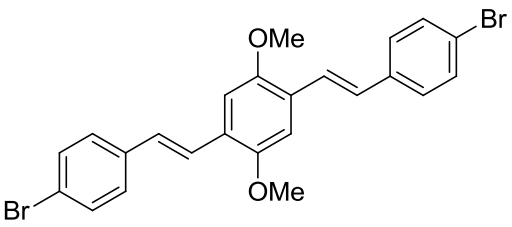

A two neck round bottom flask was charged with 1, 4-diiodo dimethoxy benezene (0.2 g, 0.512mmol), methyl triphenylphosphine iodide (0.416 g, 0.102 mmol), 4-bromobenzaldehyde (0.189 g, 0.102 mmol), K_2CO_3 (0.496 g,

0.358mmol), palladium acetate (0.0011 g, 0.00512 mmol), dppp (0.0042 g, 0.0102 mmol), TBAB (0.066 g, 0.205 mmol) in N,N-dimethyl acetamide (10 mL) and was stirred at 140 ^{o}C under N_2 atmosphere for 40 h. The cooled mixture was then poured in water (100 mL) and extracted with ethyl acetate (3 × 50 mL). The organic layer was washed with water (2 × 20 mL) and dried over anhydrous sodium sulfate. The solution was concentrated under reduced pressure to obtain a viscous liquid, which was purified by column chromatography on silica gel and petroleum ether-ethyl acetate mixture as eluent to give pure product.

Yield: 0.069 g, 27.27%, Yellow solid; Melting point: 222-224 ^{o}C (Lit.[6] 225-230 ^{o}C)

^{1}H-NMR ($CDCl_3$, 400 MHz) δ7.50-7.42 (m, 5H), 7.13 (s, 1H), 7.07 (d, *J*=16.4Hz, 1H), 3.94 (s, 3H).

MS (EI) m/z : 501 (16), 499 (32)[M^+], 497 (17), 97 (78), 83 (100).

IR (KBr): υ 2893, 2823, 1693, 1674, 1483, 1210, 1044, 852 cm.$^{-1}$

5,5'-((2,5-dimethoxy-1,4-phenylene)bis(ethene-2,1-diyl))bis(benzo[d][1,3]dioxole) **(7)**

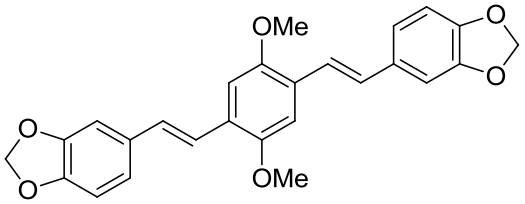

A two neck round bottom flask was charged with 1, 4-diiodo dimethoxy benezene (0.2 g, 0.512 mmol), methyl triphenylphosphine iodide (0.416 g, 0.102 mmol), piperonal (0.153 g, 0.102 mmol), K_2CO_3 (0.496 g, 0.358 mmol), palladium acetate (0.0011 g, 0.00512 mmol), dppp (0.0042 g, 0.0102 mmol), TBAB (0.066 g, 0.205 mmol) in N,N-dimethyl acetamide (10 mL) and was stirred at 140 ^{o}C under N_2 atmosphere for 40 h. The cooled mixture was then poured in water (100 mL) and extracted with ethyl acetate (3 × 50 mL). The organic layer was washed with water (2 × 20 mL) and dried over anhydrous sodium sulfate. The solution was concentrated under reduced pressure to obtain a viscous liquid, which was purified by column chromatography on silica gel and petroleum ether-ethyl acetate mixture as eluent to give pure product.

Yield: 0.098 g, 44.72%, Yellow solid; Melting point: 238 ^{o}C (Lit.[7] 237-239 ^{o}C)

^{1}H-NMR ($CDCl_3$, 400 MHz) δ7.30 (d, *J*=16.4Hz, 1H), 7.11-6.96 (m, 4H), 6.79 (d, *J*=8Hz, 1H), 5.98 (s, 2H), 3.91 (s, 3H).

***4,4'-((1E,1'E)-(((1E,1'E)-(2,5-dimethoxy-1,4-phenylene)bis(ethene-2,1-diyl))bis(4,1-phenylene))bis(ethene-2,1-diyl))dipyridine* (8)**

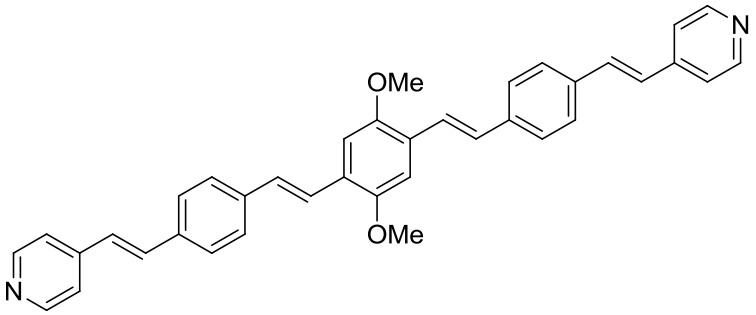

A two neck round bottom flask was charged with 2,5-dimethoxyterephthalaldehyde (0.150 g, 0.773 mmol), 4-bromo benzyl triphenylphosphine bromide (0.792 g, 1.546 mmol), 4-vinyl pyridine (0.178 g, 1.546 mmol), K_2CO_3 (0.854 g, 6.180 mmol), palladium acetate (0.0034 g, 0.0154 mmol), dppp (0.0095 g, 0.023 mmol), TBAB (0.049 g, 0.154 mmol) in N,N-dimethyl acetamide (10 mL) and was stirred at 140 ^oC under N_2 atmosphere for 40 h. The cooled mixture was then poured in water (100mL) and extracted with ethyl acetate (3 × 50 mL). The organic layer was washed with water (2 × 20 mL) and dried over anhydrous sodium sulfate. The solution was concentrated under reduced pressure to obtain a viscous liquid, which was purified by column chromatography on silica gel and petroleum ether-ethyl acetate mixture as eluent to give pure product.

Yield: 0.336 g, 79.40%, Orange solid; Melting point: >250^oC (d) (Lit.[8])

^{1}H-NMR (400 MHz, $CDCl_3$) δ 8.61-8.59 (d, J = 6Hz, 4H), 7.64-7.30 (m, 14H), 7.18-7.14 (m, 4H), 7.10-7.018 (m, 4H), 3.96 (s, 6H).

IR (KBr): υ 3050, 1589, 1438, 1189, 1120, 721 cm.$^{-1}$

***4-((E)-4-((E)-styryl)styryl)pyridine* (9)**

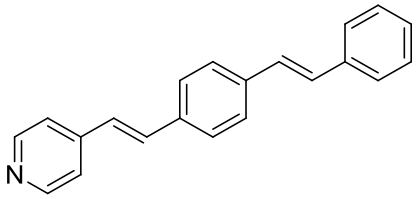

A two neck round bottom flask was charged with 4-bromo benzyl triphenylphosphine bromide (0.500 g, 0.976 mmol), benzaldehyde (0.124 g, 1.171 mmol), 4-vinyl pyridine (0.122 g, 1.171 mmol), K_2CO_3 (0.539 g, 3.90 mmol), palladium acetate (0.0021 g, 0.00976 mmol), dppp (0.0060 g, 0.014 mmol), TBAB (0.031 g, 0.097 mmol) in N,N-dimethyl acetamide (10 mL) and was stirred at 140 ^oC under N_2 atmosphere for 40 h. The cooled mixture was then poured in water (100 mL) and extracted with ethyl acetate (3 × 50 mL). The organic layer was washed with water (2 × 20 mL) and dried over anhydrous sodium sulfate. The solution was concentrated under reduced pressure to obtain a viscous liquid, which was purified

by column chromatography on silica gel and petroleum ether-ethyl acetate mixture as eluent to give pure product.

Yield: 0.229g, 85%, Yellow solid; Melting point: 276-278 ^{o}C (Lit.[9] 283-284^{o}C)

^{1}H-NMR (400 MHz, $CDCl_3$) δ 8.61-8.59 (d, *J* = 6Hz, 2H), 7.61-7.51 (m, 6H), 7.41-7.30 (m, 6H), 7.21-7.17 (d, *J* = 16.4Hz, 1H), 7.15-7.11 (d, *J* = 16.4Hz, 1H), 7.07-7.03 (d, *J* = 16.4Hz, 1H).

***4-((E)-4-((E)-4-methoxystyryl)styryl)pyridine* (10)**

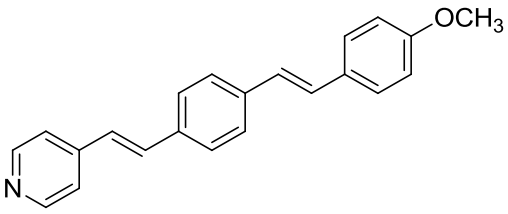

A two neck round bottom flask was charged with 4-bromo benzyl triphenylphosphine bromide (0.500 g, 0.976 mmol), 4-methoxy benzaldehyde (0.159 g, 1.171 mmol), 4-vinyl pyridine (0.122 g, 1.171 mmol), K_2CO_3 (0.539 g, 3.90 mmol), palladium acetate (0.0021 g, 0.00976 mmol), dppp (0.0060 g, 0.014 mmol), TBAB (0.031 g, 0.097 mmol) in N,N-dimethyl acetamide (10 mL) and was stirred at 140 ^{o}C under N_2 atmosphere for 40 h. The cooled mixture was then poured in water (100 mL) and extracted with ethyl acetate (3 × 50 mL). The organic layer was washed with water (2 × 20 mL) and dried over anhydrous sodium sulfate. The solution was concentrated under reduced pressure to obtain a viscous liquid, which was purified by column chromatography on silica gel and petroleum ether-ethyl acetate mixture as eluent to give pure product.

Yield: 0.196 g, 64%, Pale yellow solid; Melting point: 260^{o}C (Lit.[9] 263-264^{o}C)

^{1}H-NMR (400 MHz, $CDCl_3$) δ 8.599 (m, 2H), 7.57-7.52 (m, 4H), 7.51-7.46 (m, 4H), 7.39-7.35 (d, *J* = 16 Hz, 1H), 7.17-7.13 (d, *J* = 16 Hz, 1H), 7.08-7.04 (d, *J* = 16.4 Hz, 1H), 7.02-6.98 (d, *J* = 16.4 Hz, 1H), 6.95-6.91 (m, 2H), 3.86 (s, 3H).

MS (EI) m/z : 313 (100) [M^{+}], 312 (38).

IR (KBr): υ 3021, 2838, 1604, 1587, 1512, 1256, 969, 833 cm.$^{-1}$

***4-((E)-4-((E)-4-nitrostyryl)styryl)pyridine* (11)**

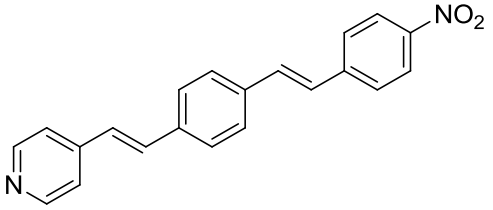

A two neck round bottom flask was charged with 4-bromo benzyl triphenylphosphine bromide (0.500 g, 0.976 mmol), 4-nitro benzaldehyde (0.177 g, 1.171 mmol), 4-vinyl pyridine (0.122 g, 1.171 mmol), K_2CO_3 (0.539 g, 3.90 mmol), palladium acetate (0.0021 g, 0.00976 mmol), dppp (0.0060 g, 0.014 mmol), TBAB (0.031 g, 0.097 mmol) in N,N-dimethyl acetamide (10 mL) and was stirred at 140

^{o}C under N_2 atmosphere for 40 h. The cooled mixture was then poured in water (100 mL) and extracted with ethyl acetate (3 × 50 mL). The organic layer was washed with water (2 × 20 mL) and dried over anhydrous sodium sulfate. The solution was concentrated under reduced pressure to obtain a viscous liquid, which was purified by column chromatography on silica gel and petroleum ether-ethyl acetate mixture as eluent to give pure product.

Yield: 0.306g, 95.6%, Pale yellow solid; Melting point: 252-255^{o}C (Lit.[10] 256-260 ^{o}C)

^{1}H-NMR (400 MHz, $CDCl_3$) δ 8.62-8.60 (d, *J* = 5.2Hz, 2H), 8.27-8.23 (m, 2H), 7.68-7.65 (m, 2H), 7.59 (s, 4H), 7.41-7.39 (m, 2H), 7.35-7.27 (two doublets with *J* = 16.4Hz and *J* = 16Hz merged together, 2H), 7.22-7.18 (d, *J* = 16.4Hz, 1H), 7.10-7.06 (d, *J* = 16.4Hz, 1H).

IR (KBr): υ 3025, 1589, 1332, 1107, 967, 844 cm.$^{-1}$

***4-((E)-4-((E)-3,4,5-trimethoxystyryl)styryl)pyridine* (12)**

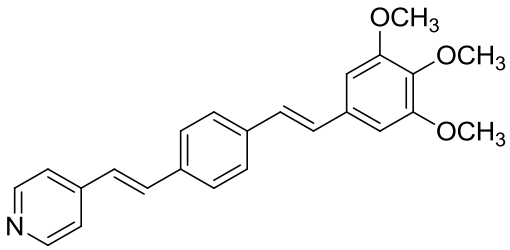

A two neck round bottom flask was charged with 4-bromo benzyl triphenylphosphine bromide (0.500 g, 0.976 mmol), 3,4,5-trimethoxybenzaldehyde (0.229 g, 1.171 mmol), 4-vinyl pyridine (0.122 g, 1.171 mmol), K_2CO_3 (0.539 g, 3.90 mmol), palladium acetate (0.0021 g, 0.00976 mmol), dppp (0.0060 g, 0.014 mmol), TBAB (0.031 g, 0.097 mmol) in N,N-dimethyl acetamide (10 mL) and was stirred at 140 ^{o}C under N_2 atmosphere for 40 h. The cooled mixture was then poured in water (100 mL) and extracted with ethyl acetate (3 × 50 mL). The organic layer was washed with water (2 × 20 mL) and dried over anhydrous sodium sulfate. The solution was concentrated under reduced pressure to obtain a viscous liquid, which was purified by column chromatography on silica gel and petroleum ether-ethyl acetate mixture as eluent to give pure product. Yield: 0.324g, 89.01%, Orange solid; Melting point: 196-198 ^{o}C

^{1}H-NMR (400 MHz, $CDCl_3$) δ 8.59 (d, *J*=6Hz, 2H), 7.56 (s, 4H), 7.39 (d, *J*=6.4Hz, 2H), 7.32 (d, *J*=16.4, 1H), 7.11(d, *J*=16, 1H), 7.08-7.02 (two doublets with *J*=16.4Hz and *J*=16Hz, 2H), 6.78 (s, 2H), 3.95 (s, 6H), 3.89 (s, 3H).

***4,4'-((1E,1'E)-(2,5-dimethoxy-1,4-phenylene)bis(ethene-2,1-diyl))dipyridine* (21)**

A two neck round bottom flask was charged with 1, 4-diiodo dimethoxy benezene (0.5 g, 1.28 mmol), K_2CO_3 (0.707 g, 5.12 mmol), palladium acetate (0.0028 g, 0.0128 mmol),

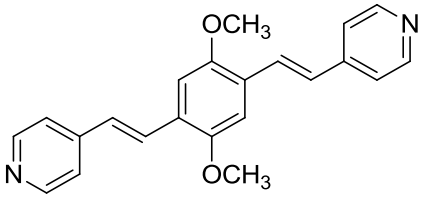

dppp (0.010 g, 0.025 mmol), TBAB (0.082 g, 0.256 mmol) in N,N-dimethyl acetamide (10 mL) under N_2 atmosphere and was stirred. The temperature was raised to 100 ^oC and 4-vinyl pyridine (0.295 g, 2.81 mmol) was added to the reaction. Further the temperature was raised to 140 ^oC and was continued for 40 h. Reaction mixture was allowed to cool and then poured in water (100 mL) and extracted with MDC (3 × 50 mL). The organic layer was washed with water (2 × 20 mL) and dried over anhydrous sodium sulfate. The solution was concentrated under reduced pressure to obtain a viscous liquid, which was purified by column chromatography on silica gel and petroleum ether-ethyl acetate mixture as eluent to give pure product.

Yield: 0.316 g, 71.65%, Orange solid; Melting point: 272^oC (273^oC)[11]

^{1}H-NMR (400 MHz, $CDCl_3$) δ 8.59-8.56 (d, J = 5.4Hz, 4H), 7.72-7.64 (d, J = 16.4Hz, 2H), 7.41-7.39 (d, J = 5.4Hz, 4H), 7.14 (s, 2H), 7.09-7.02 (d, J = 16.6Hz, 2H), 3.95 (s, 6H).

IR (KBr): υ 3032, 2829, 1592, 1409, 1212, 1034, 851, 804 $cm.^{-1}$

Spectral data for OPVs (Section 3.2.1)

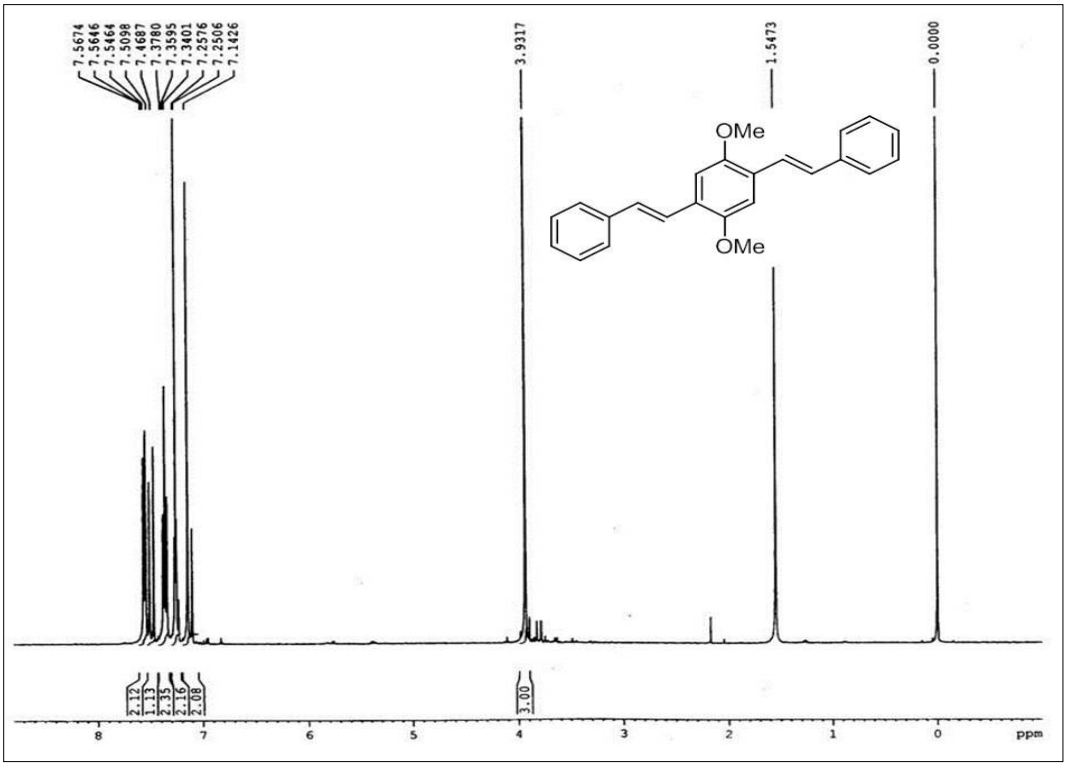

^{1}H-NMR of compound OPV 1

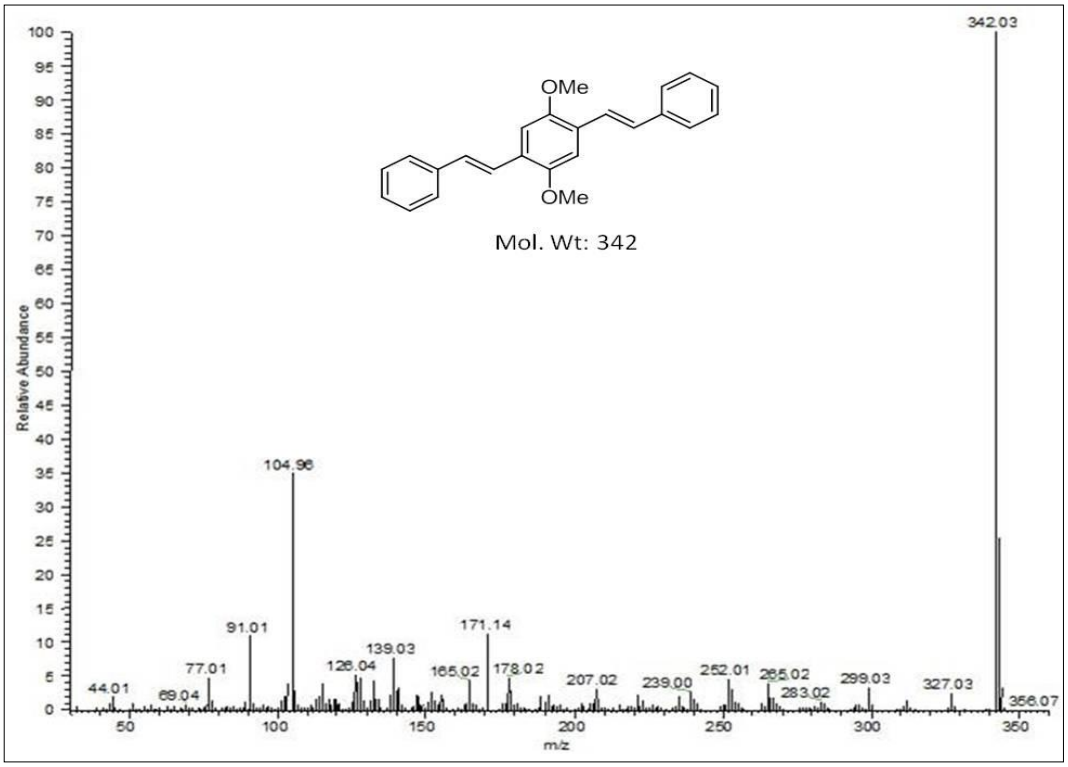

Mass spectra of OPV 1

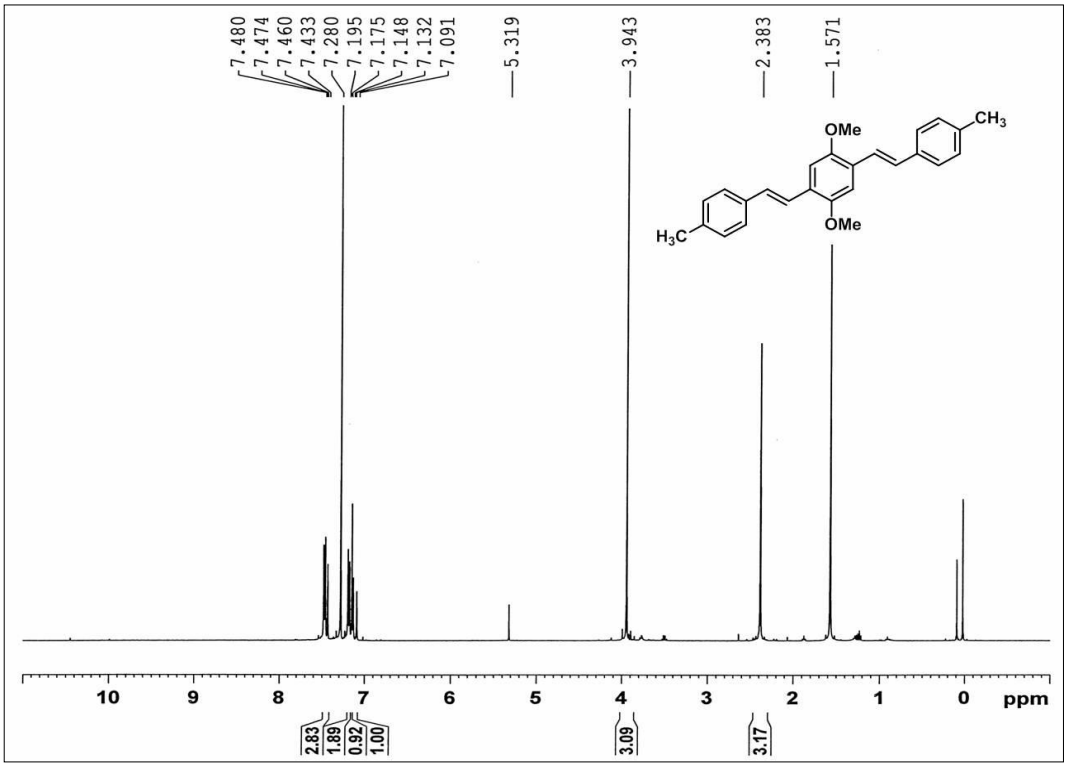

[1]H-NMR of compound OPV 2

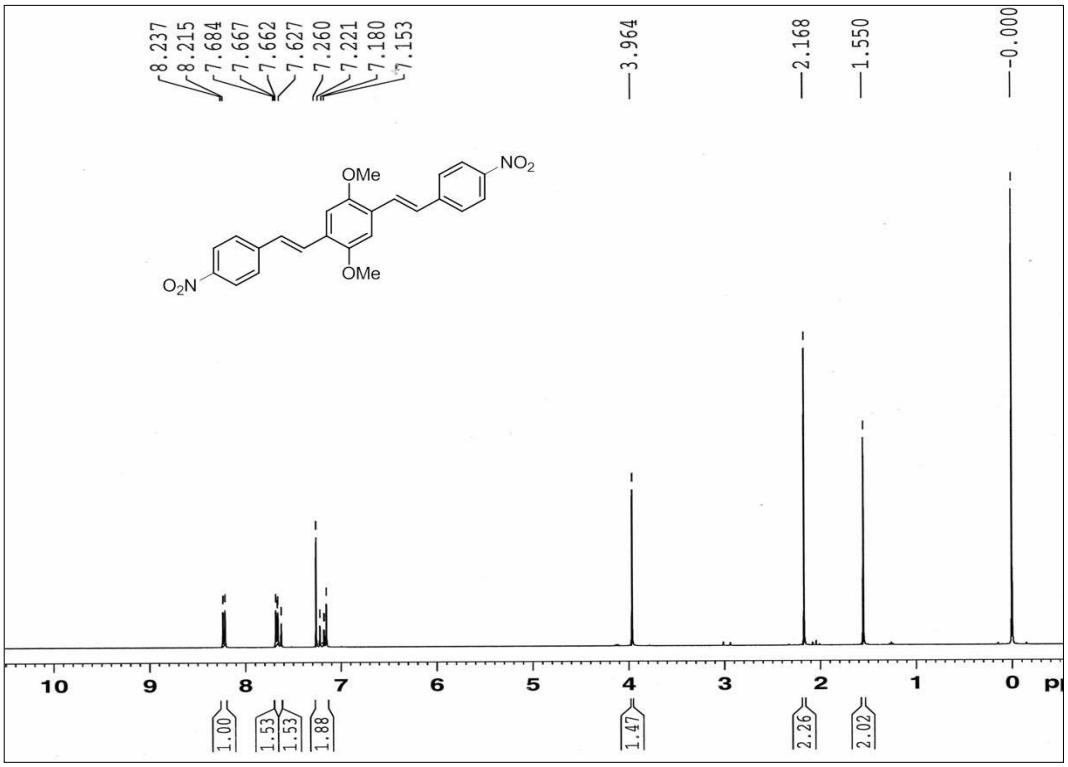

[1]H-NMR of compound OPV 3

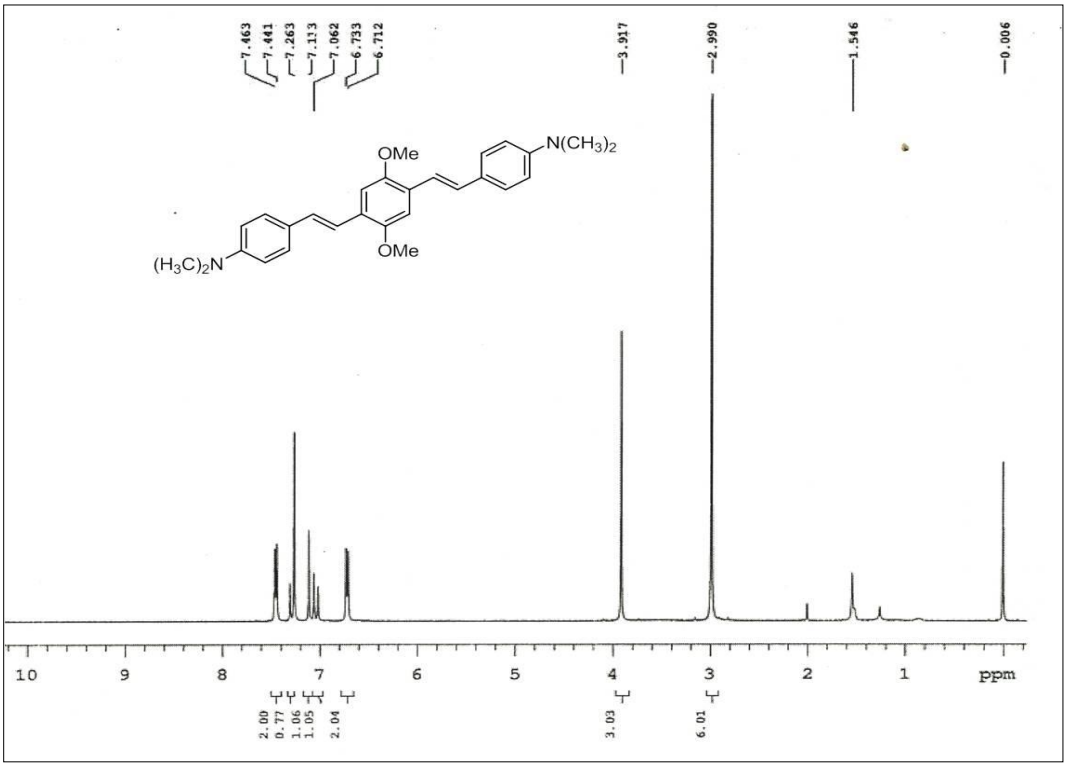

^{1}H-NMR of compound OPV 4

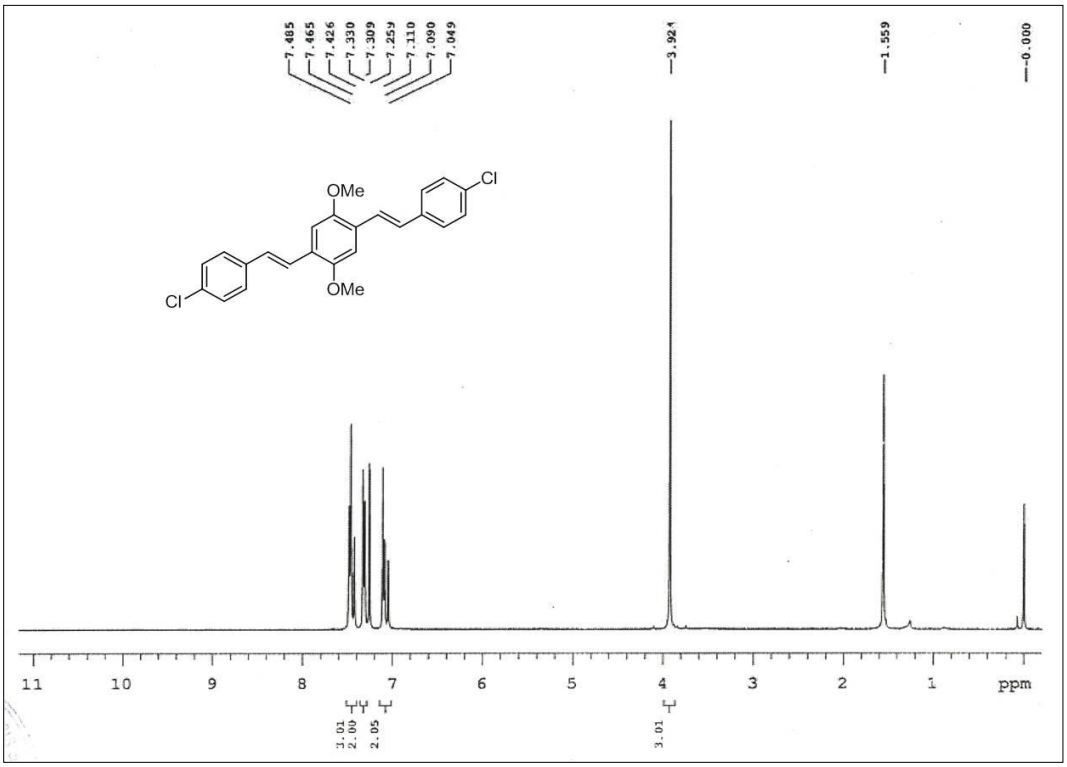

^{1}H-NMR of compound OPV 5

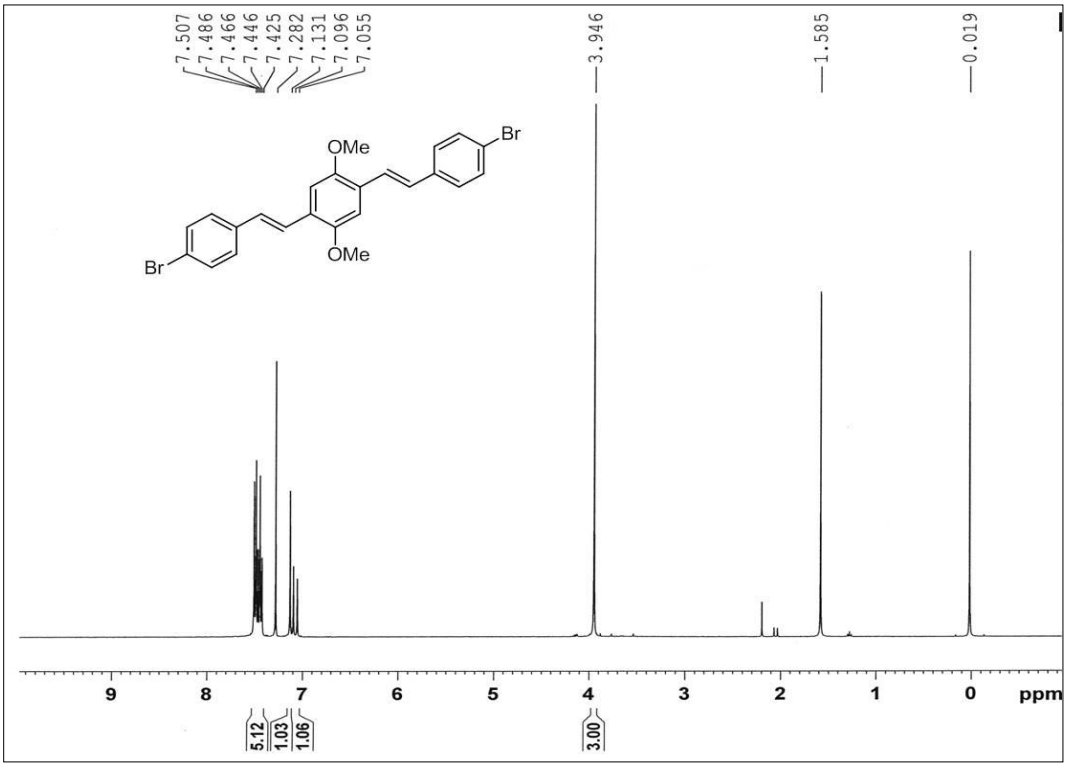

[1]H-NMR of compound OPV 6

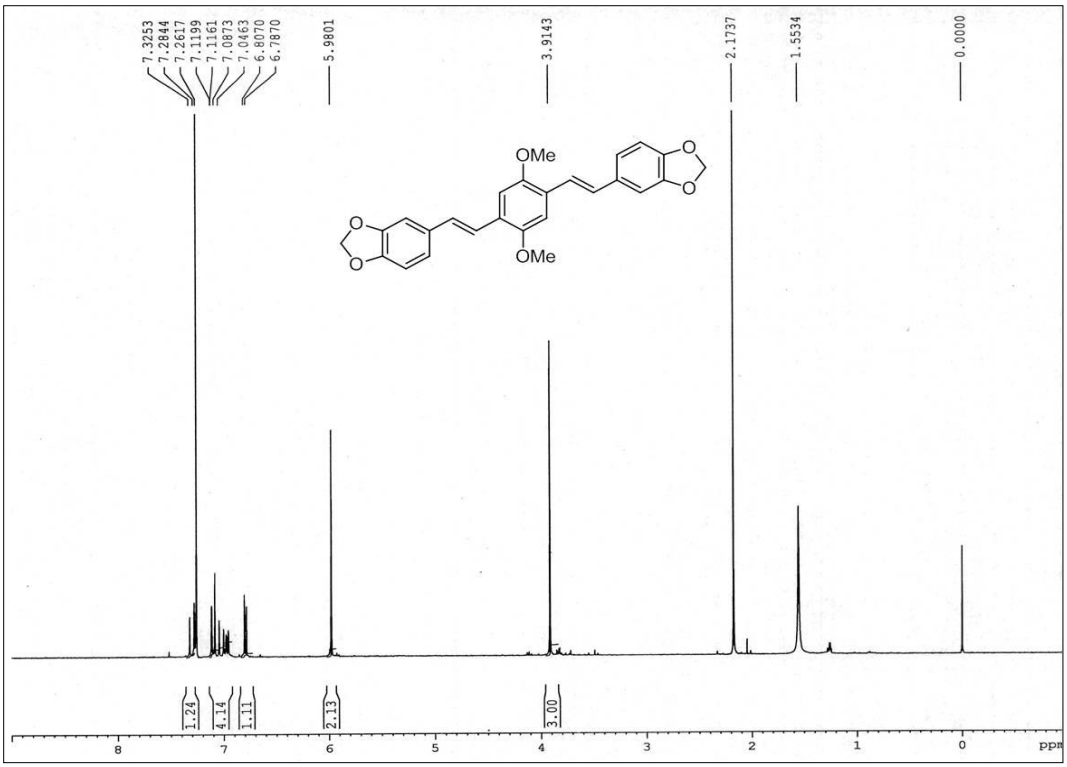

[1]H-NMR of compound OPV 7

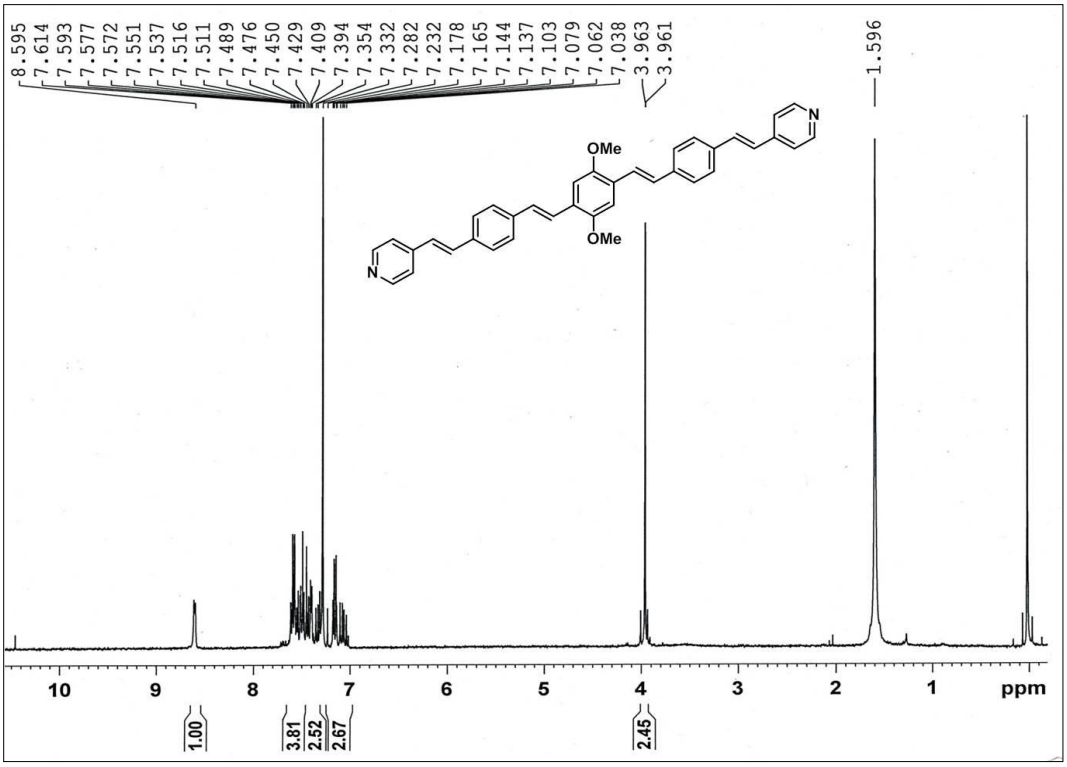

[1]H-NMR of compound OPV 8

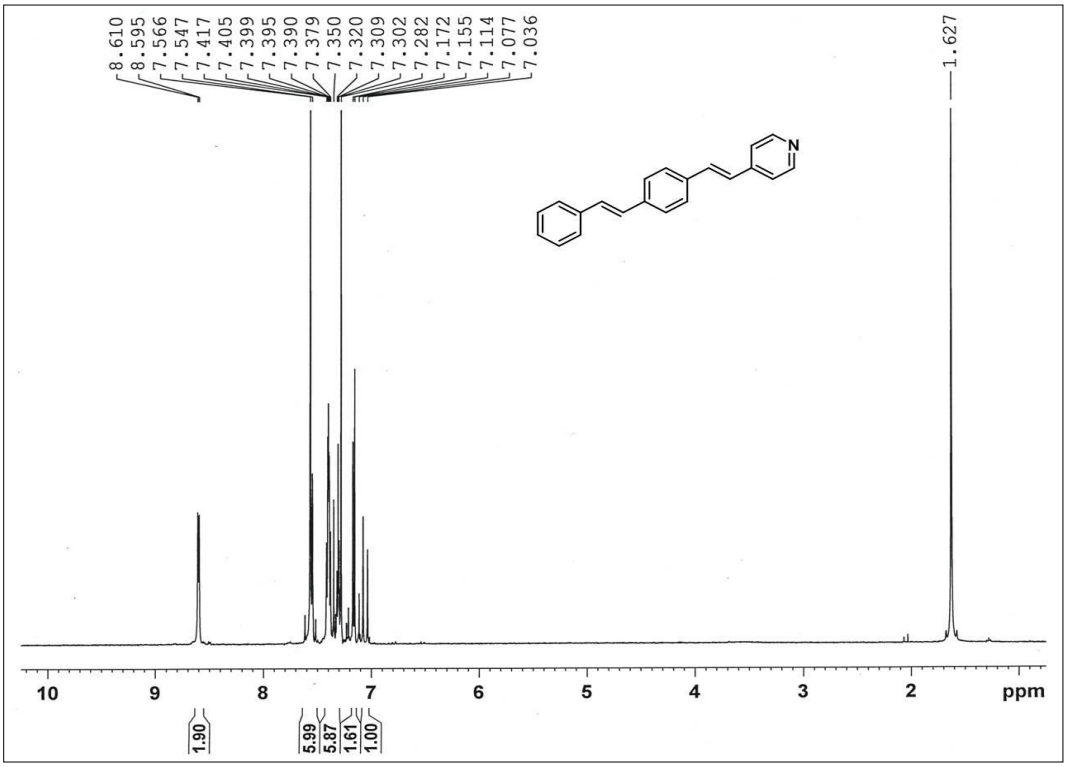

[1]H-NMR of compound OPV 9

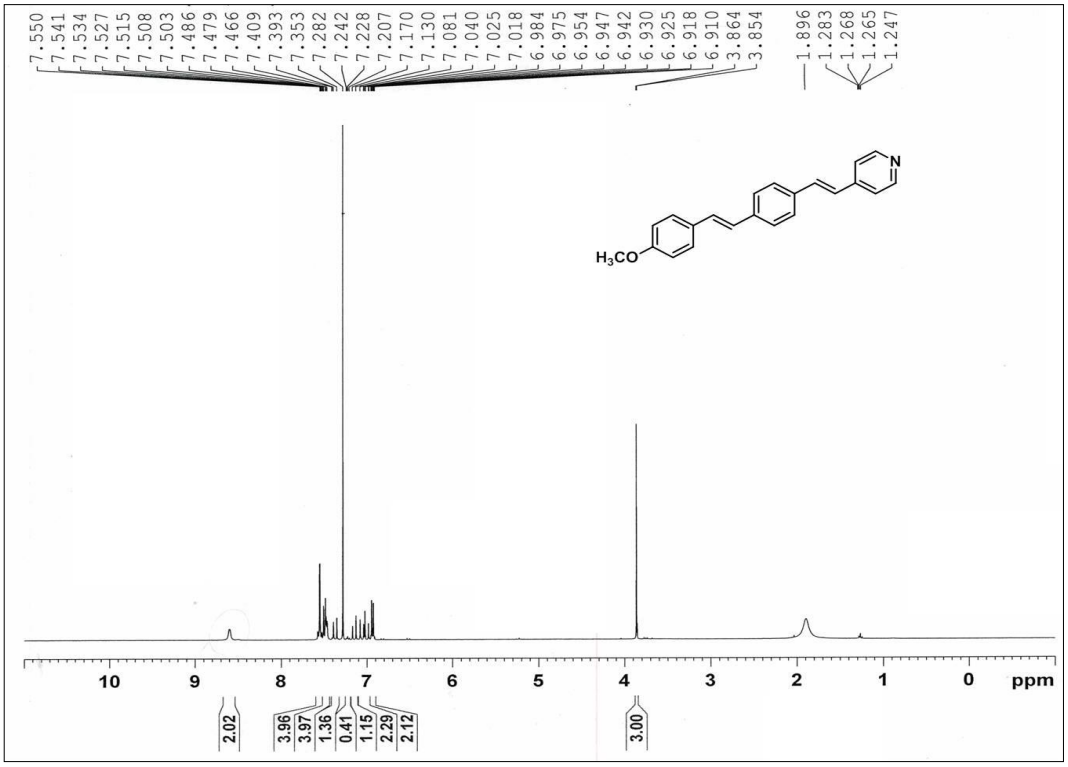

[1]H-NMR of compound OPV 10

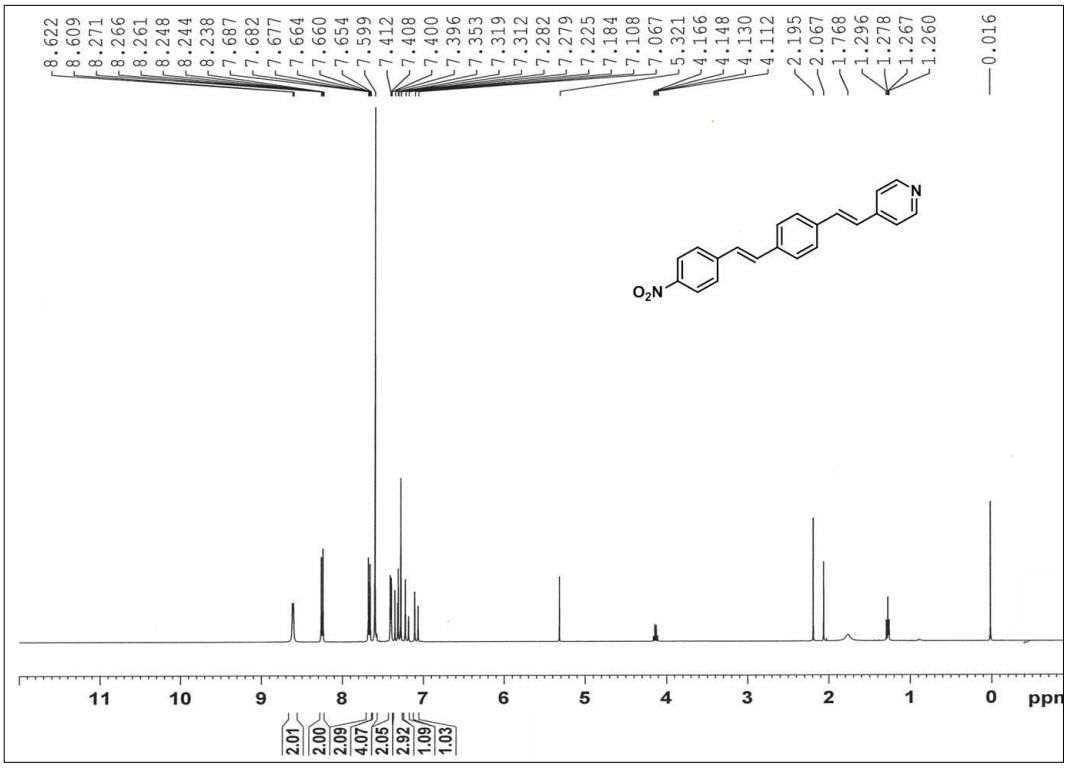

[1]H-NMR of compound OPV 11

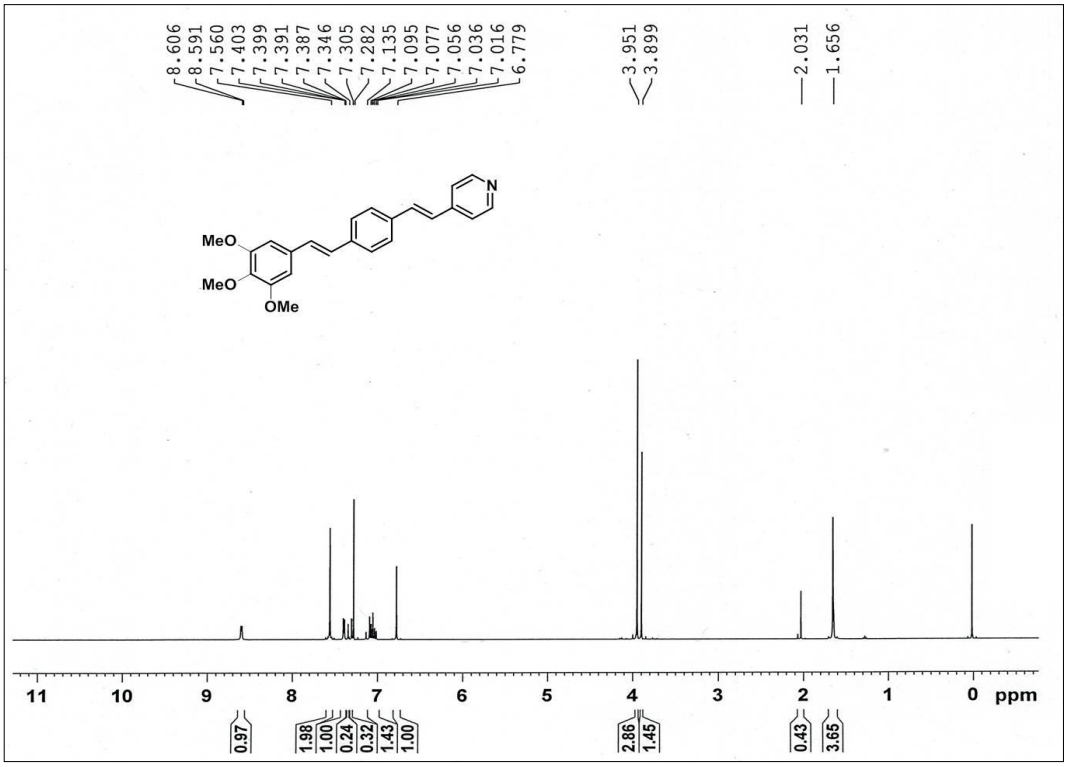

^{1}H-NMR of compound OPV 12

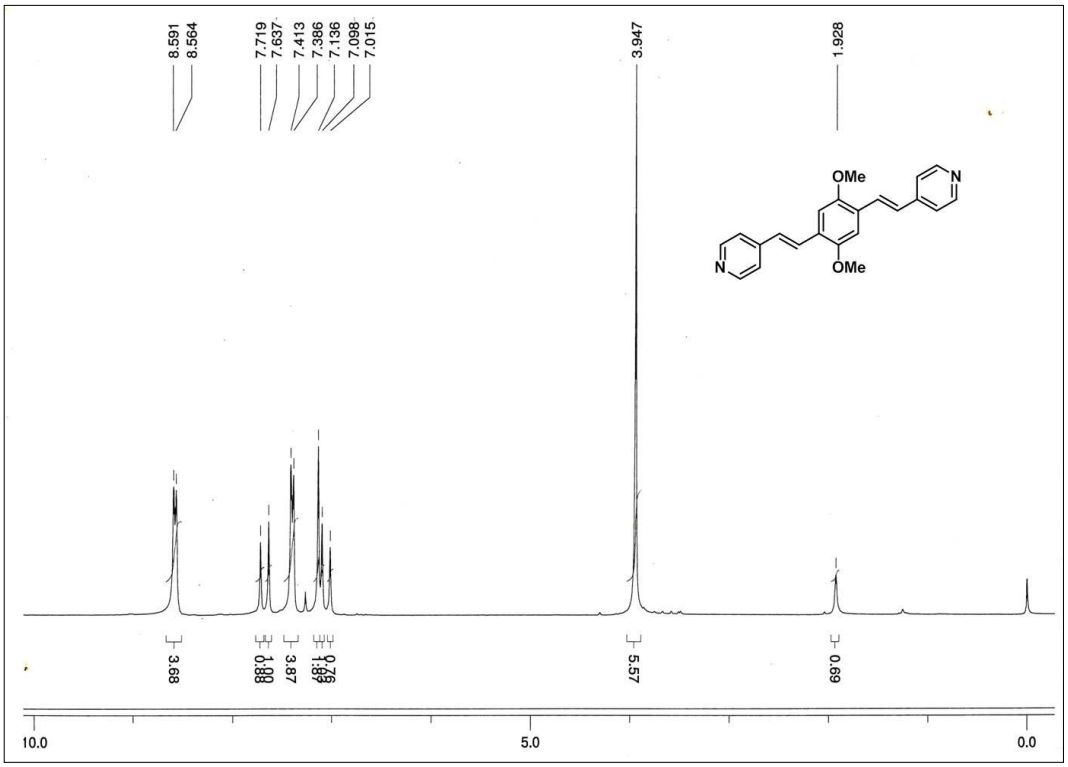

^{1}H-NMR of compound OPV 21

3.2.2 Synthesis and study of spectroscopic behavior of symmetrical cyclohexanone derived bis-chalcone

In this section, we will present the synthesis and study of another class of conjugated compounds i.e. symmetrical cyclohexanone derived bis-chalcones. Claisen–Schmidt reaction is one of the most important reactions meant for the synthesis of donor-acceptor conjugated dienes or chalcones.[12] Chalcones are categorized as bichromophoric molecules that possesses keto-vinyl moiety. The photophysical and optical properties of several derivatives of chalcones with different substituents have been studied. These compounds find applications in various optical devices including photo-alignment layer of liquid crystals display and fluorescent probes for sensing DNA and metal ions.[13] Many chalcone type compounds are known in the literature for their biological applications. Also some derivatives of this class of compounds are known as inhibitors of ovarian cancer cell proliferation[14] and pulmonary carcinogenesis.[15] In recent years, chalcones are used in the field of material science and for the development of pH sensors. Although the determination of pH with traditional electrochemical sensors is well-established, optical sensors can be still valuable alternative. Chalcones are generally synthesised by reacting compounds with active methylene group, aldehyde, catalysed by acid or base. Different synthetic methods such as, refluxing in organic solvent,[16] solvent-free solid-phase reaction,[17] ultrasonication,[18] photosensitization[19] and microwave radiation[20] have been reported.

Y. Shan *et al* have reported the synthesis of three nitro substituted chalcone derivatives with diethylamino **23**, carbazolyl **24** and pyrene **25** as terminal group via typical condensation reaction of 2-hydroxy-4-nitro-acetophenone with related arylaldehydes and it was found that all the compounds exhibit UV–Visible absorption and fast fluorescence response to cyanide anions in aqueous solution.[21]

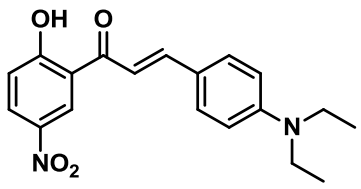

23

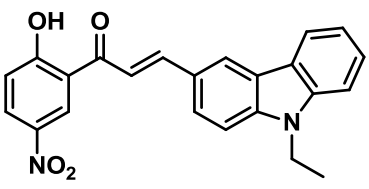

24

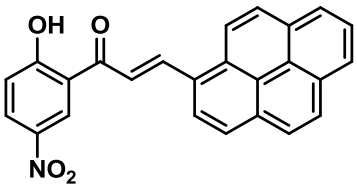

25

Compound **23** exhibits fluorescence change from orange to green with fluorescence turn-on response upon the addition cyanide anions.

Apart from that Kamal *et al*. developed chromogenic, voltammetric and potentiometric sensors based upon the novel ferrocene appended chalcone (FAC) for the selective detection of Cu (II) ions [**Figure 7**].

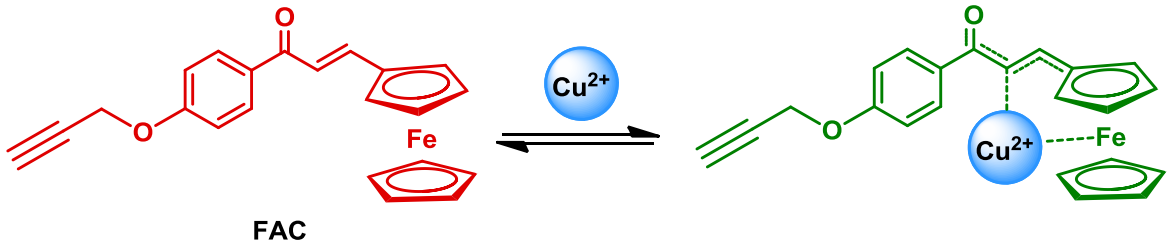

FAC

Figure 7: Structure of ferrocene appended chalcone (FAC) and its proposed co-ordination mechanism with Cu (II) ions

The UV-vis binding studies of FAC (3.00×10−5 M) in CH_3CN showed excellent selectivity towards Cu (II) ions over series of alkali (Li^+, Na^+, K^+), alkaline earth (Mg^{2+}, Ca2+) and transition metal ions ($Co^{2+,}$ Hg^{2+}, Ni^{2+}, Pb^{2+}, Cu^{2+}, Fe^{3+}, Fe^{2+}, Cd^{2+} and Zn^{2+}). On the addition of Cu (II) ions to FAC, the UV/Vis absorption bands and CV peaks get perturbed, together with the change in colour of FAC from red to olive-green.[22]

So, owing to the applicability of the chalcone derivatives we present the synthesis of α,α'-bis-(substitutedbenzylidene)cyclohexanone derivatives by solvent free Claisen-Schmidt reaction.[23] These compounds were characterized by spectroscopic techniques. Acidochromic behavior and their interactions with different metal ions were studied by UV-Visible spectroscopy. Compounds **26-32** were synthesized by solvent free chemical synthesis, also known as "mechanochemistry" which has received much attention in recent years.[24] This synthetic approach has several distinct advantages over the conventional reactions and therefore applied for the synthesis of present series of chalcones [**Scheme 6]**.

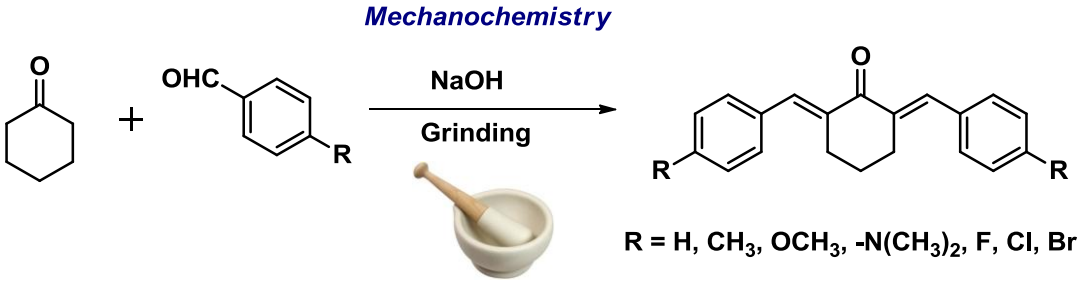

Scheme 6: Synthetic scheme for bis-chalcones **26-32**

Compound	R	Yield (%)	mp(^{o}C)(lit. value)[ref]
26	-H	93	116, (117)[25]
27	-CH_3	88	157, (162-163)[26]
28	-OMe	82	200, (204)[26]
29	-$N(CH_3)_2$	74	250-252, (250-252)[28]
30	-F	89	150, (156)[30]
31	-Cl	84	144 , (149-151)[29]
32	-Br	85	160-164, (165-168)[27]

Photophysical properties of symmetrical Cyclohexanone derived Bis-chalcone (26-32)

The optical properties of the synthesized bis-chalcone derivatives were studied by UV-Visible spectroscopy [**Table 2**, **Figure 8]**. All the compounds were soluble in most organic solvents and showed absorption above 320 nm. It was observed that 2,6-bis-(benzylidene)cyclohexanone **26** absorbed at 323 nm, 2,5-bis-(4-methoxybenzylidene)cyclohexanone **28** absorbed at 354 nm and 2,6-bis-(4-N,N-dimethylaminobenzylidene)cyclohexanone **29** showed distinctly high absorption at 421 nm. This bathochromic absorption of **28** and **29** can be attributed to the presence of electron donating -OMe and $–N(Me)_2$ substituent. Further, compounds **30**, **31** and **32** showed absorption at 324, 328 and 329 nm respectively with the marginal difference of 4 to 5 nm as compared to **26**, indicating the absorption could be mainly due to the basic chalcone framework. Probably the halogen substituent contributed very little to the absorption.

Entry	Substituents (R)	λ_{max} (nm)
26	H	323
27	4-CH_3	334
28	4-OMe	354
29	4-$N(CH_3)_2$	421
30	F	324
31	Cl	328
32	Br	329

Table 2: UV-Vis data for bis-chalcones

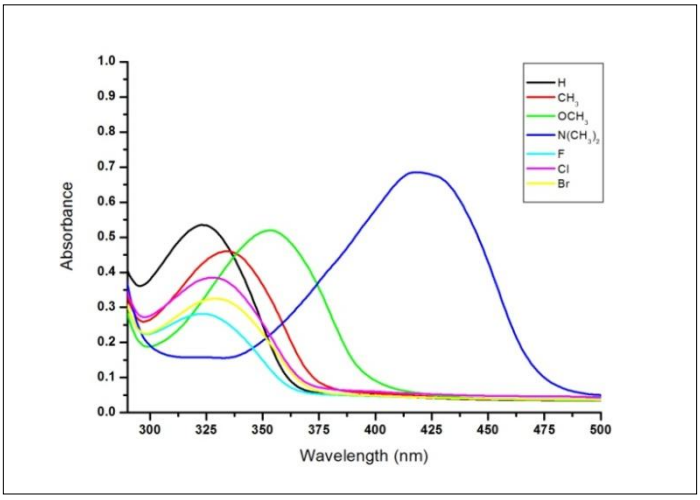

Figure 8: UV-Visible absorption of compound **26**-**32** in THF

Visual response of *2,6-bis-(4-methoxybenzylidene)cyclohexanone* 28 and *2,6-bis-(4-N,N-dimethylaminobenzylidene)cyclohexanone* 29 to H^+

It was observed that 2,5-bis-(4-methoxybenzylidene)cyclohexanone **28** and 2,6-bis-(4-N,N-dimethylaminobenzylidene)cyclohexanone **29** showed acidochromic behaviour. In presence of protic acid a clear colour change from yellow to red [**Figure 8**] was observed for the compound **28** but the compound **29** showed colour change from yellow to colourless [**Figure 9**].

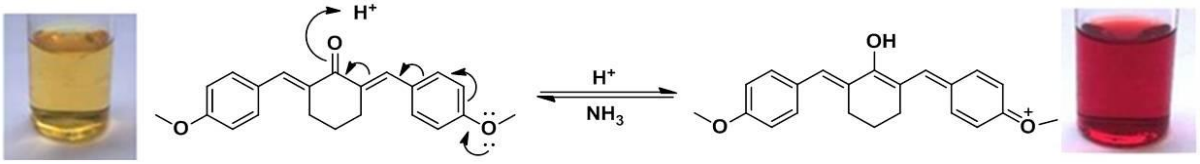

Figure 8: Response of compound **28** with Acid

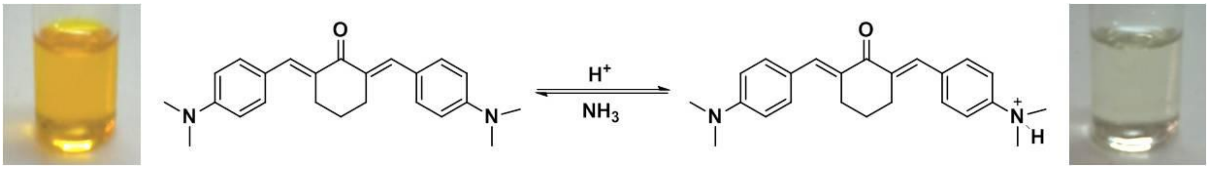

Figure 9: Response of compound **29** with Acid

On neutralizing the acidified solutions with aqueous NH_3, the original colour of compound **28** and **29** was restored, indicating the reversibility of the process. The phenomenon of pH dependence was systematically studied by varying the ratio of acid to compound. The effect of variable ratio was studied by treating the solution of **28** in acetonitrile (0.01 M) with equimolar solution of p-TSA in the same solvent and as a result a gradual red shift was observed, which in turn can be used for determination of pH [**Figure 10**].

A = only 28	B = 28 + 0.15 eq. p-TSA	C = 28 + 0.25 eq. p-TSA	D = 28 + 0.50 eq. p-TSA	E = 28 + 1.00 eq. p-TSA

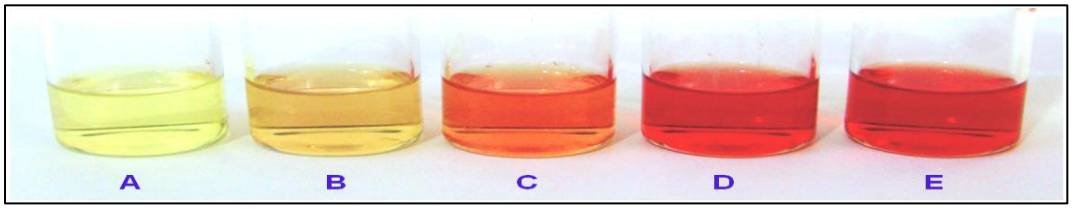

Figure 10: Compound **28** with varying concentration of p-TSA

During solvent study of compound **28** and **29** a bathochromic shift in the absorption maxima with the increasing polarity of solvent was observed [**Table 3**]. This solvatochromism could be due to the decrease in energy of the excited state as a function of increase in solvent polarity, which is in the order: toluene < THF < DCM < MeCN < DMSO. Due to the larger dipole moment of the fluorophore in the excited state, the energy level is lowered by the reorientation or relaxation of the solvent dipoles.[31] It was observed that both compounds **28** and **29** showed largest λ_{max} in DMSO, whereas no significant change was observed in other solvents.

Table 3: Effect of solvent on UV-Visible absorption

Compound	Solvent	Absorption λ_{max}	λ_{max} after acidifying
28	Toluene	354	356
	THF	354	361
	DCM	358	361
	MeCN	354	358
	DMSO	362	367
29	Toluene	416	328
	THF	421	319
	DCM	434	319
	MeCN	430	318
	DMSO	444	323

UV-Visible titration of *2,6-bis-(4-methoxybenzylidene)cyclohexanone* 28 and *2,6-bis-(4-N,N-dimethylaminobenzylidene)cyclohexanone* 29 with HCl in THF

The pH dependent behaviour was further studied by UV-Visible titration. In case of **28**, addition of HCl showed a marginal bathochromic shift from 354 to 361 nm [**Figure 11**]. But a considerable hypsochromic shift from 421 to 319 nm was seen in the case of **29**. The bathochromic shift in **28** could possibly be explained on the basis of initial protonation of the carbonyl oxygen, which may lead to the formation of the quinonoid structure. This postulated quinonoid form **28a** with a conjugation of fourteen atoms might be stabilized by an internal charge transfer (ICT) assisted by the lone pair of methoxy as shown in **Figure 8**.

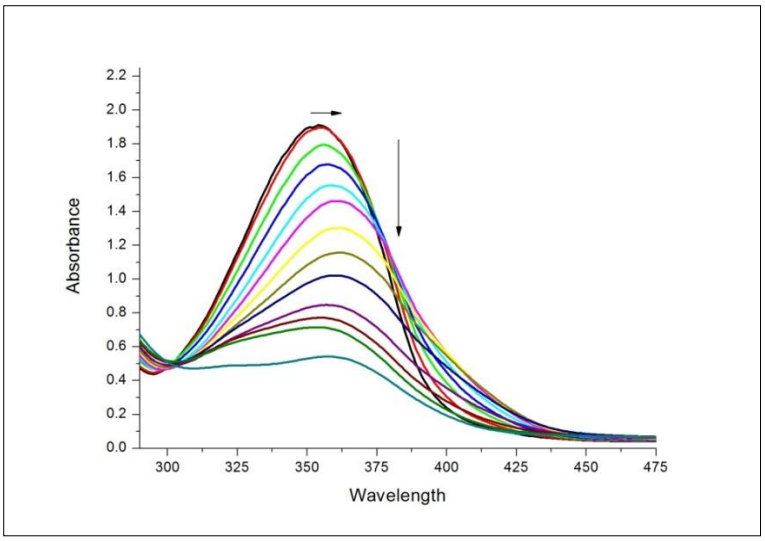

Figure 11: UV-Visible titration of compound **28** with HCl in THF

The considerable hypsochromic shift from 421 to 319 nm in case of compound 2,6-bis-(4-N,N-dimethylaminobenzylidene)cyclohexanone **29** can be attributed to the preferential protonation of chromophoric *N*,*N*-dimethyl group, owing to its more basic nature, and resulting into quaternary salt formation. This quaternary system makes the ring strongly deactivated, resulting in the observed shift to 319 nm [**Figure 12**].

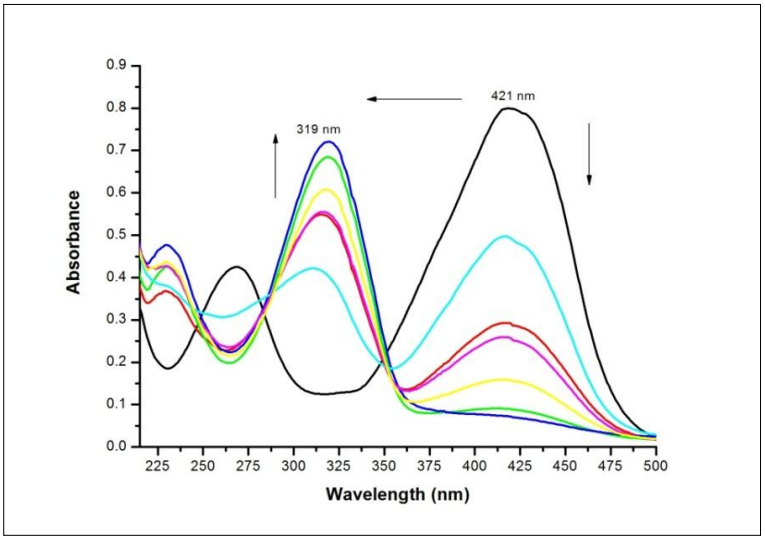

Figure 12: UV-Visible titration of compound **29** with HCl in THF

Similar study was performed by treating 2,6-bis-(4-methoxybenzylidene)cyclohexanone **28** with different mineral and organic acids. The former class of acids were strong enough to bring a noticeable change, but the later class was not as effective to induce colour change. This suggested the need of strongly acidic condition for the proposed protonation for the visual change in colour. **Figure 13** shows colour change of **28** in presence of different acids at a 1:1 mole ratio: Blank (vial-1), 4-chloro-3,5-dinitro benzoic acid (vial-

2), *m*-chlorobenzoic acid (vial-3), *o*-nitro benzoic acid (vial-4), p-TSA (vial-5), H_2SO_4 (vial-6), and HCl (vial-7) [**Figure 13**].

Figure 13: Response of compound **28** with different acids

Visual response of *2,6-bis-(4-methoxybenzylidene)cyclohexanone* 28 with different metal ions

Compound **28** was further investigated for its complexation with different metal ions as detected by visual colour change. Solution of **28** in acetonitrile was mixed with equimolar solutions of different metal ions and the following results were obtained [**Figure 14**]

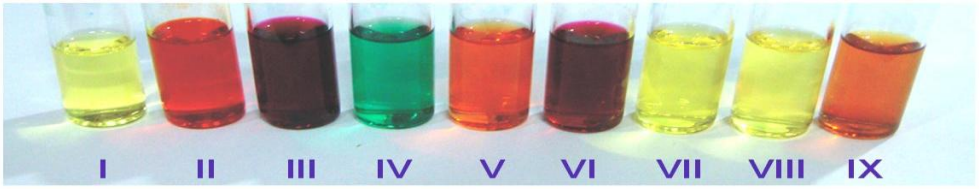

Figure 14: Response of compound **28** with different metal ions

The colour of compound **28** in presence of different metal salts in a 1:1 mole ratio was studied [**Figure 14]**: blank **28** (vial-I), $Sc(OTf)_3$ (vial-II), $FeCl_3$ (vial-III), $CoCl_2$ (vial-IV), $CuCl_2$ (vial-V), $Cu(OTf)_2$ (vial-VI), $ZnCl_2$ (vial-VII), $HgCl_2$ (vial-VIII), $PdCl_2$ (vial-IX). A variation in colours with different metal ions was observed. It was seen that $CuCl_2$ (vial-V) gave orange colour whereas $Cu(OTf)_2$ (vial-VI) gave deep pink colour suggesting the effect of counter ion in the colour change. Moreover the later is much stronger Lewis acid and may contribute strongly towards the interaction with **28** resulting into deep coloration (vial-VI).

In summary, seven substituted bis-chalcone derivatives were synthesized by solvent free methodology and substituent effect on absorption pattern was studied. Bis-chalcones **28** and **29** showed visually reversible response to the acid which was systematically studied by UV-Visible spectroscopy. Internal charge transfer in case of **28** was shown to be responsible for reversible acidochromism. These compounds can be used for the synthesis of pH sensitive probes.

Experimental Section (Section 3.2.2)

General Procedure for the preparation of α,α'-bis-(substituted-benzylidene)cyclohexanone

A mixture of cyclohexanone (1 eq.), substituted benzaldehyde (2 eq.) and solid NaOH (2.2 eq.) was ground in a mortar and pestle for 10 minutes at room temperature and then the reaction mixture was poured in to dilute HCl (2 N), separated solid material was filtered and dried. The solid obtained was recrystallized from petroleum ether and ethyl acetate mixture.

***2,6-bis-(benzylidene)cyclohexanone* (26)**

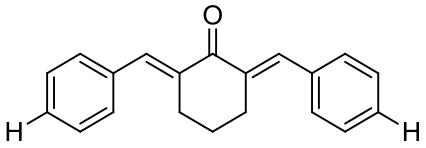

Compound **26** was synthesized from cyclohexanone and benzaldehyde, as per the above procedure. Yield: 93%, Yellow solid; Melting point: 116°C (117°C)[25]

^{1}H-NMR (400 MHz, $CDCl_3$) δ 7.83 (s, 2H), 7.51-7.33 (m, 10H), 2.98-2.92 (m, 4H), 1.85-1.78 (m, 2H).

MS (EI) m/z (%): M^+274(78), 273(100), 217(20), 114(41).

IR (KBr): υ 3023, 2929 ,2355 , 1954, 1811, 1684 , 1660 , 1605 , 1487 , 1440 , 1317 , 1274 , 1204 , 1140 , 1070 , 1030 , 968 $cm.^{-1}$

***2,6-bis-(4-methylbenzylidene)cyclohexanone* (27)**

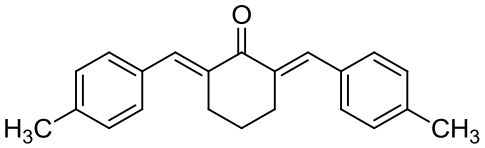

Compound **27** was synthesized from cyclohexanone and 4-methyl benzaldehyde, as per the above procedure. Yield: 88%, Yellow solid, Melting point: 157°C (162-163°C)[26]

^{1}H-NMR (400 MHz, $CDCl_3$) δ 7.80 (s, 2H), 7.42-7.39 (d, J = 8 Hz, 4H), 7.25-7.23 (d, J = 8 Hz, 4H), 2.95-2.91 (m, 4H), 2.40 (s, 6H), 1.84-1.78 (m, 2H).

MS (EI) m/z (%): M^+ 302 (37), 301(39), 287(100), 115(25).

IR (KBr): υ 3025, 2916, 2862, 1788, 1659, 1599, 1506, 1410, 1311, 1268, 1197, 1154, 956, 819 cm^{-1}

2*,6-bis-(4-methoxybenzylidene)cyclohexanone* (28)

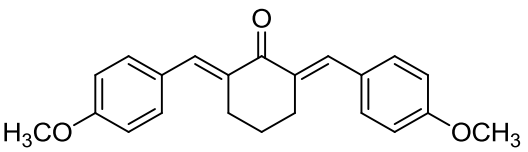

Compound **28** was synthesized from cyclohexanone and 4-methoxy benzaldehyde, as per the above procedure. Yield: 82%, Yellow solid; Melting point: 200°C (204°C)[26]

^{1}H-NMR (400 MHz, $CDCl_3$) δ 7.79 (s, 2H), 7.49-7.47 (d, *J* = 8.8 Hz, 4H), 6.97-6.95(d, *J* = 8.8 Hz, 4H), 2.96-2.93 (m, 4H), 1.86-1.79 (m, 2H).

MS (EI) m/z (%): M^+334 (100), 333 (79), 303 (25), 275 (28), 115 (28).

IR (KBr): υ 3200, 2827, 2364, 1656, 1594, 1503, 1415, 1308, 1247, 1138, 829 cm^{-1}

***2,6-bis-(4-N,N-dimethylaminobenzylidene)cyclohexanone* 29**

Compound **29** was synthesized from cyclohexanone and 4-(dimetylamino) benzaldehyde as per the above procedure. Yield: 74%, Yellow solid; Melting point: 250-252^{o}C (250-252^{o}C)[28]

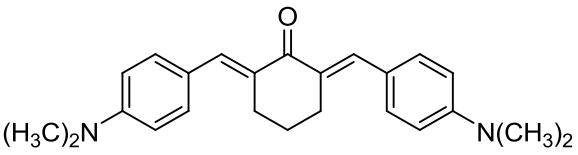

^{1}H-NMR (400 MHz, $CDCl_3$) δ 7.78 (s, 2H), 7.48-7.46 (d, *J* = 8.8 Hz, 4H), 6.75-6.72 (d, *J* = 8.8 Hz, 4H), 3.04 (s, 12H), 2.97-2.94 (m, 4H), 1.86-1.80 (quin, *J* = 6.4 Hz, 2H).

MS (EI) m/z (%): M^+360 (76), 359 (24), 358 (100), 331 (19), 303 (16).

IR (KBr): υ 2830, 1643, 1610, 1573, 1516, 1429, 1359, 1282, 1222, 1191, 1160, 1063, 959, 867, 817 cm^{-1}

***2,6-bis-(4-fluorobenzylidene)cyclohexanone* 30**

Compound **30** was synthesized with cyclohexanone and p-fluoro benzaldehyde as per the above procedure. Yield: 89%, Yellow solid; Melting point: 150^{o}C (156^{o}C)[30]

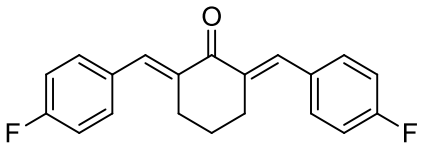

^{1}H-NMR (400 MHz, $CDCl_3$): δ 7.77 (s, 2H), 7.49-7.46 (m, 4H), 7.14-7.10 (t, *J* = 8.2 Hz, 4H), 2.94-2.90 (m, 4H), 1.86-1.80 (quin, *J* = 6.4 Hz, 2H).

MS (EI) m/z (%): M^+310 (35), 309 (100), 253 (16).

IR (KBr): υ 3064, 2954, 2932, 2870, 1661, 1593, 1498, 1409, 1306, 1268, 1221, 1147, 1010, 961, 842 cm^{-1}

***2,6-bis-(4-chlorobenzylidene)cyclohexanone* 31**

Compound **31** was synthesized with cyclohexanone and *p*-chloro benzaldehyde as per the above procedure. Yield: 84%, Yellow solid; Melting point: 144^{o}C (149-151^{o}C)[29]

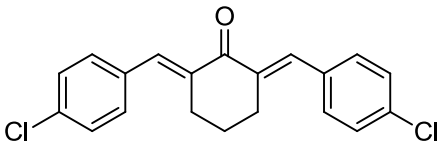

^{1}H-NMR (400 MHz, $CDCl_3$) δ 7.75 (s, 2H), 7.43-7.39 (m, 8H), 2.93-2.90 (m, 4H), 1.86-1.79 (quin, *J* = 6.4 Hz, 2H).

MS (EI) m/z (%): M^+343 (77), 342 (59), 340 (100), 306 (67), 278 (52), 250 (15).

IR (KBr): υ 3061, 2938, 2872, 1912, 1666, 1579, 1483, 1401, 1300, 1261, 1146, 1087, 1003, 829 cm^{-1}

***2,6-bis-(4-bromobenzylidene)cyclohexanone* 32**

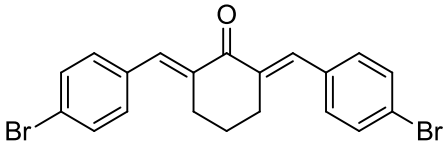

Compound **32** was synthesized with cyclohexanone and p-chloro benzaldehyde as per the above procedure. Yield: 85%, Yellow solid; Melting point: 160-164^oC (165-168^oC)[27]

^{1}H-NMR (400 MHz, $CDCl_3$) δ 7.69 (s, 2H), 7.54-7.49 (d, *J* = 10Hz, 4H), 7.32-7.28 (d, *J* = 8Hz, 4H), 2.90-2.82 (m, 4H), 1.84-1.72 (quin, *J* = 6Hz, 2H).

MS (EI) m/z (%): M^+ 433 (33), 432 (39), 431 (72), 430 (67), 352 (93), 350 (98), 244 (100), 115 (97).

IR (KBr**)**: υ 2924, 1661, 1600, 1479, 1395, 1300, 1267, 1155, 1135, 1068, 822, 730 cm.$^{-1}$

Spectral Data for symmetrical Cyclohexanone derived Bis-chalcone (Section 3.2.2)

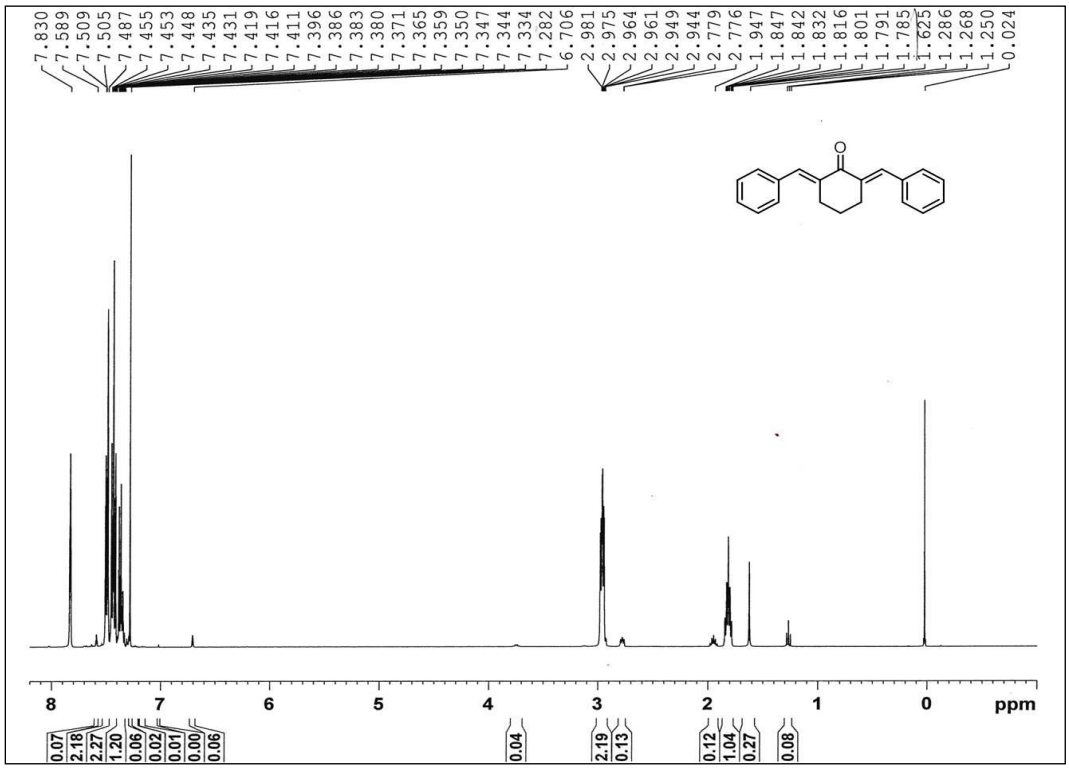

^{1}H-NMR of compound 26

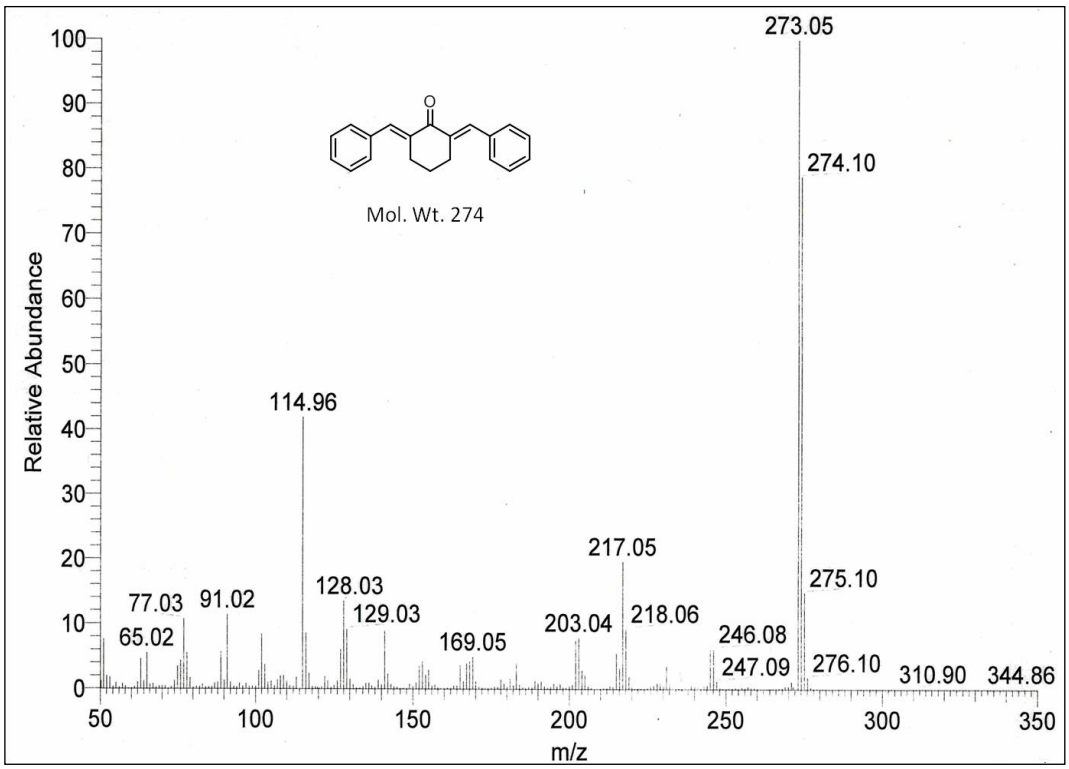

Mass spectra of compound 26

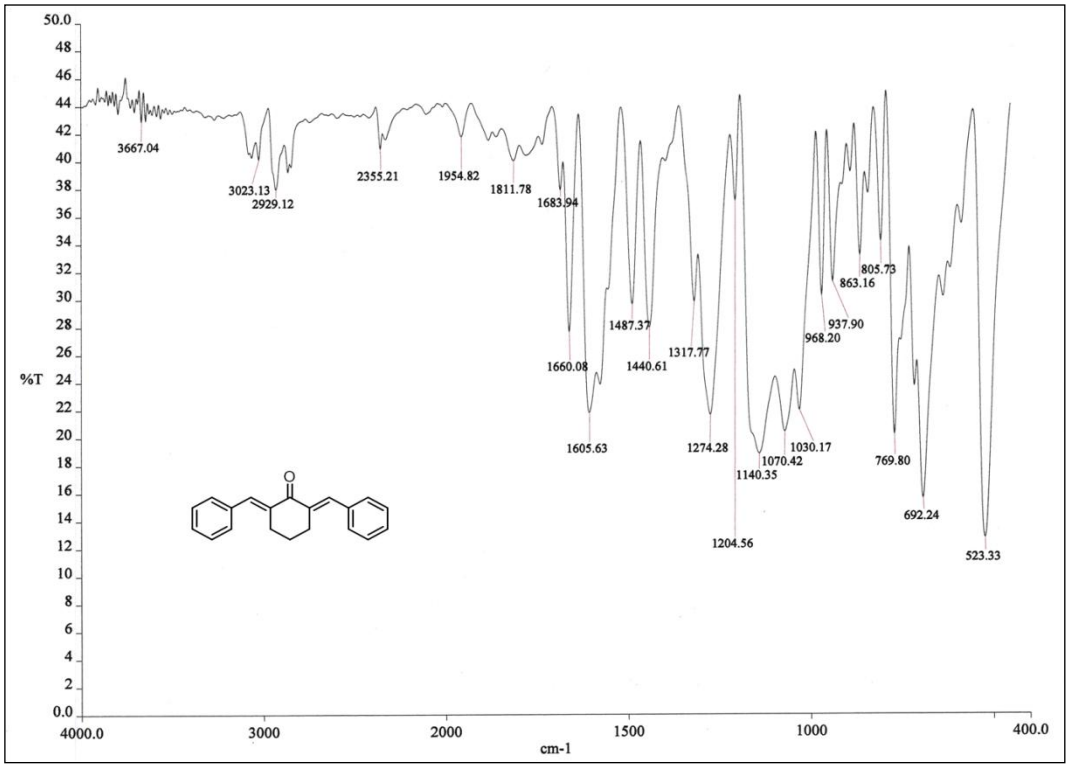

IR spectra of compound 26

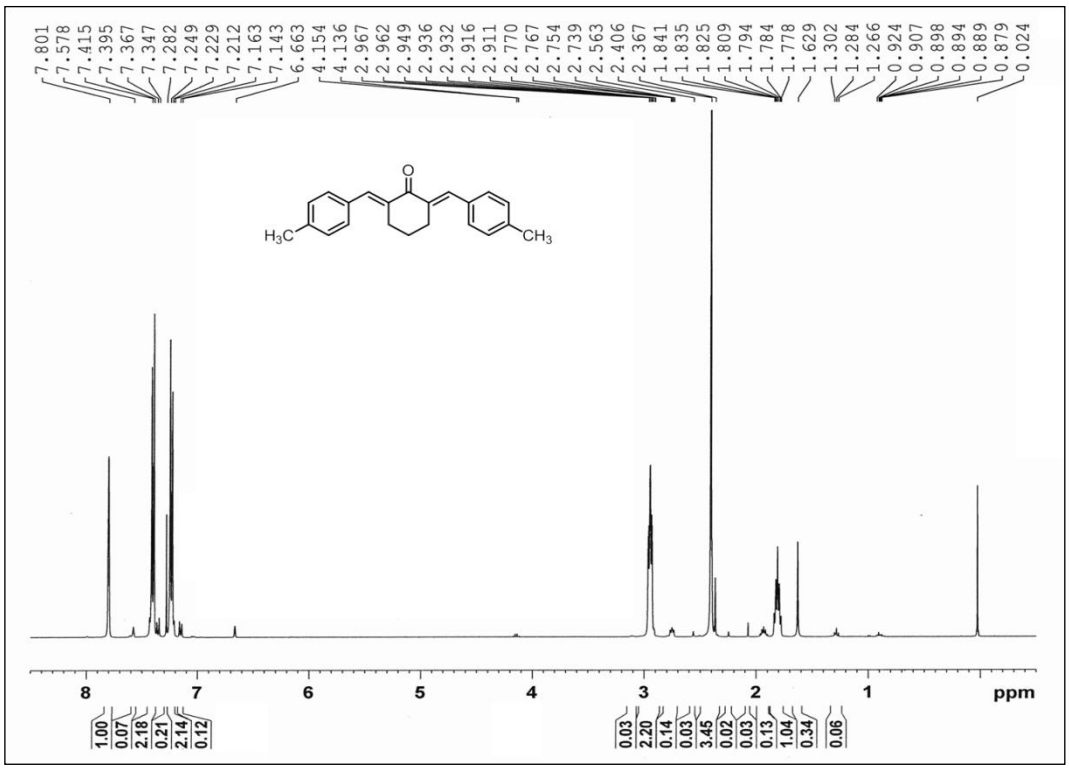

^{1}H-NMR of compound 27

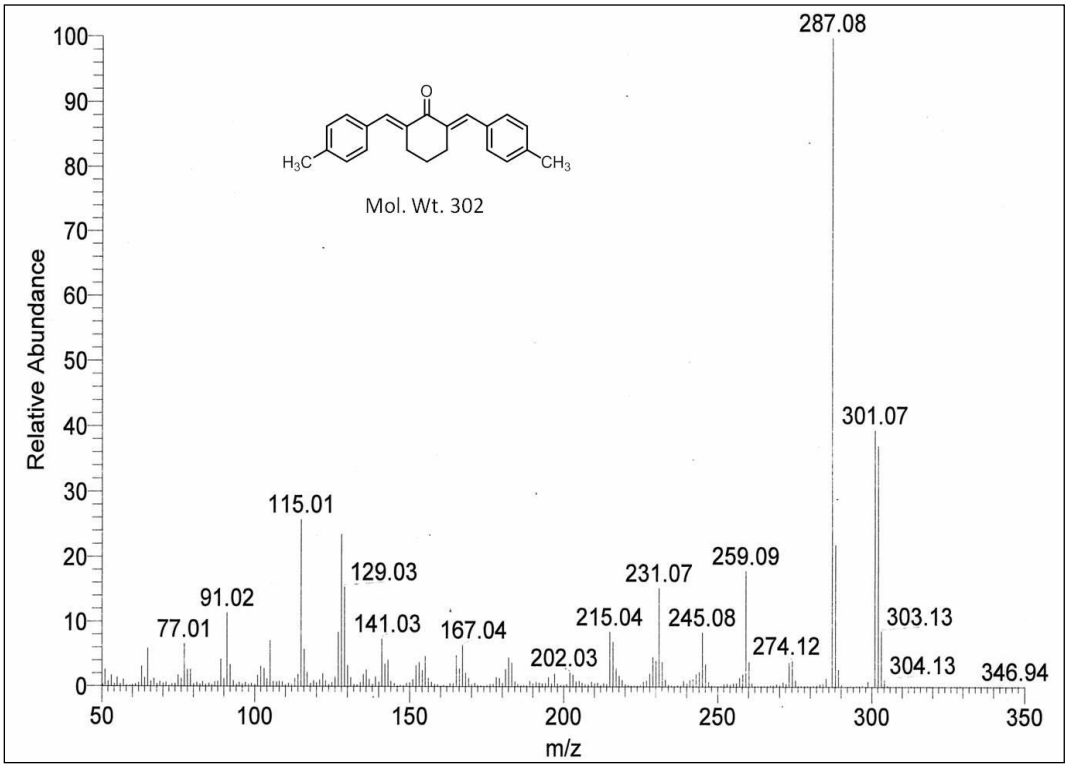

Mass spectra of compound 27

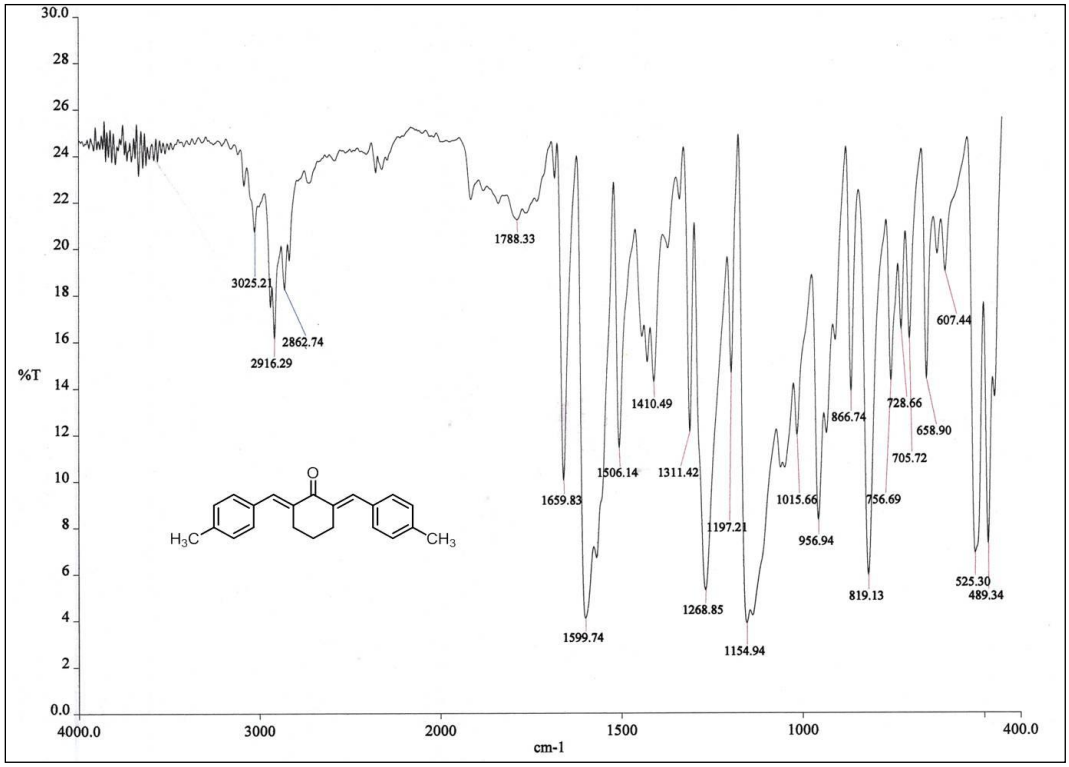

IR spectra of compound 27

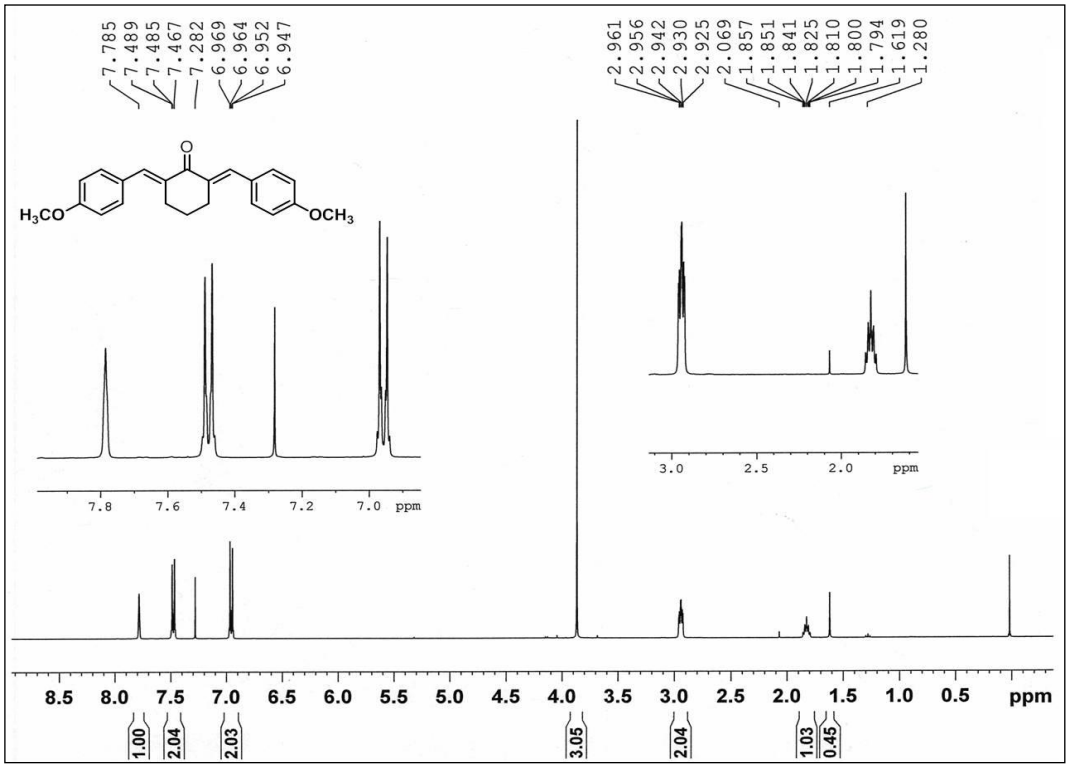

^{1}H-NMR of compound 28

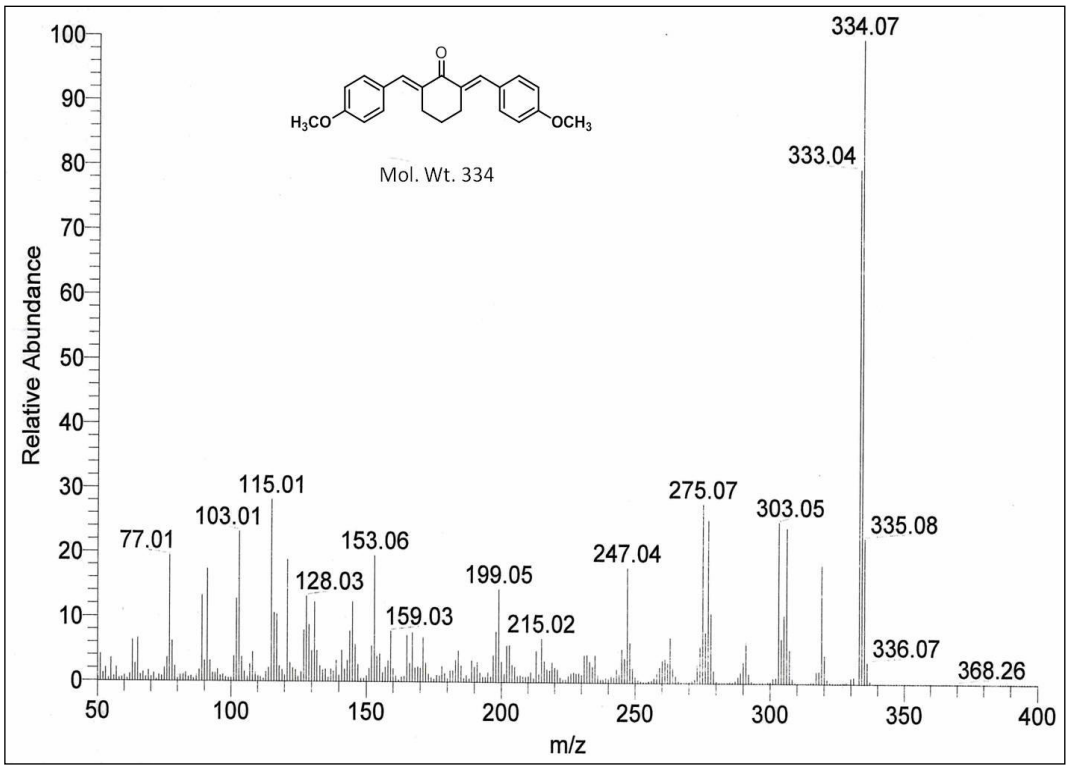

Mass spectra of compound 28

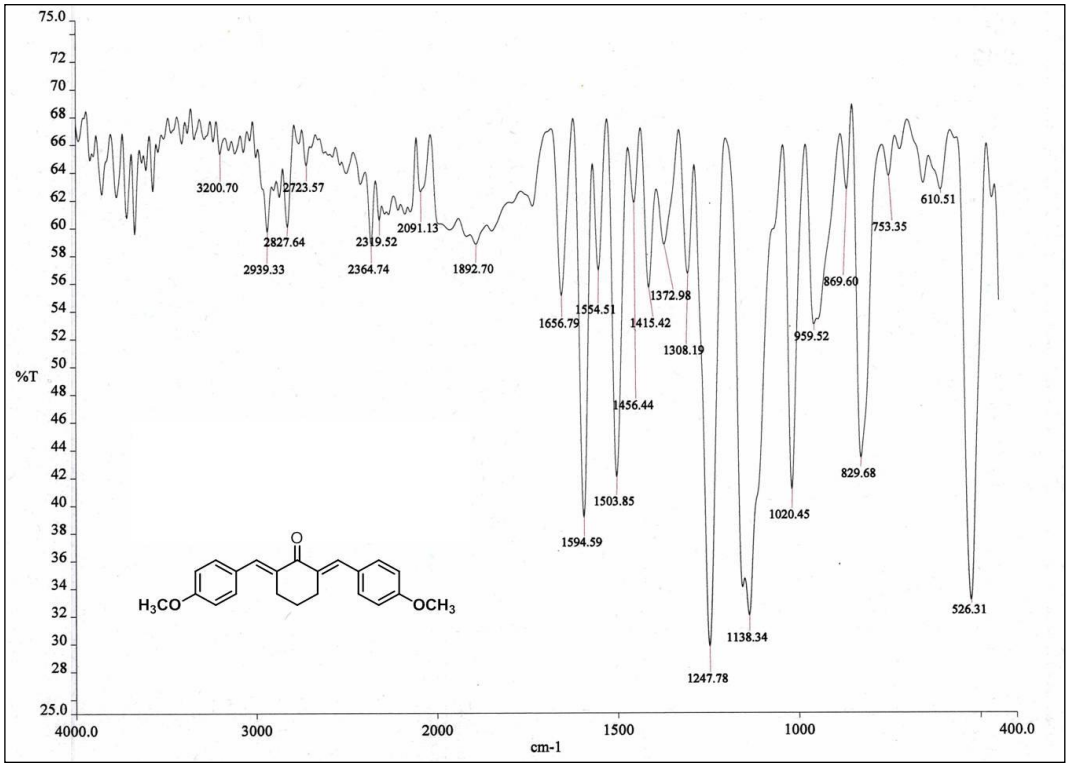

IR spectra of compound 28

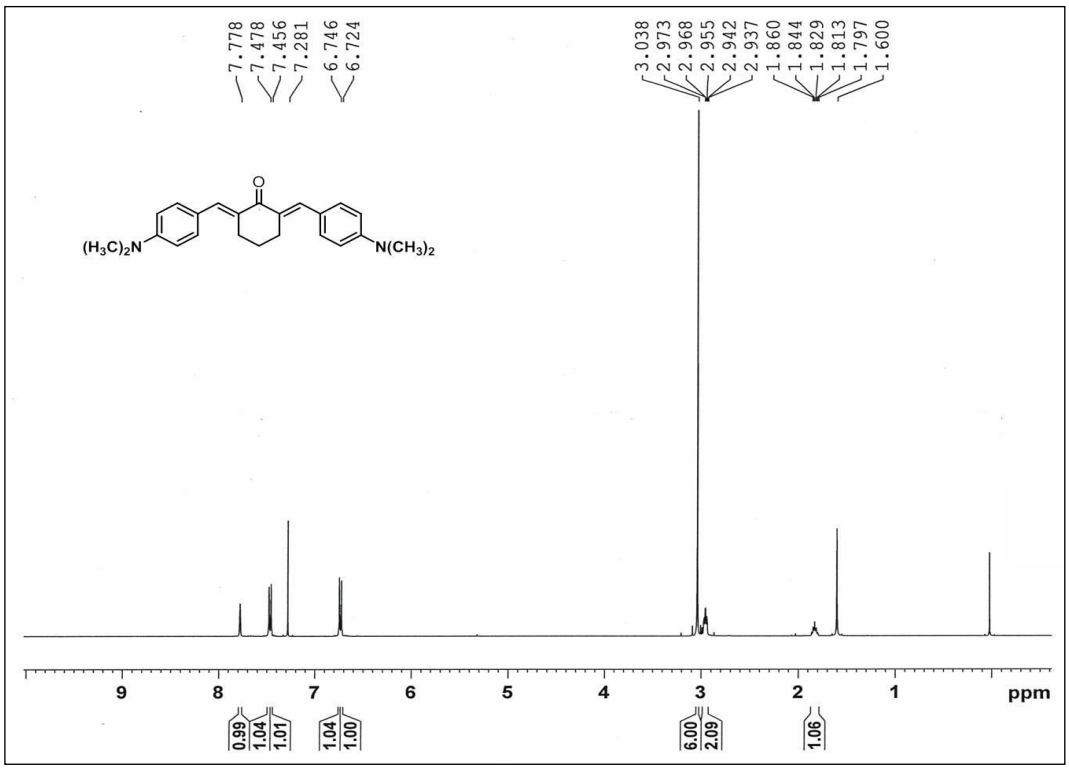

^{1}H-NMR of compound 29

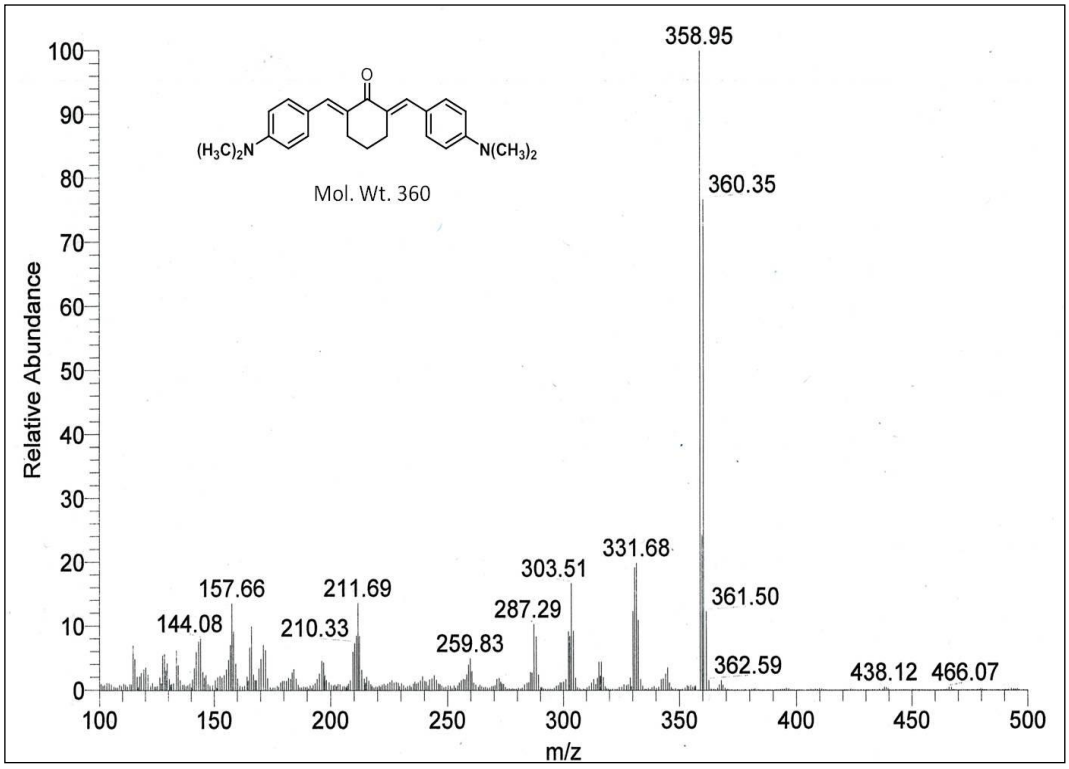

Mass spectra of compound 29

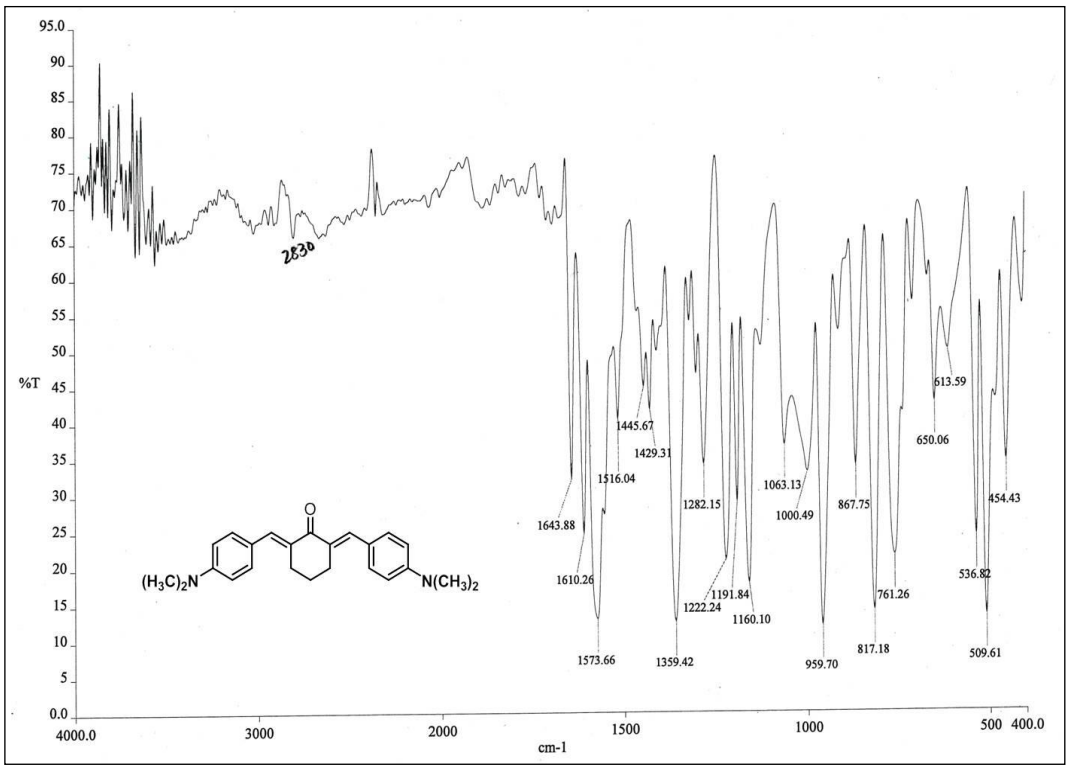

IR spectra of compound 29

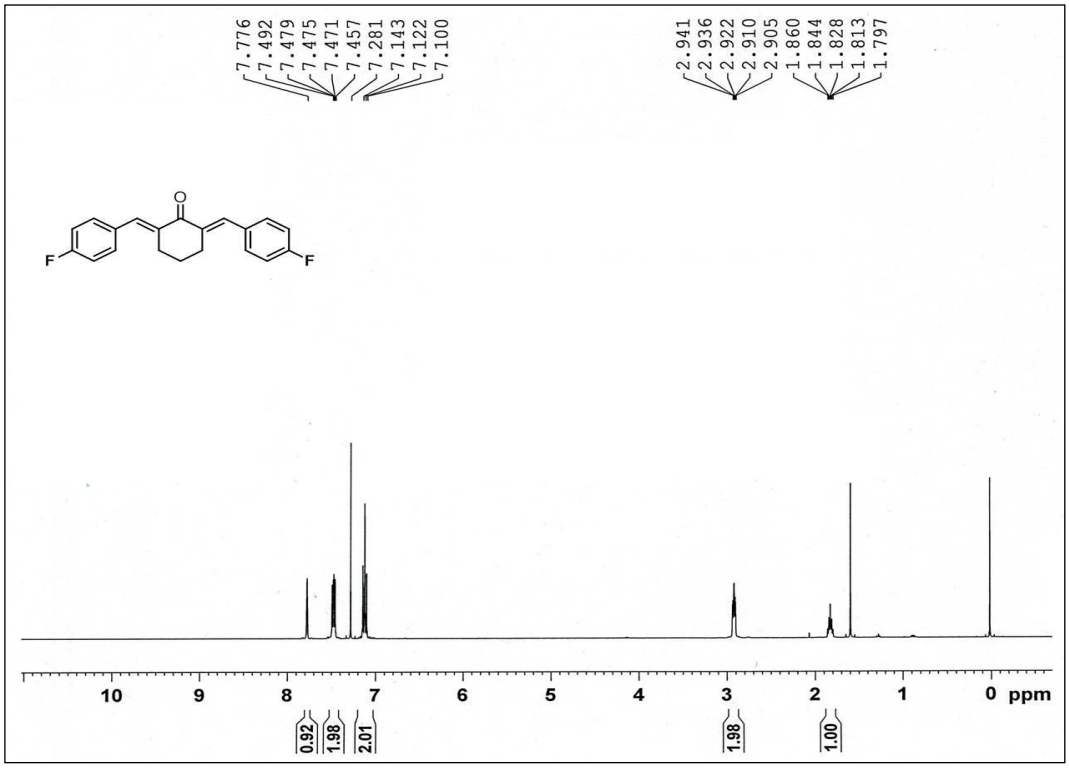

^{1}H-NMR of compound 30

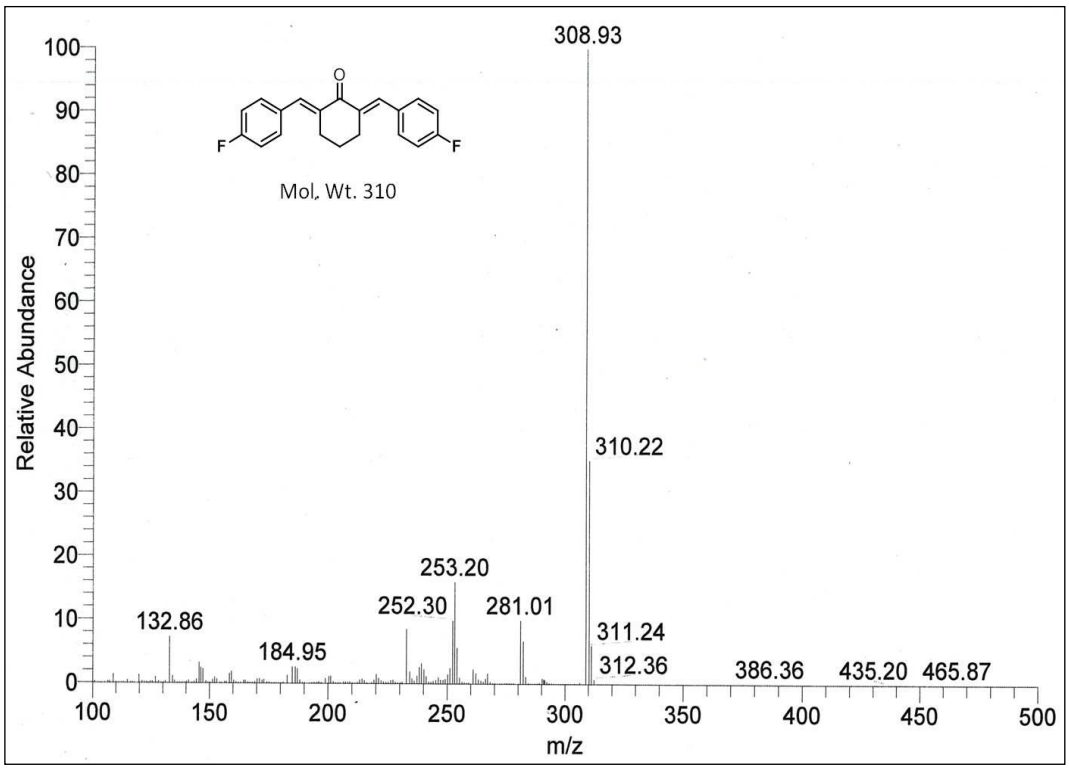

Mass spectra of compound 30

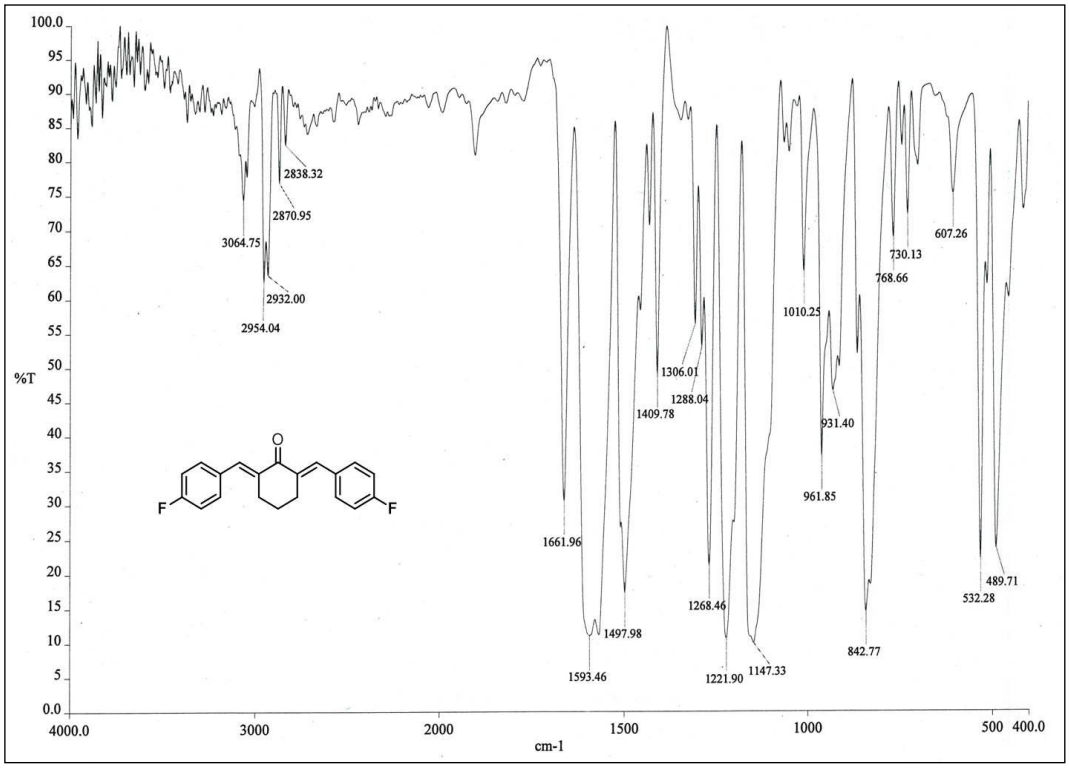

IR spectra of compound 30

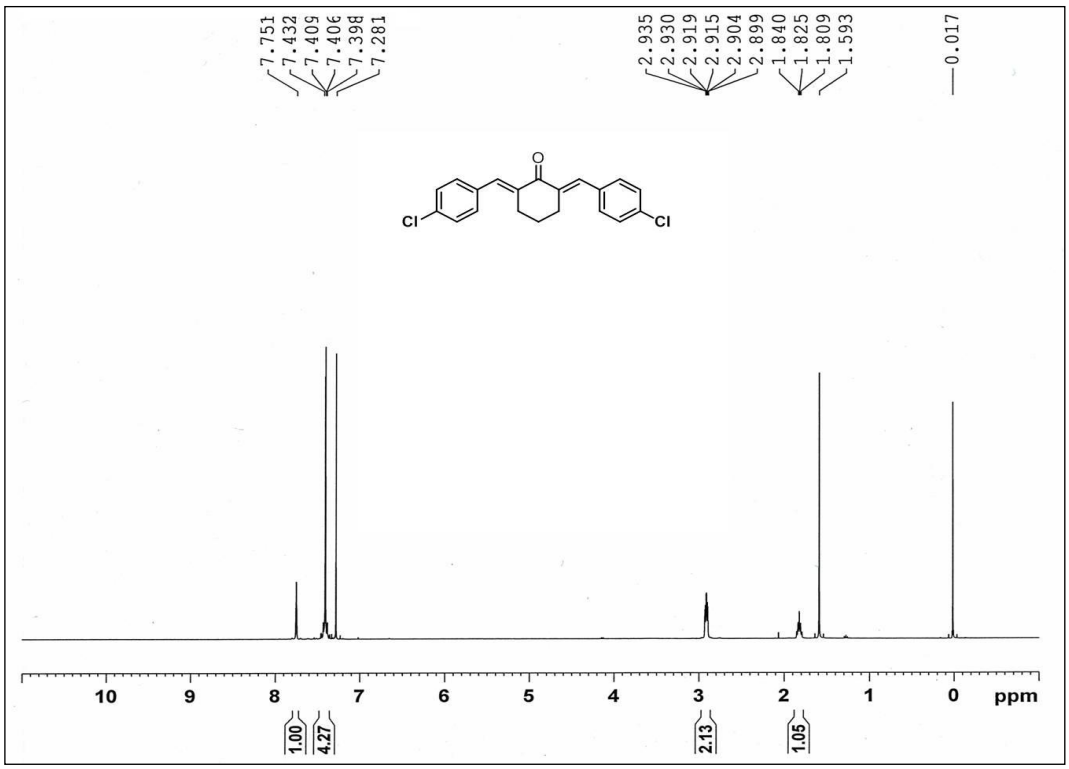

^{1}H-NMR of compound 31

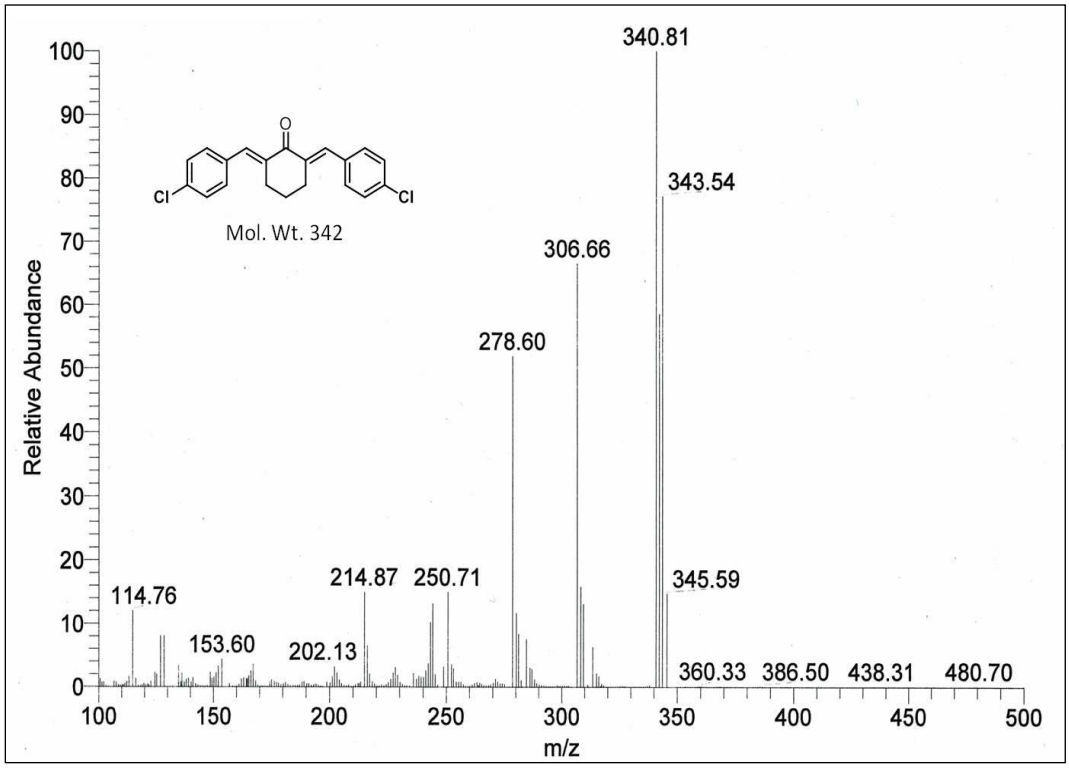

Mass spectra of compound 31

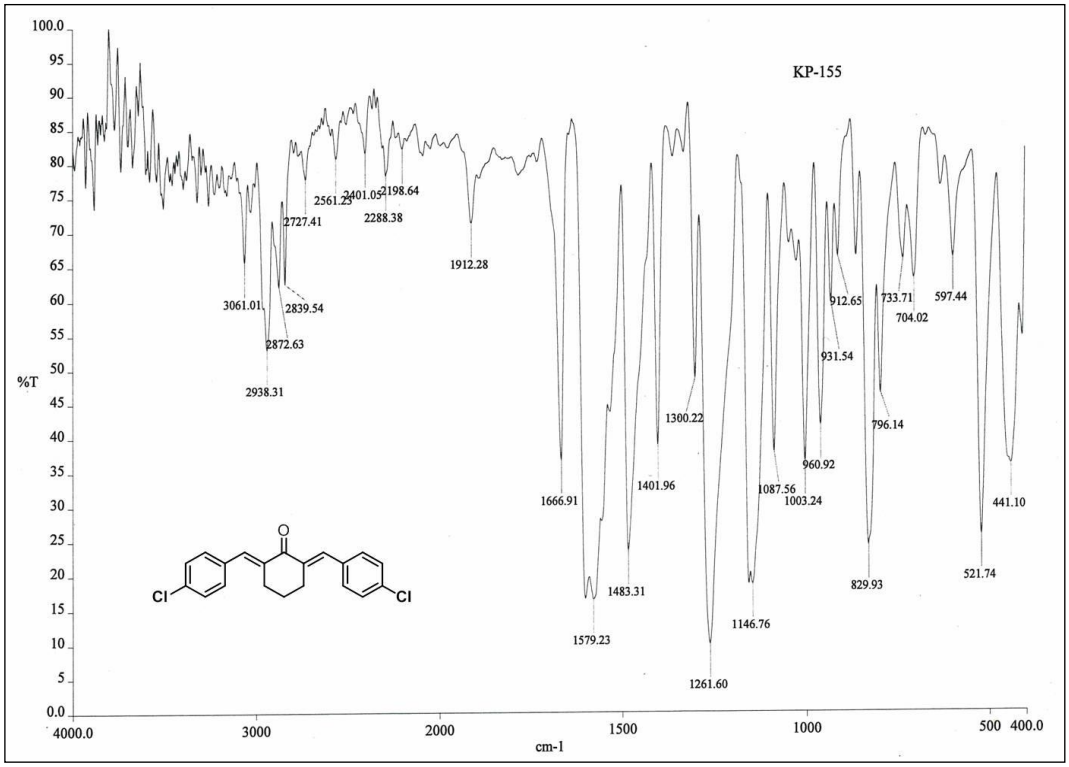

IR spectra of compound 31

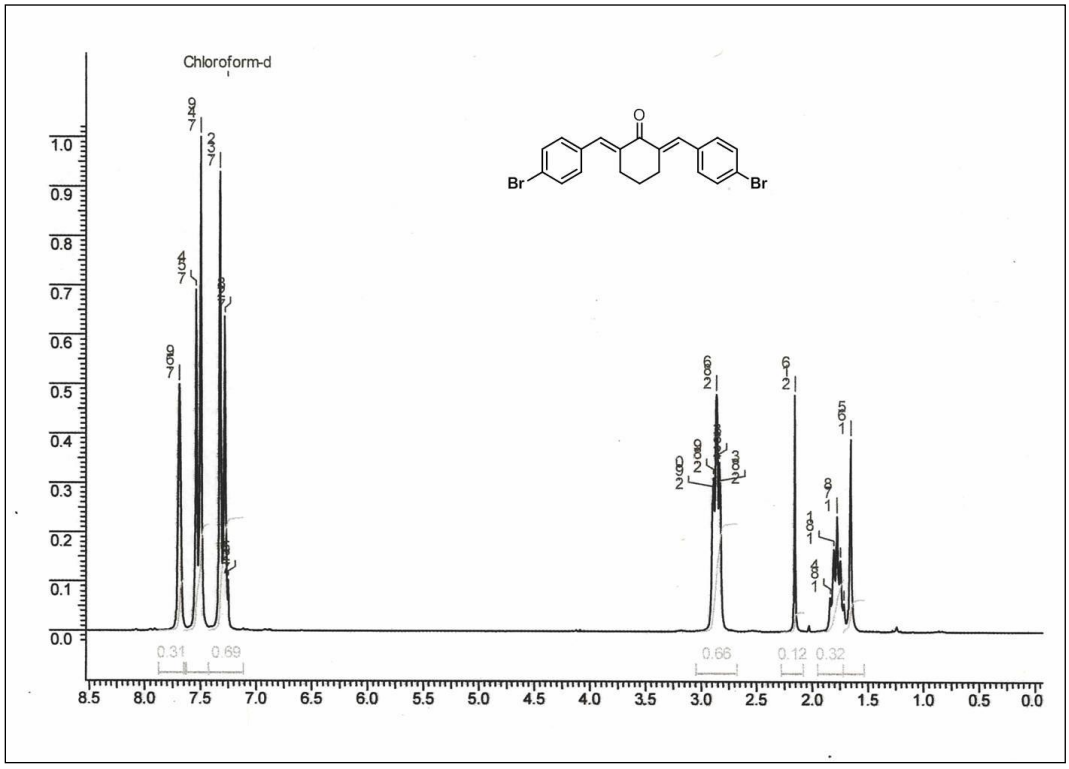

^{1}H-NMR of compound 32

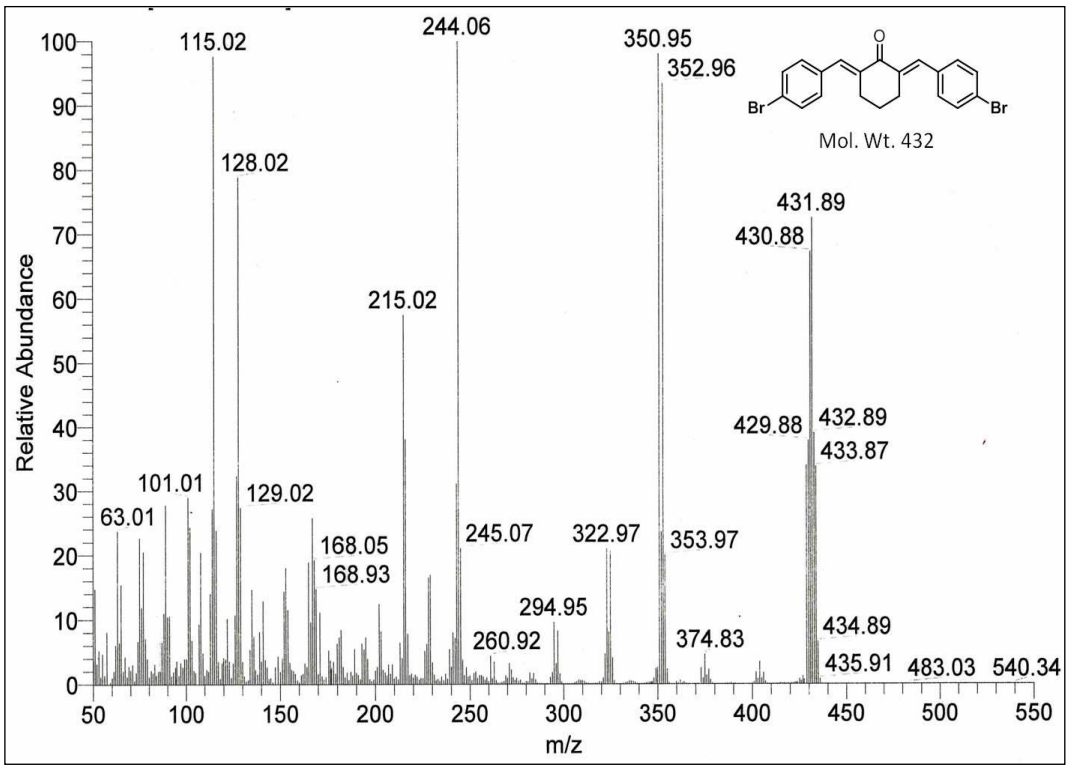

Mass spectra of compound 32

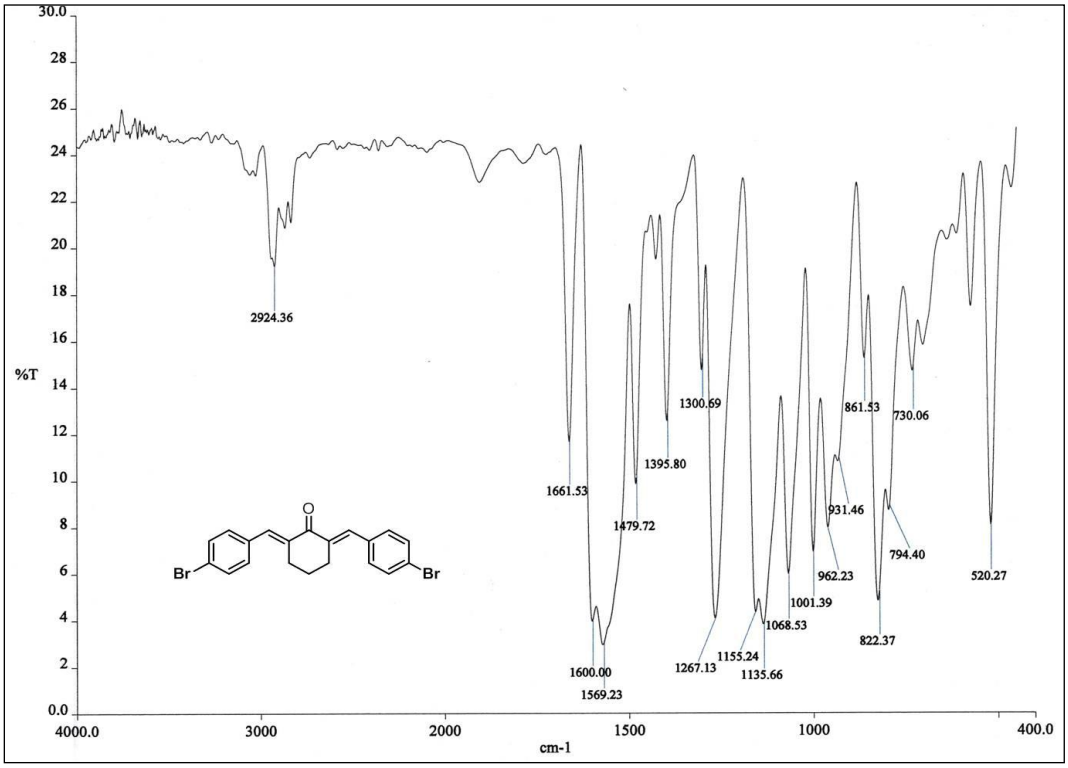

IR spectra of compound 32

3.2.3 Synthesis and mesomorphic properties of unsymmetrical Cyclohexanone derived Bis-chalcones

In the third part of the chapter, we will be presenting the synthesis of unsymmetrical cyclohexanone derived bis-chalcones and its liquid crystalline properties. Design, synthesis and study of organic molecules with specific applications is an important aspect of modern chemistry. Liquid crystalline compounds are one such class of materials which has triggered massive research activity and has resulted in commercial development of many materials of interesting applications. Liquid crystals (LC) are recognized as orientationally ordered fluids formed by shape-anisotropic organic molecules.[32,33] They are matter in a state that has properties between those of conventional liquid and of solid crystal, i.e. liquid crystal may flow like a liquid, but its molecules may be oriented in a crystal-like way. In 1888, Austrian botanical physiologist Friedrich Reinitzer first examined the physico-chemical properties of various derivatives of cholesterol which now belong to the class of materials known as cholesteric liquid crystals.

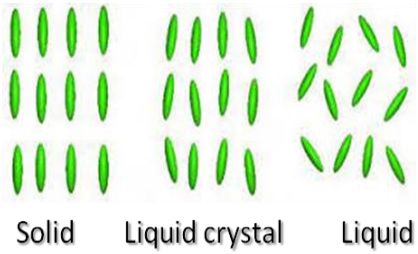

Reinitzer described three important features of liquid crystalline materials which are as follows:

1. *existence of two melting points*
2. *reflection of circularly polarized light*
3. *ability to rotate the polarization direction of light*

For many years aromatic compounds based on benzene, biphenyl or terphenyl core unit were the most commonly studied liquids crystals, partly because of their easy synthesis and partly due to the link between highly polarizable π-electron system and over emphasized mesogenicity.[34-36] As a result of further study, it became clear that saturated systems are also excellent units when placed appropriately in relation to other planer or high polarizable moieties. In some cases the entire saturated systems are also key for this behavior. Examples of such type of mesogenic, non-aromatic structures include *trans*-1,4-disubstituted cyclohexanes and 1,4-disubstituted bicyclo[2.2.2]octanes.[37,38] The presence of slightly flexible cyclohexane based core offers a possibility of introducing an element of mobility in these compounds. From the available literature on different types of liquid crystalline compounds such type of compounds are scarcely known to show mesogenicity. This includes an early report on 2,5-bis(4-methoxybenzylidene)cyclopentanone and 2,6-bis(4-methoxybenzylidene)cyclohexanone and their mesogenic property, though without much details about the transition

temperatures.[39,40] More recently Matsunaga and Miyamoto[41] have reported synthesis and systematic study of the mesogenic property of symmetrically substituted derivatives of cyclic ketones. A series of alkoxy derivatives **34** of the basic compound **33** were reported with the details of the comparison of their mesogenic properties. Structurally similar liquid crystalline copolyarylidene ethers derived from 4-methyl cyclohexanones and 4-*tert*-butyl cyclohexanone[42] along with poly(azomethine ether)s[43] were also reported. In the present work we propose to modify the cyclohexanone based compounds and prepare unsymmetrical derivatives of the type **35**, where we expect the crystal packing to be different than the symmetrical compounds **34**. We present the synthesis of a series of such compounds, study of their crystal packing and phase transition behavior.

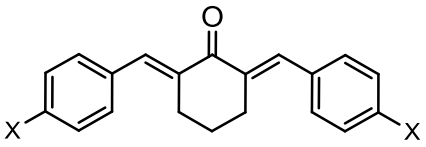

33, X = H
34, X = OR (R = C_1 to C_{10}, C_{12}, C_{14} & C_{16})

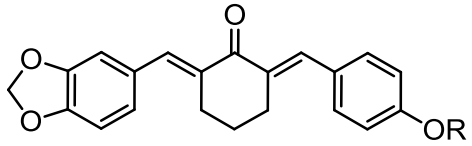

35, R = C_4, C_6,C_7, C_8, C_{10}, C_{12}, C_{14} & C_{16}

The design of the chalcone derivative **35** involves introduction of a benzo[1,3]dioxolyl unit as structurally flat component in the unsymmetrical molecule. This bis-chalcone units can be introduced by base mediated stepwise condensation reaction of cylohexanone, first with piperonal followed by 4-alkoxy benzaldehyde.

Result and Discussion

Synthesis of the title compound **35** is outlined in **Scheme 7**, where mono chalcone **38** of cyclohexanone **36** and piperonal **37** was prepared by base mediated condensation reaction. The intermediate mono chalcone **38** was separated and purified. The chalcone **38** was then subjected to second condensation reaction with appropriate 4-alkoxy benzaldehyde **39a-39h** with methanolic sodium hydroxide at slightly elevated temperature. The unsymmetrical bis-chalcones, **35a - 35h**, were isolated in good yields and were fully characterized.

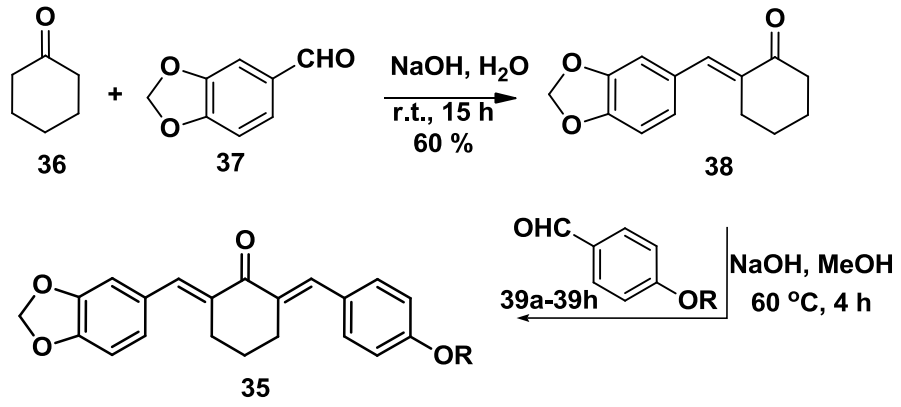

35a, R = C_4H_9 (83 %); **35b**, R = C_6H_{13} (78 %); **35c**, R = C_7H_{15} (75 %);
35d, R = C_8H_{17} (84 %); **35e**, R = $C_{10}H_{21}$ (78 %); **35f**, R = $C_{12}H_{25}$ (74 %);
35g, R = $C_{14}H_{29}$ (70 %); **35h**, R = $C_{16}H_{33}$ (62 %)

Scheme 7: Synthesis of the title compound **35**, by stepwise double condensation

One of the compounds **35d**, with octyloxy substituent was further studied by single crystal X-ray diffraction analysis.[44] The crystal packing indicated the presence of two molecules in the unit cell arranged in opposite way in a head-tail manner [**Figure 15**]. The carbonyl of one cyclic ketone is showing interaction with the C-H of alkyl chain of the other molecule, while they are further held together by additional Ar-H·····H-C interaction. The interactions result in the distance at these sites to be of the order of 2.593 and 2.356 Å.

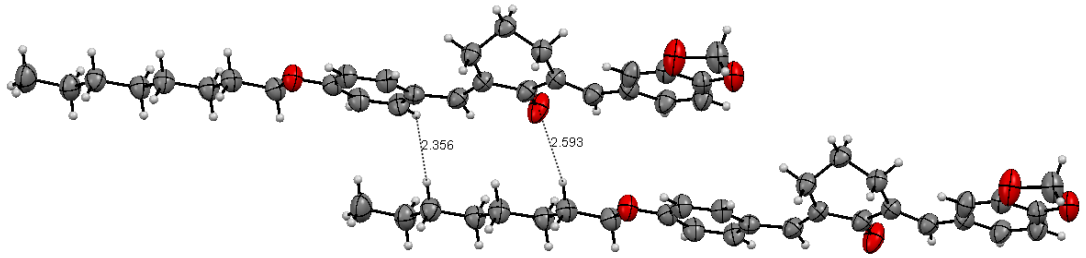

Figure 15: ORTEP diagram of **35d**.

Further it is observed that the crystal is packed in the ordered pattern where the average inter layer distance is observed to be 3.505 Å [**Figure 16**].

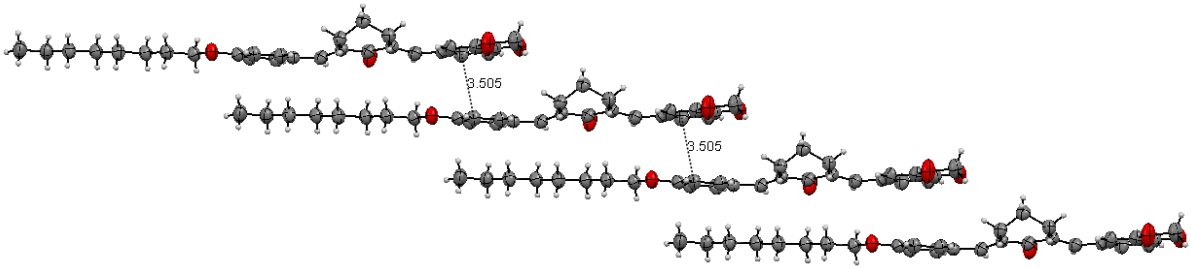

Figure 16: Crystal packing of **35d**.

The eight compounds of the series **35a** – **35h** were then evaluated for their mesogenic properties. The compounds were examined by using a polarizing optical microscope (POM). Thin film of the sample was obtained by sandwiching between a glass plate and a cover slip. Members with small alkoxy chains (**35a** n = 4 and **35b** n = 6) did not exhibit mesomorphic property. On cooling the isotropic liquids on an ordinary slide, **35c** to **35h** gave tiny spherical droplets [**Figure 17a**] which coalesced in to the Schlieren texture [**Figure 17b**], which is a characteristic of the nematic mesophase. There was no fundamental difference in the texture through all the derivatives of this series. Differential scanning calorimetry (DSC) is a valuable method for the detection of phase transition. It yields quantitative results, therefore conclusions may be drawn concerning the nature of the phases which participate in the transition. In the present study enthalpies of all the liquid crystalline unsymmetrical bis-chalcones **35c-35h** were measured by DSC (cryo-DSC model DSC 822^e, Mettler Toledo, Switzerland having Star^e software). Data is presented in **Table 4**.

Table 4: Transition temperatures (^oC) and enthalpies [J/g] of the series **35a - 35h**

Entry	Compound No	R = $C_nH_{2n+1}O$-(n)	Phase sequence	
			Heating	Cooling
1	**35a**†	4	Cr 140 Iso	Iso 121 Cr
2	**35b**†	6	Cr 125 Iso	Iso 114 Cr
3	**35c**	7	Cr 134.88 [114.86] Iso	Iso 90.43 [1.22] N 75.77 [77.03] Cr
4	**35d**	8	Cr_1 125.65 [128.31] Cr 132.15 [151.43] Iso	Iso 93.0 [1.02] N 87.43 [110.67] Cr 72.32 [105.60] Cr_1
5	**35e**	10	Cr 110.67 [92.51] Iso	Iso 90.94 [1.76] N 73.28 [77.34] Cr
6	**35f**	12	Cr 112.41 [91.93] Iso	Iso 92.43 [1.60] N 78.26 [78.54] Cr
7	**35g**	14	Cr 105.82 [89.02] Iso	Iso 92.17 [1.51] N 85.67 [84.67] Cr
8	**35h**	16	Cr_1 95.88 [4.51] Cr 108.45 [86.29] Iso	Iso 91.62 [2.49] N 80.62 [74.92] Cr

The enthalpy values are enclosed in brackets. † The phase transitions of the compounds were studied under POM only. Cr= Crystal, N= Nematic phase, Iso= isotropic liquid state.

a) b)

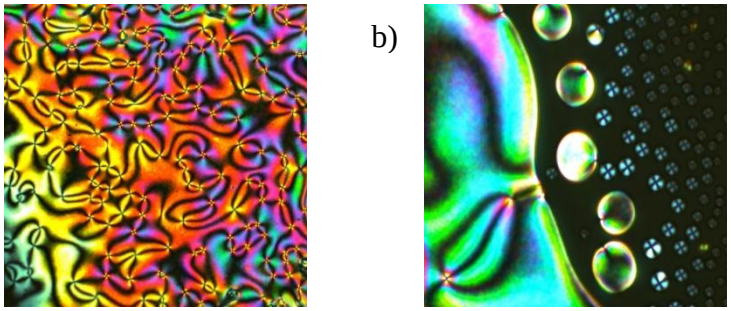

Figure 17: Optical micrographs (a) nematic droplets (Iso – N) at 92 °C [left] and (b) Schlieren texture in nematic phase at 88 °C [right] of compound **35f** (n = 12).

The enthalpy values of the phase transitions agree well with those in the literature,[45] providing further confirmations of the mesophase type. The phase transition behavior of the mesogenic bis-chalcones was studied on heating between ambient temperature and 140°C at a rate of 5°C min^{-1} and on cooling from 140°C to 30°C at a similar scanning rate. The differential scanning calorimetry thermogram of all the compounds showed one endotherm for the crystal (Cr) to isotropic phase (Iso) transition (i.e. isotropisation) peaks during the heating scan. The compounds **35d** and **35h** also showed one additional endotherm for the crystal (Cr_1) to crystal (Cr) transition (modification) during the heating scan. On cooling all the compounds showed two exotherms. The first exotherm corresponds to the isotropic liquid phase (Iso) to nematic mesophase (N) and the second exotherm corresponds to the nematic mesophase (N) to crystallisation phase (Cr). The compound **35d** also showed third exotherm corresponding to the crystal (Cr) to crystal (Cr_1) modification on cooling. The mesophase assignment by POM observation was in good agreement with the corresponding DSC thermograms. All the compounds exhibited clear-cut transition temperatures in the DSC thermograms.

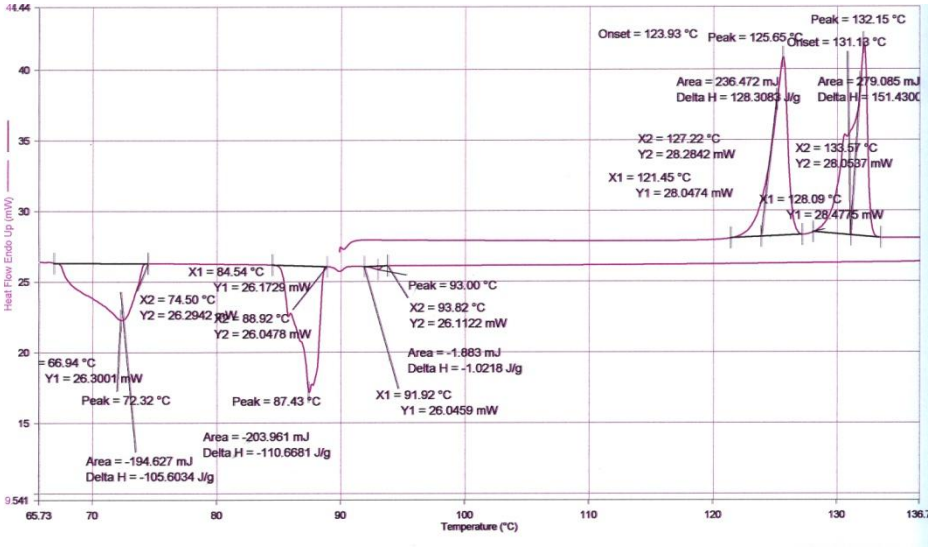

Figure 18: Representative DSC thermogram for compound **35d**

The plot of transition temperatures against the number of carbon atoms in alkoxy chain is presented in **Figure 18**, which shows initial rising tendency from n-heptyloxy (**35c**) to octyloxy derivative (**35d**) which may be is due to the usual odd-even effect. This was followed by a steady drop in the nematic isotropic (N-Iso) transition temperatures for all the synthesized derivatives, **35e - 35h**.

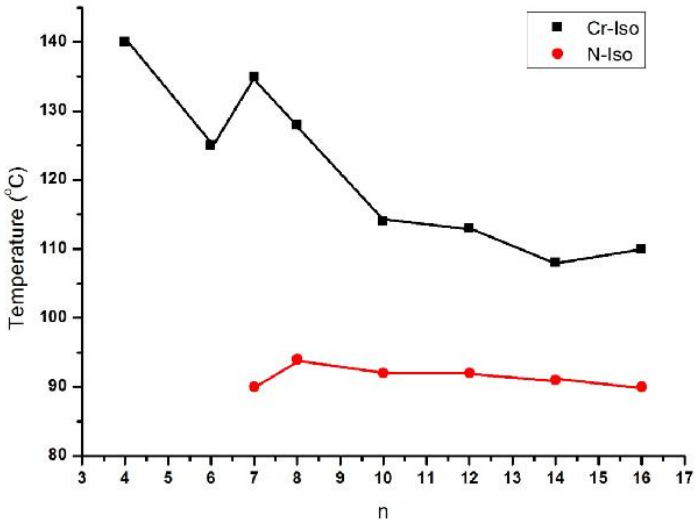

Figure 19: The phase behavior of **35a** to **35h**.

Mesogenic properties and molecular constitution

It is now well established that the thermotropic liquid crystals are highly sensitive to their molecular constitution. To determine the effects of alterations in the molecular core on the mesogenic properties of a compound, the thermal stability and mesophase length as a measure of mesomorphism can be correlated with the molecular constitution of the compounds. The present series exhibits monotropic nematic mesophase whereas in structurally related series of 2,4-bis(4-alkoxybenzylidene)cyclohexanones **34**,[41] where the methoxy to n-decyloxy homologues exhibited a nematic phase and the higher members exhibited a smectic mesophase. In addition smectic A phase also appeared in the n-nonyloxy and n-decyloxy derivatives.

The comparison of molecular structure, transition temperatures and energy minimized ball and stick model (MM2 models) with length and breadth of the n-octyloxy derivative of the present series **35d** and structurally related compound **34**[41] is presented in **Figure 19**. Compound **35d** exhibits monotropic nematic mesophase while compound **34** (n = C8) exhibits enantiotropic nematic mesophase. The nematic mesophase length and thermal stability (N-Iso transition temperatures) of compound **35d** is lower by 12 and 41 ^{o}C as compared with **34** (n = C8). The molecules have same central cyclohexanone unit, but

differ only at the side arms. The compound **35d** has piperanalidene moiety as one arm and the 4-octyloxybenzylidene as other arm; whereas similar derivative **34** has the same substituent on both sides. From **Figure 20** we can see that the length/breadth ratio (L/B) of compound **35d** (5.43) is quite lower compared to the corresponding derivative of **34** (6.78). Gray[34] has explained that decrease in the L/B ratio of the molecules reduces both the smectic and nematic thermal stabilities. These factors would contribute to the lower thermal stability of compound **35d**, and explain elimination of the smectogenic tendencies as well as monotropic nature of the mesophase observed in the present study.

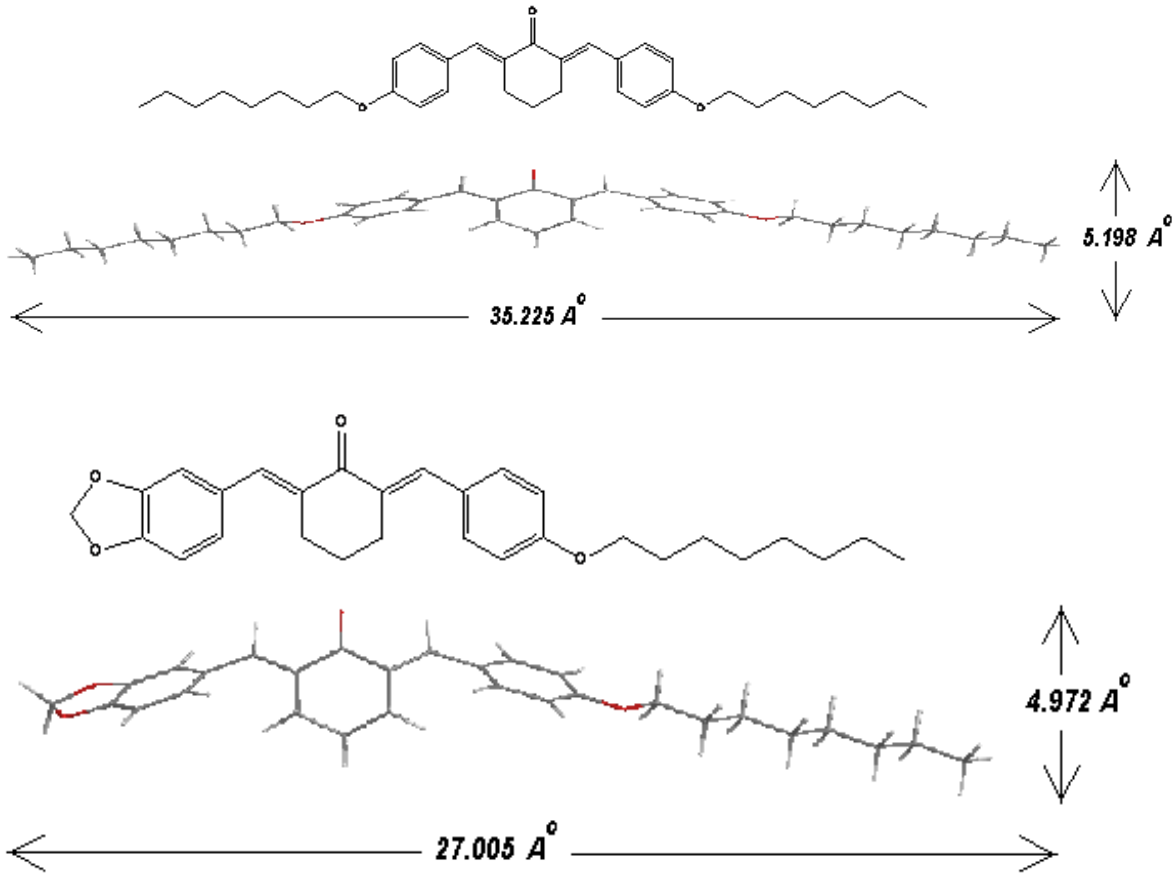

Figure 20: Comparison of the size of **3d** (bottom) with **2** (R = C8; Top).

Hence in this part of chapter we have presented the preparation and study of a series of unsymmetrical bis-chalcone derivatives of cyclohexanone. The molecules were found to show mesomorphic behavior and their properties were compared with structurally similar symmetrical analogues.

Experimental Section (Section 3.2.3)

(E)-2-((benzo[d][1,3]dioxol-6-yl)methylene)cyclohexanone (**38**)

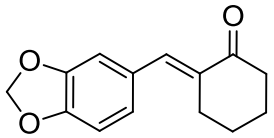

A round bottom flask was charged with piperonal (1.0 g, 6.66 mmol), cyclohexanone (0.98 g, 9.99 mmol), NaOH (0.53 g, 13.32 mmol) and water (70 mL). This mixture was heated (80^{o}C; 24 h). The reaction was quenched with water and dil. HCl and extracted with ethyl acetate (3x25 mL). The combined organic phase was washed with water and dried over anhydrous sodium sulfate. Solvent was removed in vacuum and the crude product was purified by column chromatography on silica gel to afford the product **38** as white solid (0.92 g, 60.0%); Melting point: 87 ^{o}C (Lit.[46] 87-88 ^{o}C).

^{1}H-NMR (400 MHz, $CDCl_3$) δ 7.46 (t, J = 2 Hz, 1H), 6.96 (d, J = 8 Hz, 1H), 6.95 (s, 1H), 6.85 (d, J = 8 Hz, 1H), 2.84 (t, J = 6.4 Hz, 2 Hz, 2H), 2.54 (t, J = 6.8 Hz, 2H), 1.94 (m, 2H), 1.79 (m, 2H).

IR (KBr): υ 3015, 2941, 1668, 1576, 1490, 1233, 1143, 1038, 757 cm.$^{-1}$

General procedure for the synthesis of unsymmetrical cyclohexanone derived bischalcones

(2E,6E)-2-(4-octyloxybenzylidene)-6-((benzo[d][1,3]dioxol-6-yl)methylene)cyclohexanone **(35d**)

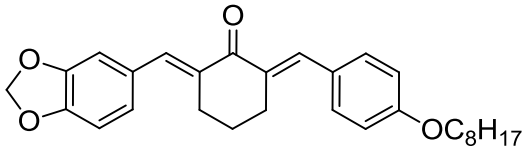

A round bottom flask was charged with **6** (0.25 g, 1.086 mmol), 4-octyloxy benzaldehyde (0.25 g, 1.086 mmol), NaOH (0.065 g, 1.63 mmol) and MeOH (15 mL). This mixture was heated (60-70 ^{o}C; 15 h). The reaction mixture was quenched with water and dilute HCl and extracted with ethyl acetate (3x25 mL). The combined organic phase was washed with water and dried over anhydrous sodium sulfate. Solvent was removed in vacuum and the crude product was purified by column chromatography on silica gel to afford **35d** as yellow crystalline solid (0.407 g, 84.43%).

(2E,6E)-2-(4-butoxybenzylidene)-6-((benzo[d][1,3]dioxol-6-yl)methylene) cyclohexanone (**35a**)

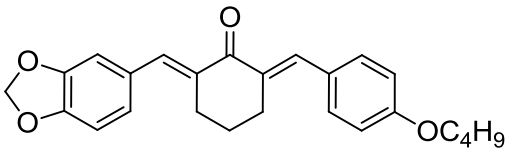

Yellow solid, Yield: 83.45%

^{1}H-NMR (400 MHz, $CDCl_3$) δ 7.77 (s, 1H), 7.72 (s, 1H), 7.46 (d, J = 8.8 Hz, 2H), 7.03-7.01 (d, J = 7.6 Hz, 1H and one singlet of aromatic H merged with doublet), 6.94 (d, J = 8.8

Hz, 2H), 6.87 (d, *J* = 8.4 Hz, 1H), 6.02 (s, 2H), 4.01 (t, *J* = 6.8 Hz, 2H), 2.95-2.90 (m, 4H), 1.85-1.76 (m, 4H), 1.55-1.49 (m, 2H), 1.00 (t, *J* = 7.6 Hz, 3H).

MS (EI) m/z (%): (M+1) 391 (1), 390 (84), 389 (64), 388 (100), 333 (61), 332 (44).

IR (KBr): υ 2945, 2865, 1659, 1593, 1555, 1504, 1444, 1246, 1164, 1035, 842 cm.$^{-1}$

(2E,6E)-2-(4-hexyloxybenzylidene)-6-((benzo[d][1,3]dioxol-6-yl)methylene) cyclohexanone (**35b**)

Yellow solid, Yield: 78.23%

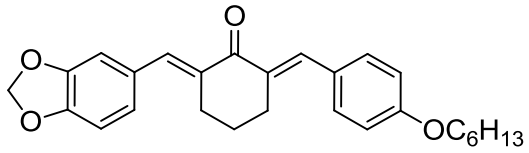

^{1}H-NMR (400 MHz, $CDCl_3$) δ 7.77 (s, 1H), 7.72 (s, 1H), 7.46 (d, *J* = 8.8 Hz, 2H), 7.03-7.01 (d, *J* = 8 Hz, 1H and one singlet of aromatic H merged with doublet), 6.94 (d, *J* = 8.8 Hz, 2H), 6.87 (d, *J* = 8.4 Hz, 1H), 6.02 (s, 2H), 4.01 (t, *J* = 6.4 Hz, 2H), 2.95-2.90 (m, 4H), 1.84-1.79 (m, 4H), 1.50-1.46 (m, 2H), 1.38-1.35 (m, 4H), 0.94-0.91 (m, 3H).

MS (EI) m/z (%): 418 (28), 417 (100), 390 (22), 389 (51), 333 (22), 332 (29).

IR (KBr): υ 2937, 2856, 1654, 1591,1557, 1507, 1443, 1295, 1248, 1162, 824 cm.$^{-1}$

(2E,6E)-2-(4-heptyloxybenzylidene)-6-((benzo[d][1,3]dioxol-6-yl)methylene) cyclohexanone (**35c**)

Yellow solid, Yield: 75.08%

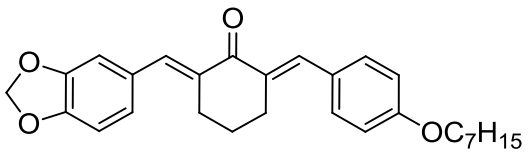

^{1}H-NMR (400 MHz, $CDCl_3$) *δ* 7.77 (s, 1H), 7.72 (s, 1H), 7.46 (d, *J* = 8.8 Hz, 2H), 7.03-7.01 (d, *J* = 8 Hz, 1H and one singlet of aromatic H merged with doublet), 6.94 (d, *J* = 8.8 Hz, 2H), 6.87 (d, *J* = 8 Hz, 1H), 6.02 (s, 2H), 4.01 (t, *J* = 6.4 Hz, 2H), 2.95-2.90 (m, 4H), 1.84-1.77 (m, 4H), 1.51-1.44 (m, 2H), 1.41-1.36 (m, 6H), 0.91(t, *J* = 6.8 Hz, 3H).

MS (EI) m/z (%): (M+1) 433 (33), 432 (100), 431 (76), 430 (98), 429 (31), 333 (64), 332 (56).

IR (KBr): υ 2935, 2853, 1654, 1590, 1507, 1443, 1297, 1248, 1162, 1035, 923, 823 cm.$^{-1}$

(2E,6E)-2-(4-octyloxybenzylidene)-6-((benzo[d][1,3]dioxol-6-yl)methylene) cyclohexanone (**35d**):

Yellow solid, Yield: 84%

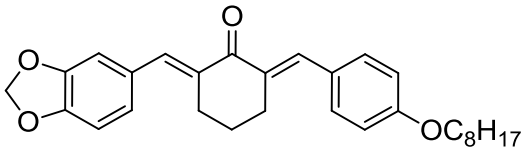

^{1}H-NMR (400 MHz, $CDCl_3$) *δ* 7.77 (s, 1H), 7.72 (s, 1H), 7.46 (d, *J* = 8.8 Hz, 2H), 7.02-7.01 (d, *J* = 7.6 Hz, 1H and one singlet of aromatic H merged with doublet), 6.94 (d, *J* =

6.8 Hz, 2H), 6.87 (d, *J* = 7.6 Hz, 1H), 6.02 (s, 2H), 4.01 (t, *J* = 6.8 Hz, 2H), 2.95-2.91 (m, 4H), 1.85-1.77 (m, 4H), 1.50-1.44 (m, 2H), 1.36-1.30 (m, 8H), 0.91 (t, *J* = 7.2 Hz, 3H).

MS (EI) m/z (%): (M+1) 447 (57), 446 (78), 445 (100), 444 (66), 431 (34), 333 (31), 332 (44).

IR (KBr): υ 3061, 2924, 2850, 1656, 1591, 1556, 1508, 1491, 1259, 1160, 924, 560 $cm.^{-1}$

(2E,6E)-2-(4-decyloxybenzylidene)-6-((benzo[d][1,3]dioxol-6-yl)methylene) cyclohexanone (**35e**):

Yellow solid, Yield: 78.26%

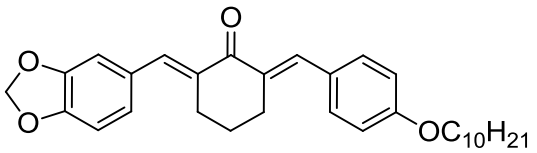

^{1}H-NMR (400 MHz, $CDCl_3$) δ 7.77 (s, 1H), 7.72 (s, 1H), 7.46 (d, *J* = 8.8 Hz, 2H), 7.03-7.01 (d, *J* = 8 Hz, 1H and one singlet of aromatic H merged with doublet), 6.94 (d, *J* = 8.8 Hz, 2H), 6.87 (d, *J* = 8.4 Hz, 1H), 6.02 (s, 2H), 4.00 (t, *J* = 6.4 Hz, 2H), 2.93-2.90 (m, 4H), 1.82-1.79 (m, 4H), 1.49-1.44 (m, 2H), 1.34-1.29 (m, 12H), 0.90 (t, *J* = 7.2 Hz, 3H).

MS (EI) m/z (%): 474 (56), 473 (100), 472 (75), 446 (31), 445 (30), 444 (36), 333 (63), 332 (53).

IR (KBr): υ 2935, 2849, 1654, 1590, 1506, 1443, 1297, 1249, 1164, 1034, 924, 823 cm^{-1}

(2E,6E)-2-(4-dodecyloxybenzylidene)-6-((benzo[d][1,3]dioxol-6-yl)methylene) cyclohexanone (**35f**):

Yellow solid, Yield: 73.76%

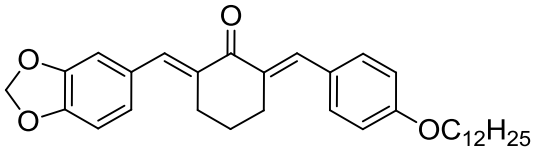

^{1}H-NMR (400 MHz, $CDCl_3$) δ 7.77 (s, 1H), 7.72 (s, 1H), 7.46 (d, *J* = 8.8 Hz, 2H), 7.03-7.01 (d, *J* = 8 Hz, 1H and one singlet of aromatic H merged with doublet), 6.94 (d, *J* = 8.8 Hz, 2H), 6.87 (d, *J* = 8.4 Hz, 1H), 6.02 (s, 2H), 4.00 (t, *J* = 6.8 Hz, 2H), 2.95-2.90 (m, 4H), 1.85-1.77 (m, 4H), 1.55-1.44 (m, 2H), 1.38-1.29 (m, 12H), 0.90 (t, *J* = 6.8, 3H).

MS (EI) m/z (%): 502, 474 (84), 473 (82), 472 (100), 333 (25), 332 (32).

IR (KBr): υ 2922, 2850, 1654, 1590, 1505, 1443, 1248, 1164, 1034, 923, 822, 566 $cm.^{-1}$

(2E,6E)-2-(4-tetradecyloxycyloxybenzylidene)-6-((benzo[d][1,3]dioxol-6-yl)methylene) cyclohexanone (**35g**):

Yellow solid, Yield: 70.43%

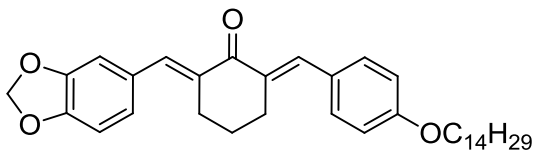

^{1}H-NMR (400 MHz, $CDCl_3$) δ 7.77 (s, 1H), 7.72 (s, 1H), 7.46 (d, *J* = 8.8 Hz, 2H), 7.03-7.01 (d, *J* = 8 Hz, 1H and one singlet of aromatic H merged with doublet), 6.94 (d, *J* = 8.8 Hz, 2H), 6.87 (d, *J* = 8.4 Hz, 1H), 6.02 (s, 2H), 4.00 (t, *J* = 6.8 Hz, 2H), 2.95-2.90 (m, 4H), 1.83-1.79 (m, 4H), 1.49-1.43 (m, 2H), 1.33-1.27 (m, 16H), 0.89 (t, *J* = 6.8 Hz, 3H).

MS (EI) m/z (%): 530 (57), 529 (39), 528 (35), 439 (24), 368 (72), 367 (100), 332 (34).

IR (KBr): υ 2920, 2850, 1654, 1592, 1506, 1298, 1249, 1163, 1035, 924, 824 cm.$^{-1}$

(2E,6E)-2-(4-hexadecyloxycyloxybenzylidene)-6-((benzo[d][1,3]dioxol-6-yl)methylene) cyclohexanone (**35h**):

Yellow solid, Yield: 61.85%

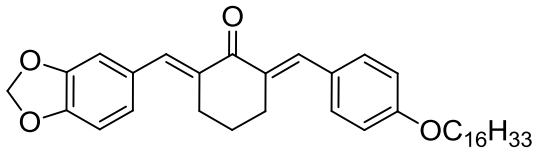

^{1}H-NMR (400 MHz, $CDCl_3$) δ 7.77 (s, 1H), 7.72 (s, 1H), 7.46 (d, *J* = 8.8 Hz, 2H), 7.03-7.01 (d, *J* = 8.8 Hz, 1H and one singlet of aromatic H merged with doublet), 6.94 (d, *J* = 8.8 Hz, 2H), 6.87 (d, *J* = 8.4 Hz, 1H), 6.02 (s, 2H), 4.00 (t, *J* = 6.4 Hz, 2H), 2.95-2.91 (m, 4H), 1.85-1.77 (m, 4H), 1.49-1.43 (m, 2H), 1.33-1.27 (m, 24H), 0.89 (t, *J* = 6.8Hz, 3H).

MS (EI) m/z (%): 558 (51), 557 (51), 556 (29), 438 (30), 369 (54), 368 (100), 367 (84), 312 (61).

IR (KBr): υ 3021, 2921, 2850, 1655, 1593, 1506, 1445, 1249, 1163, 1036, 925, 759 cm^{-1}

Spectral Data for unsymmetrical Cyclohexanone derived Bis-chalcones (Section 3.2.3)

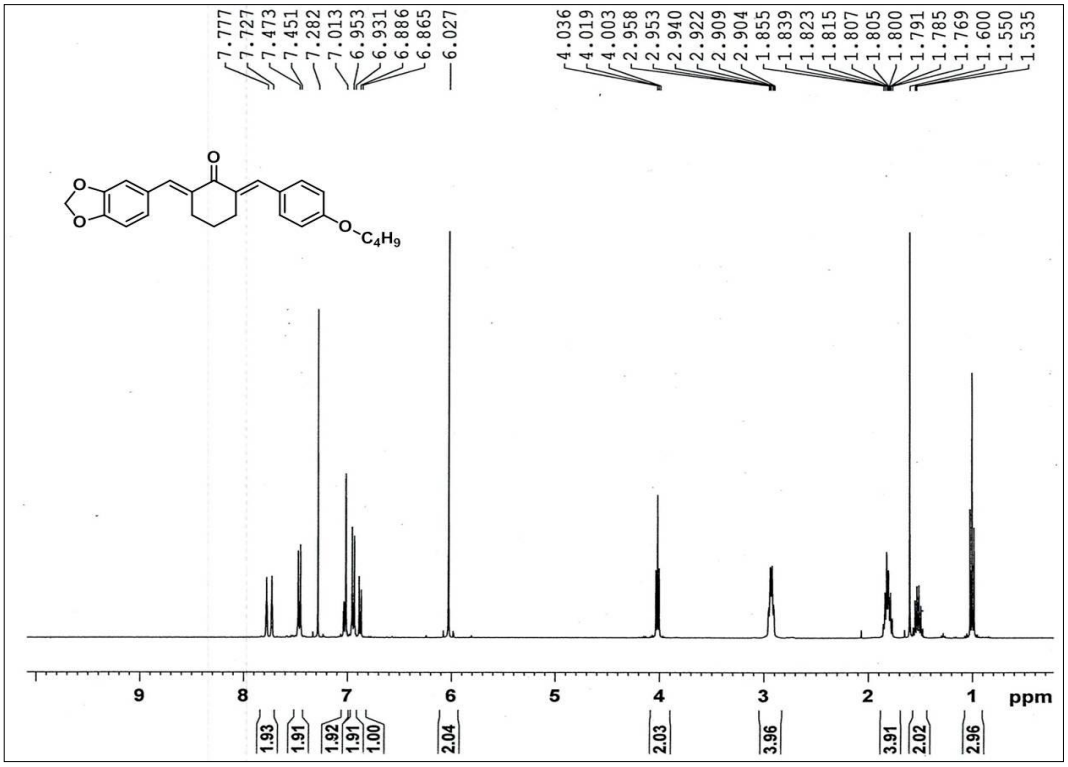

^{1}H-NMR of compound 35a

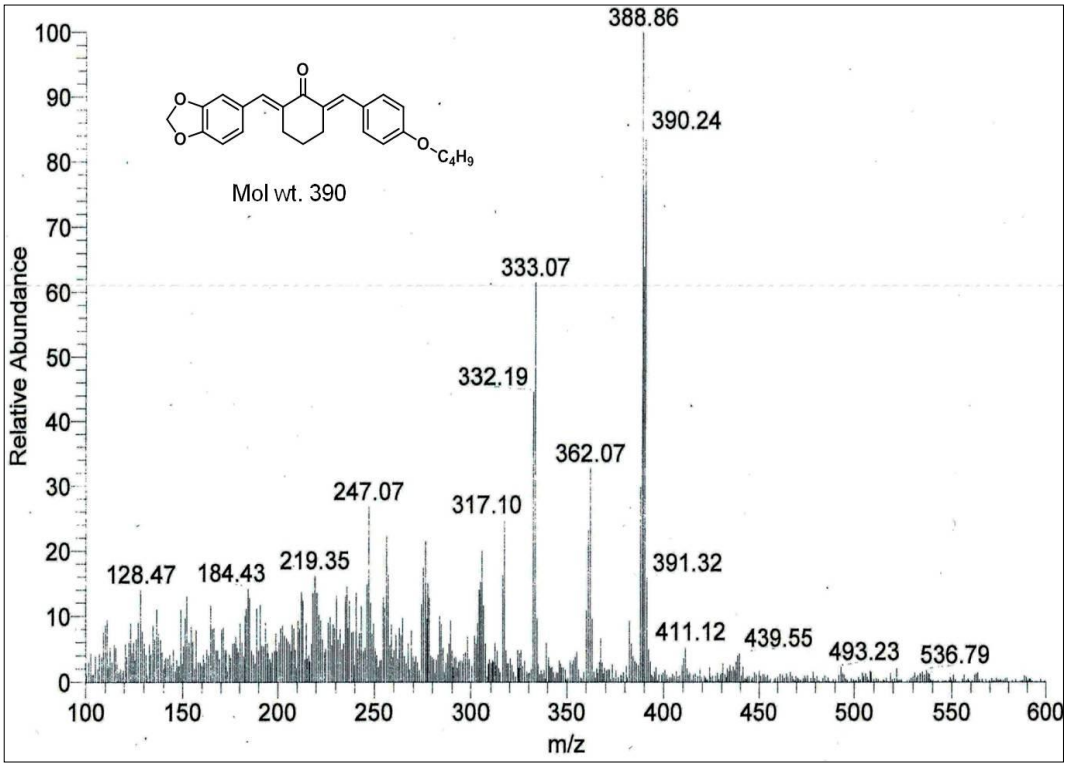

Mass spectra of compound 35a

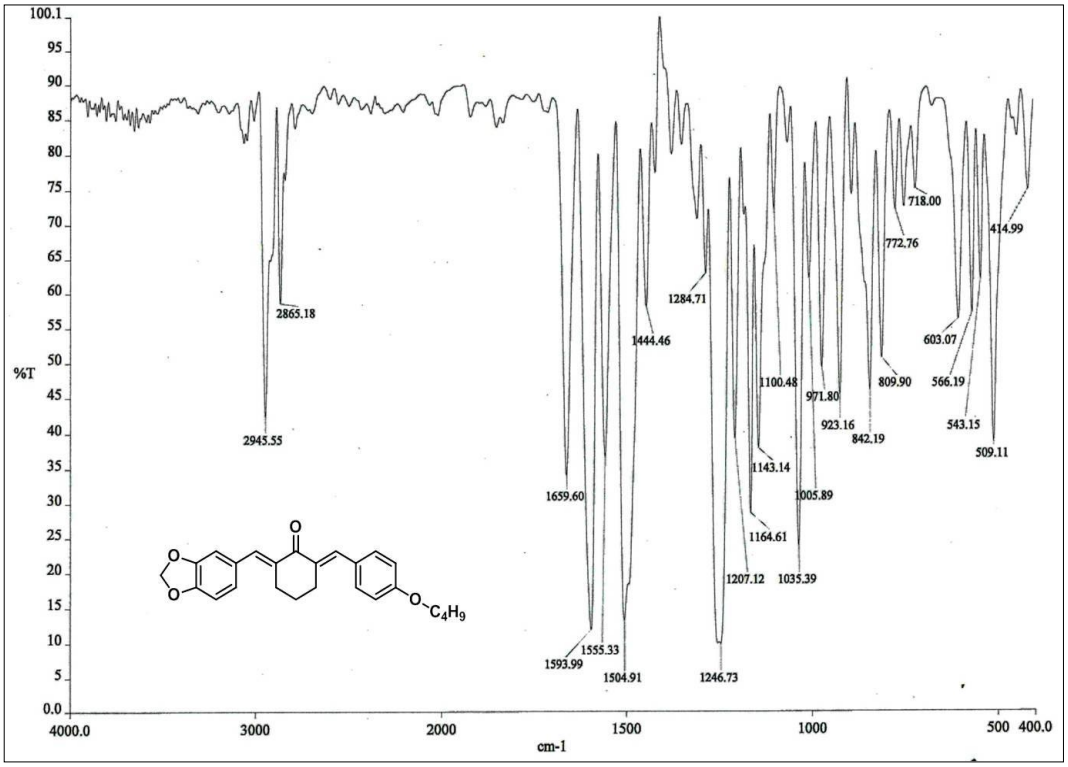

IR spectra of compound 35a

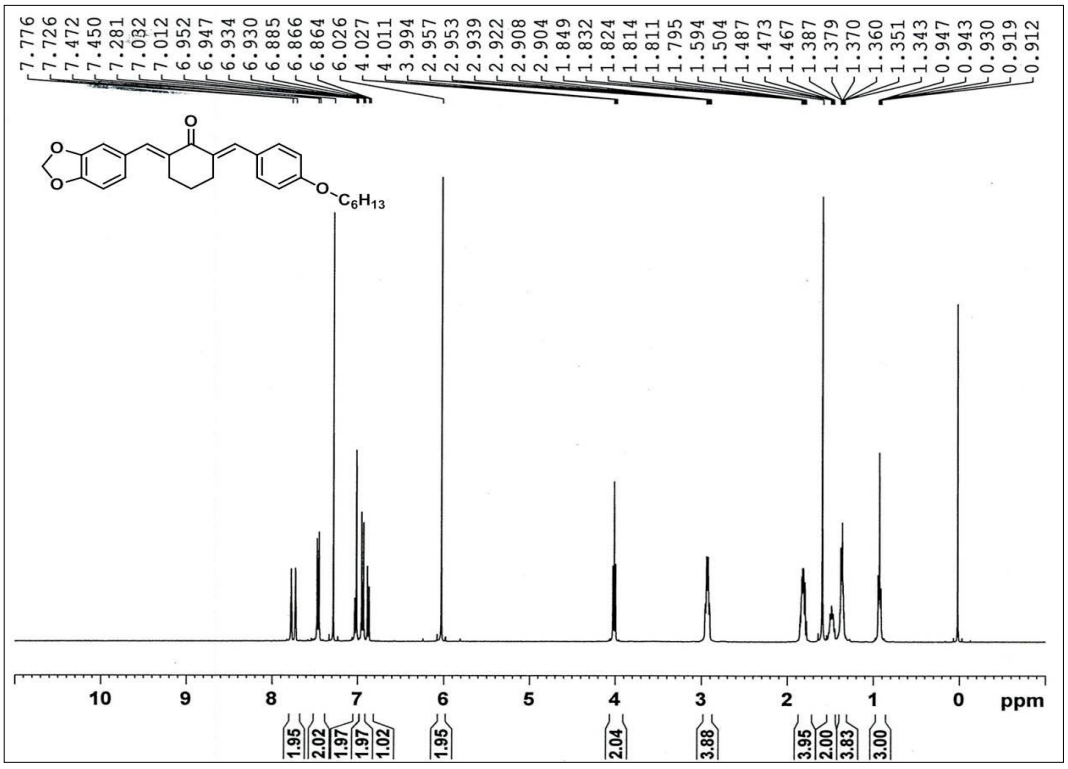

^{1}H-NMR of compound 35b

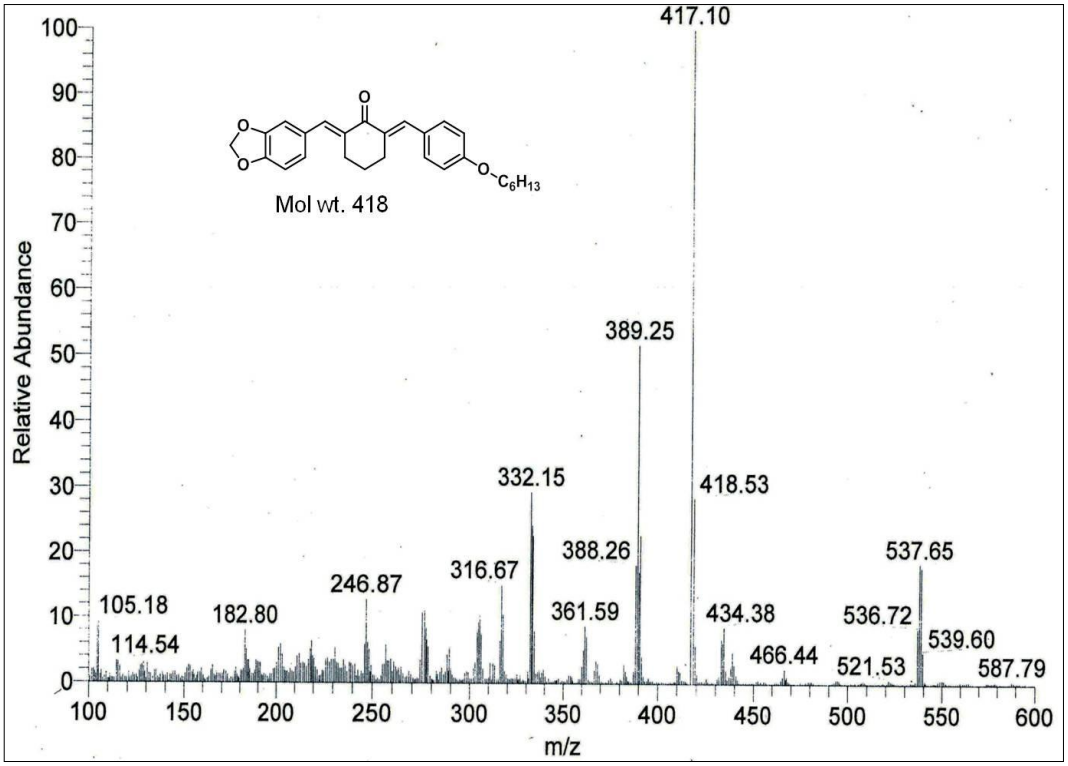

Mass spectra of compound 35b

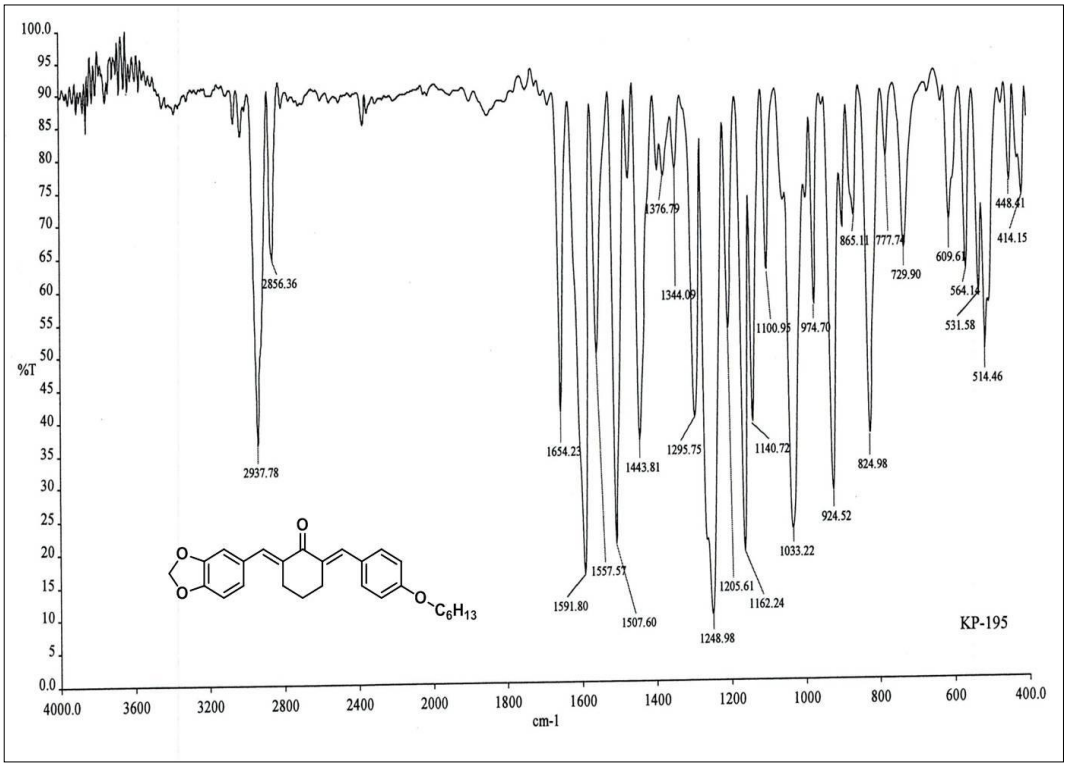

IR spectra of compound 35b

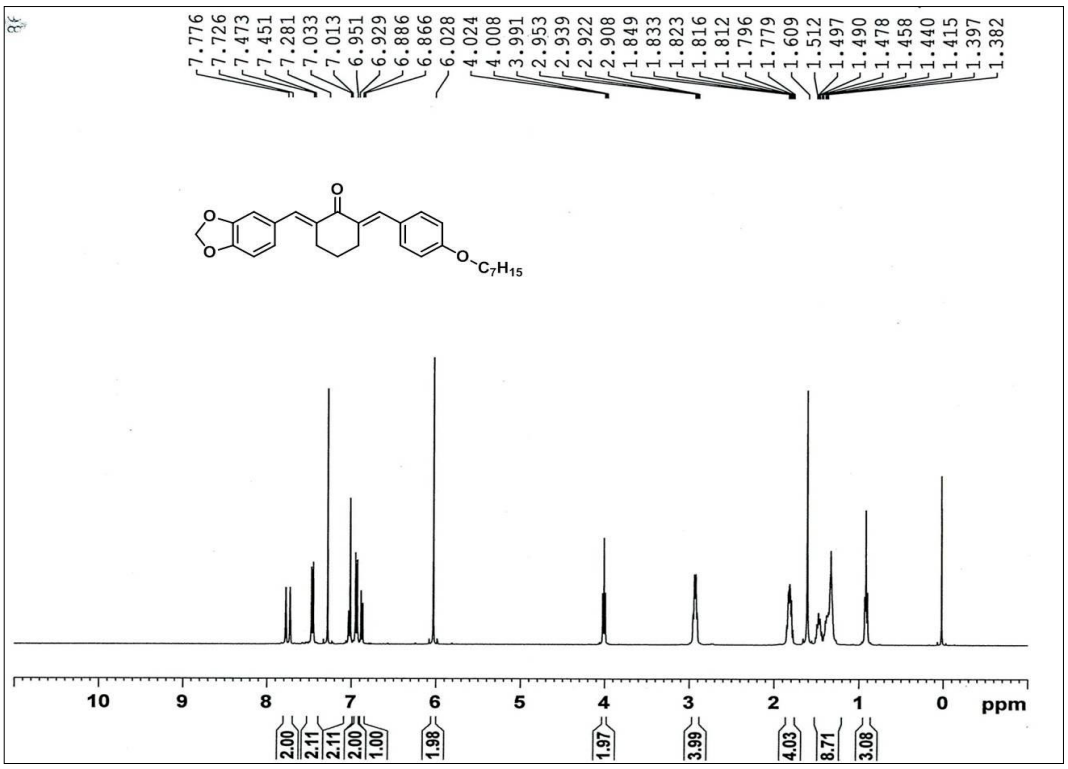

^{1}H-NMR of compound 35c

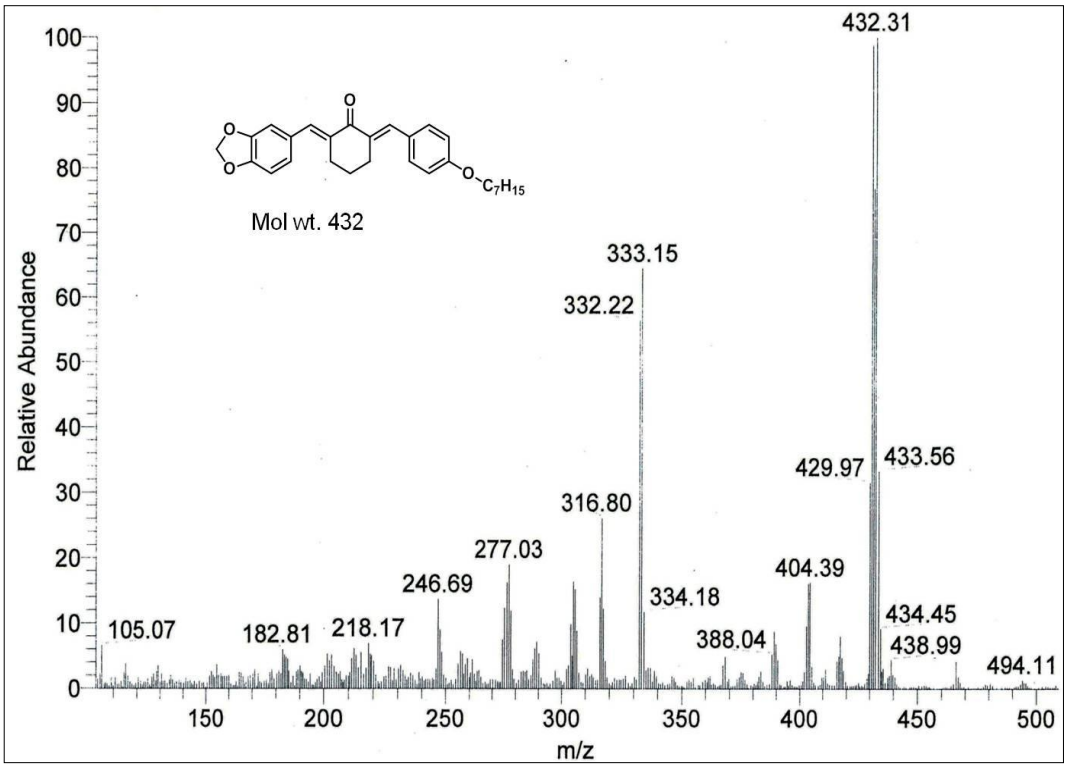

Mass spectra of compound 35c

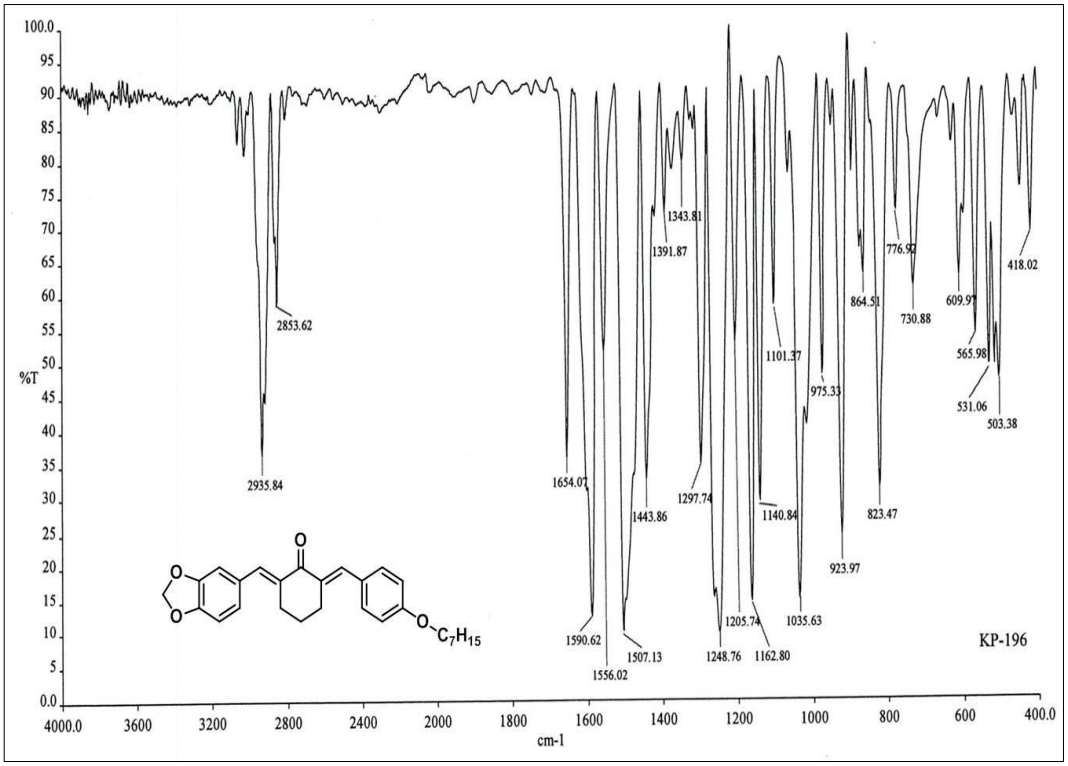

IR spectra of compound 35c

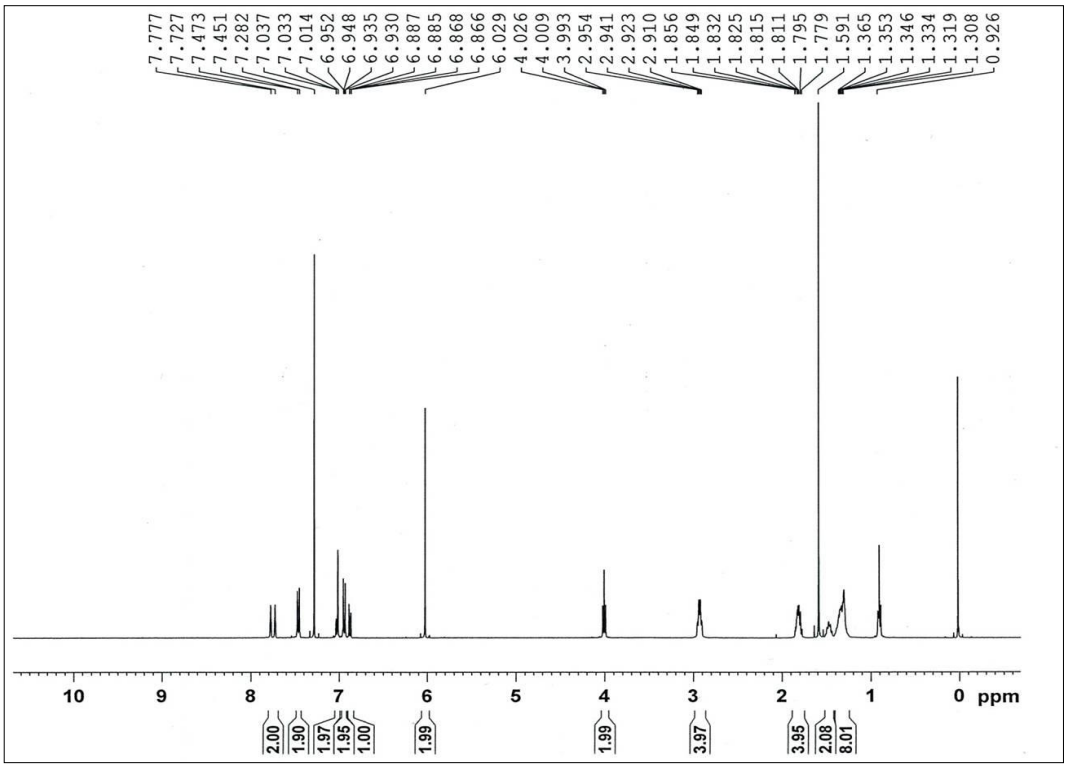

^{1}H-NMR of compound 35d

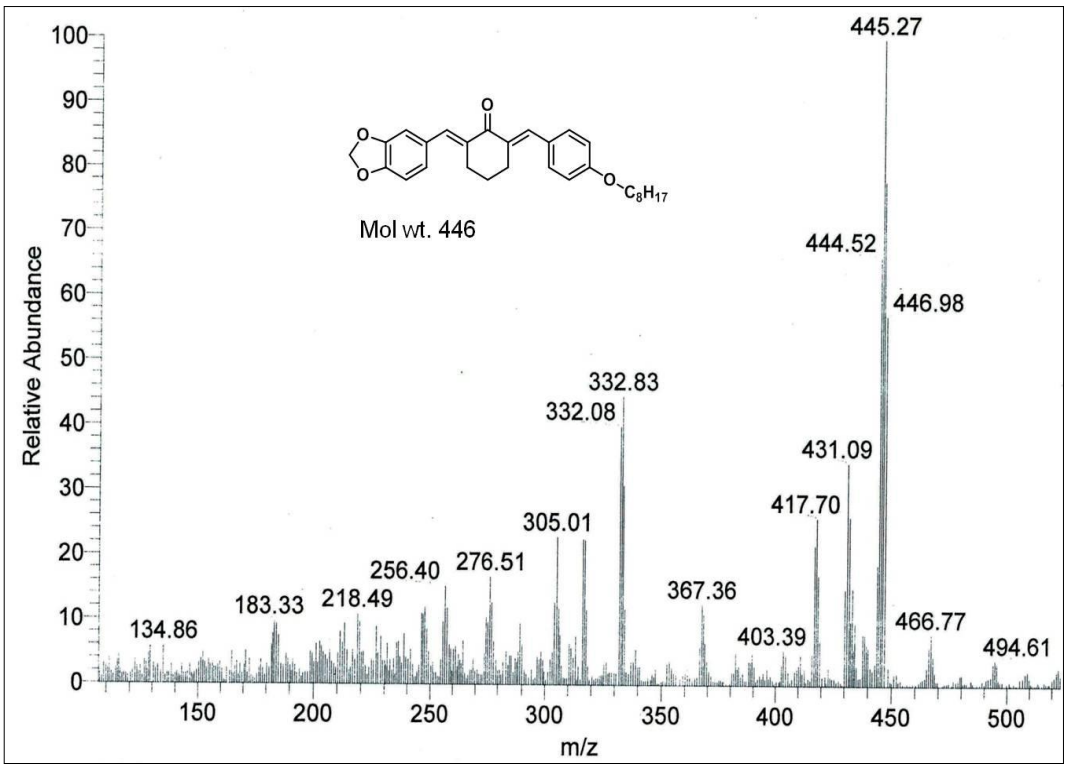

Mass spectra of compound 35d

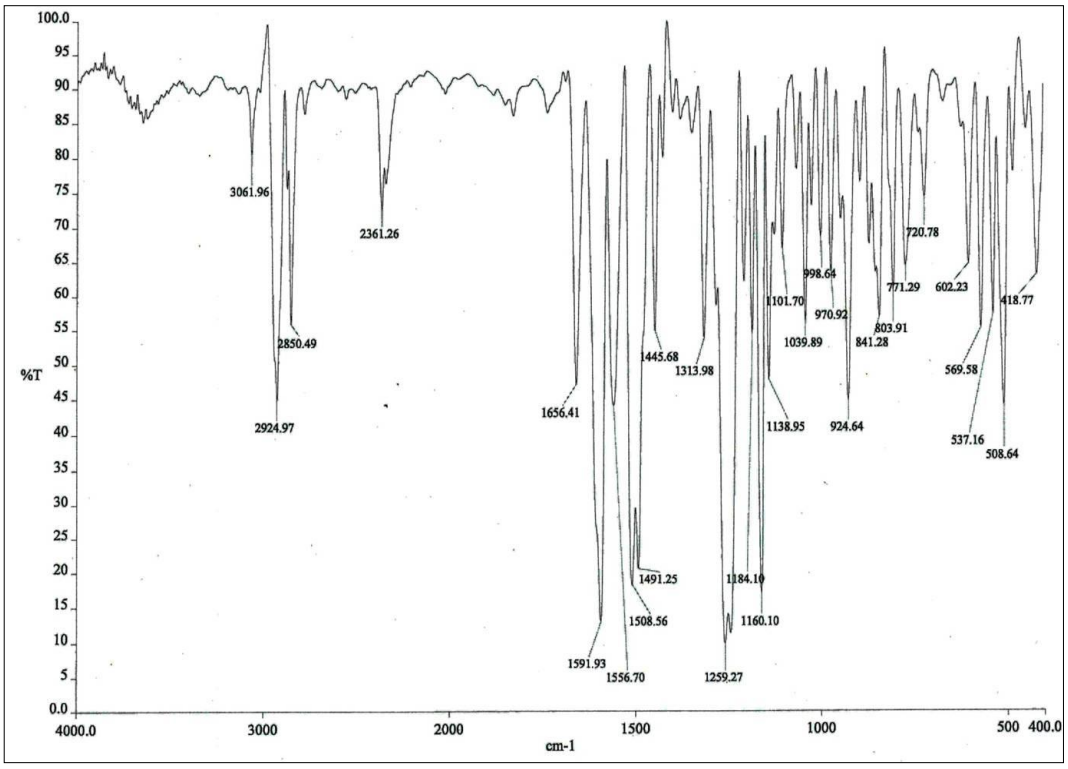

IR spectra of compound 35d

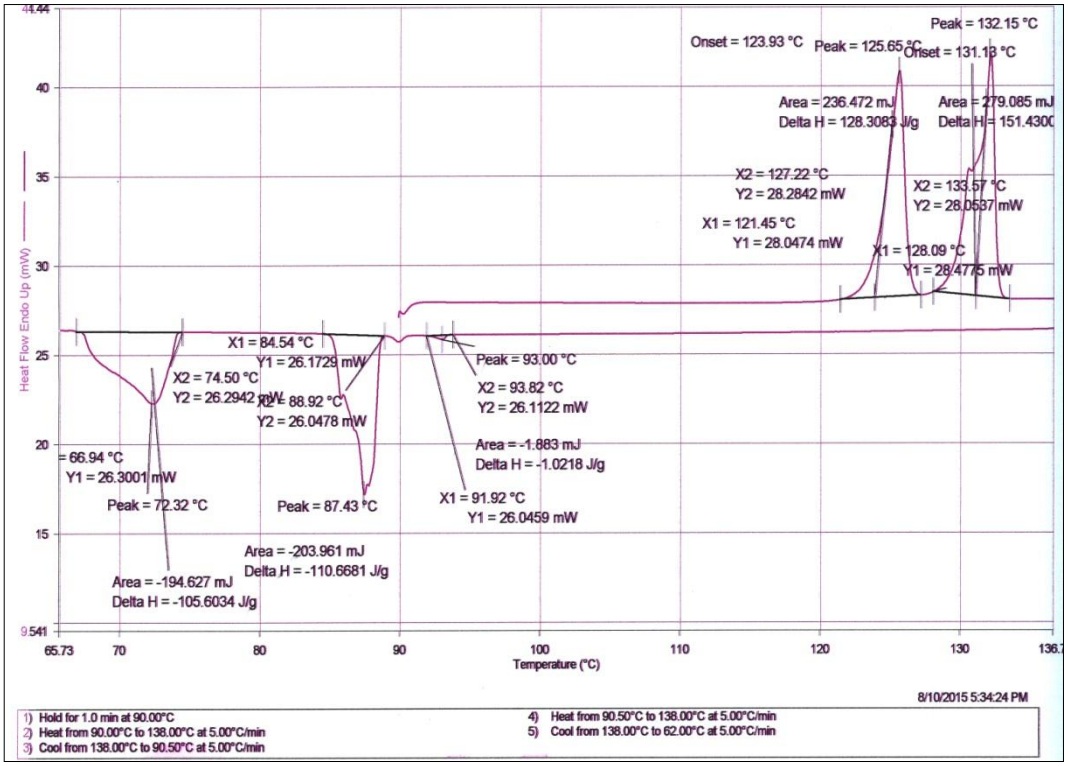

DSC thermogram of compound 35d

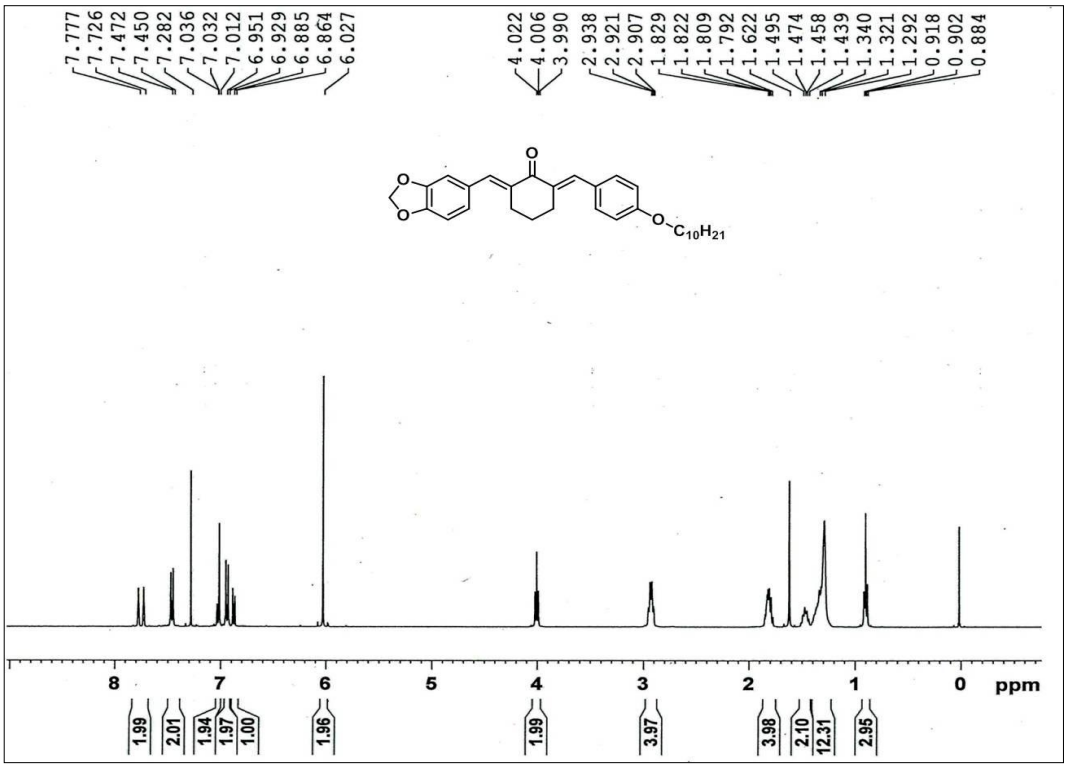

^{1}H-NMR of compound 35e

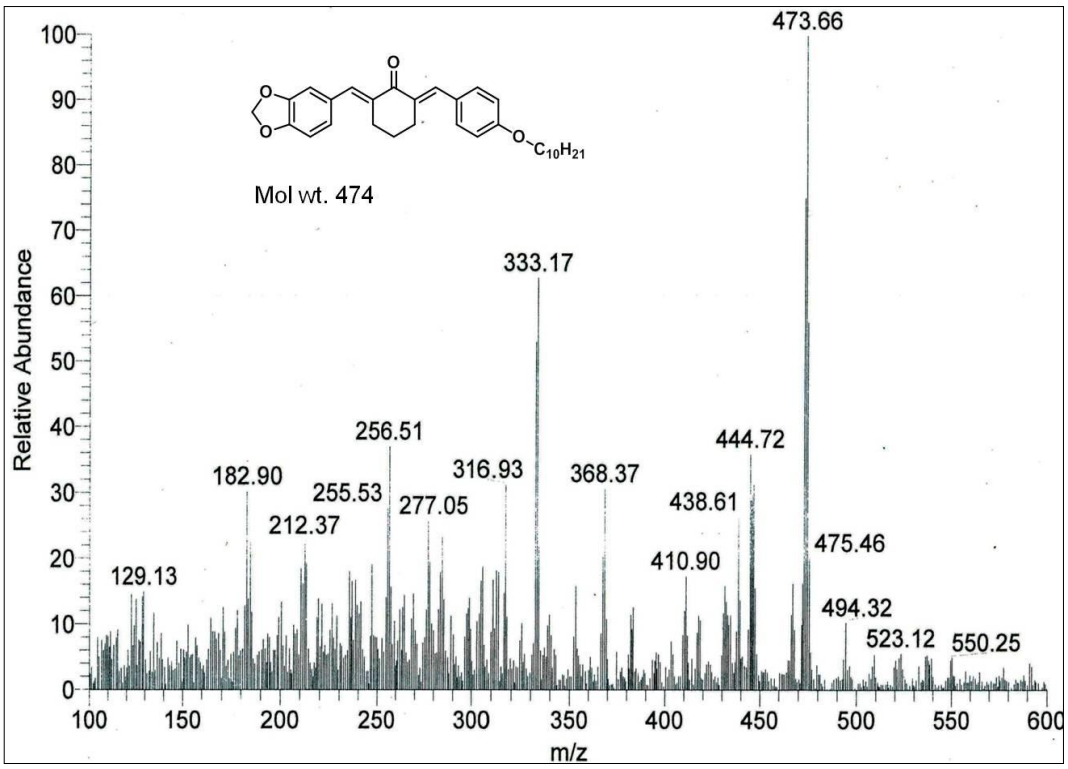

Mass spectra of compound 35e

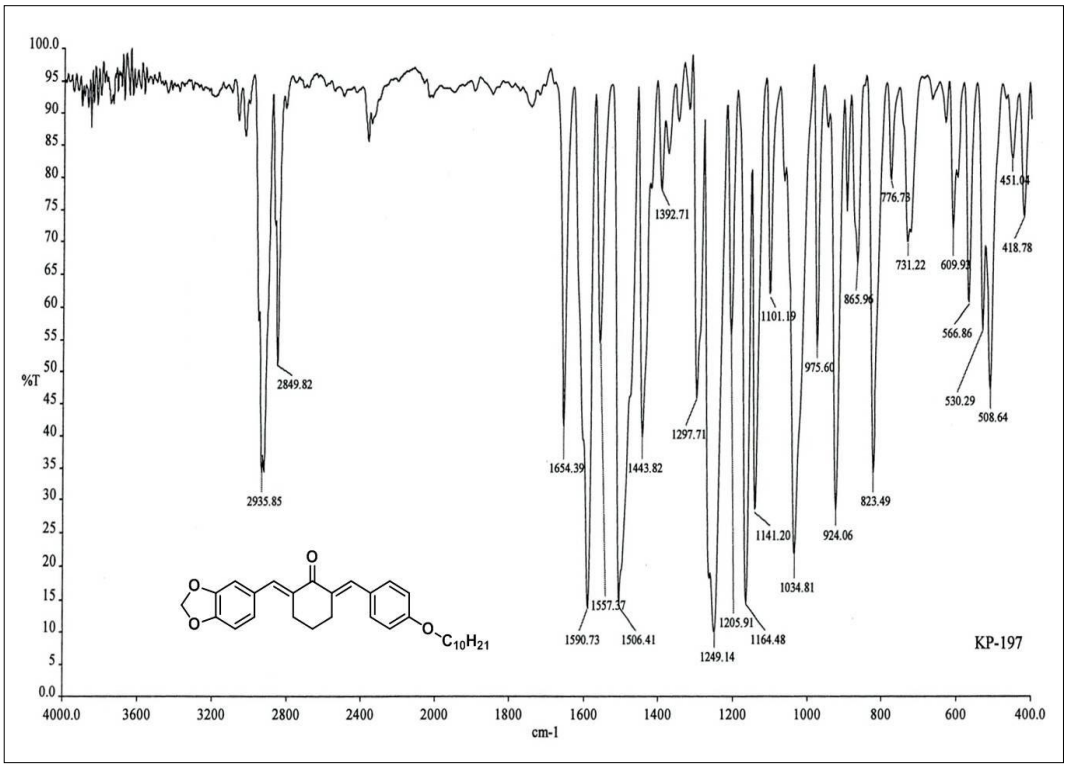

IR spectra of compound 35e

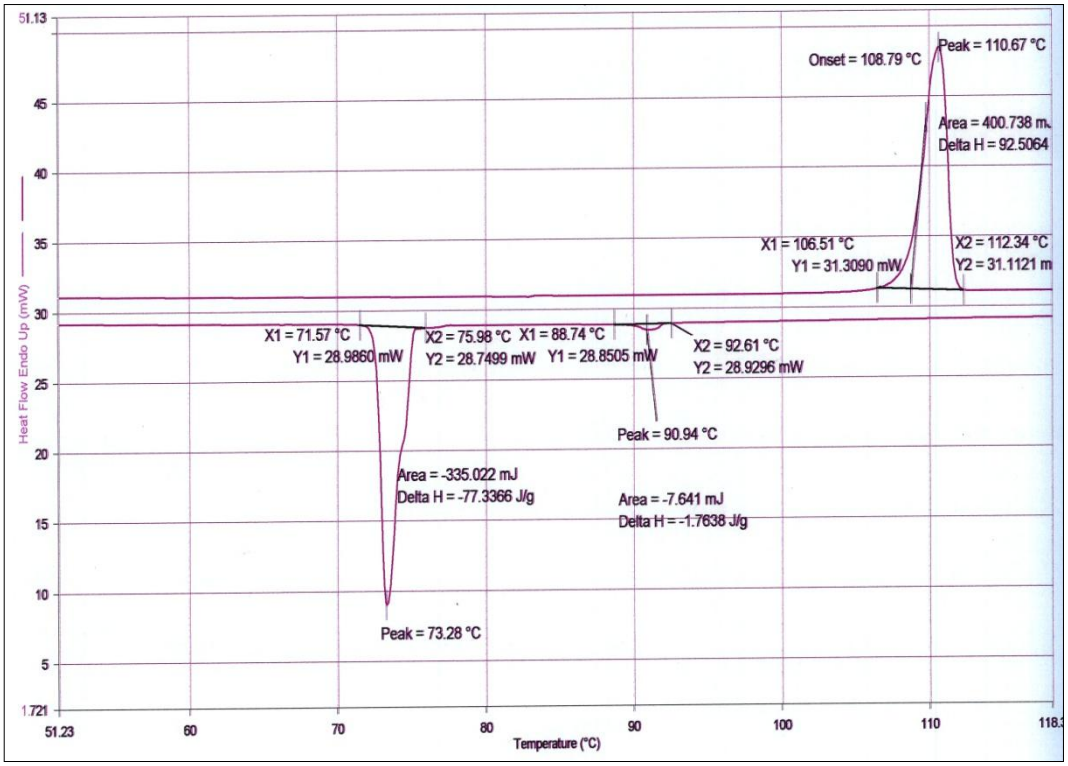

DSC thermogram of compound 35e

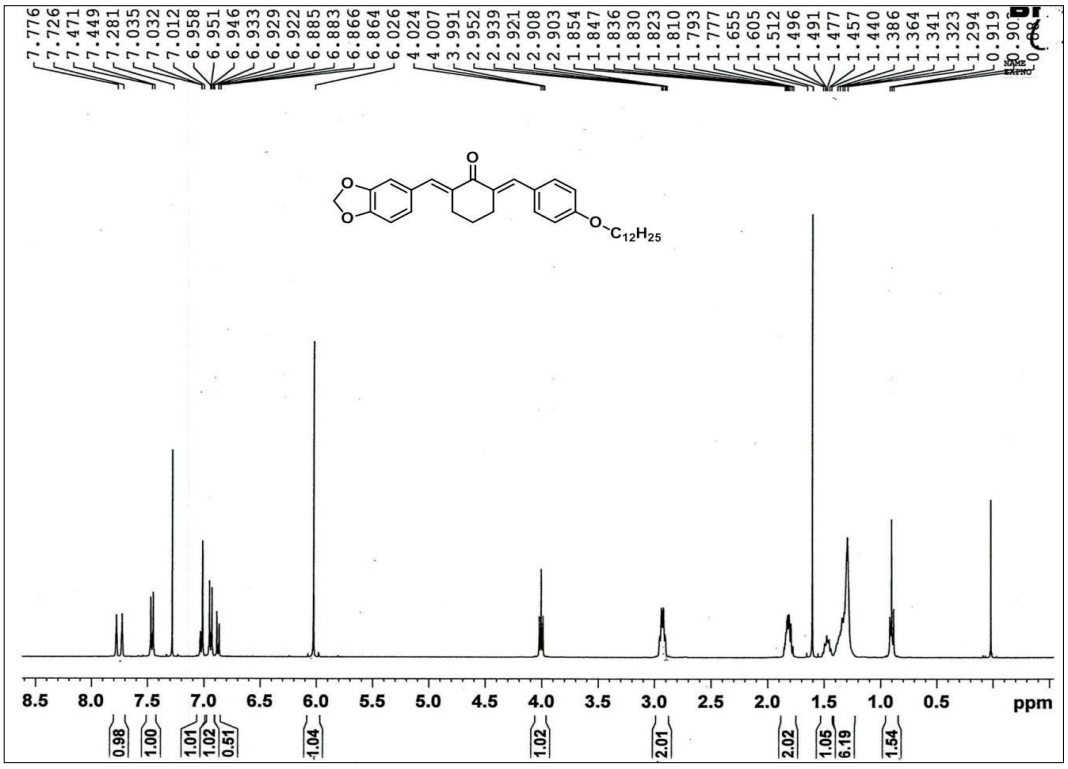

^{1}H-NMR of compound 35f

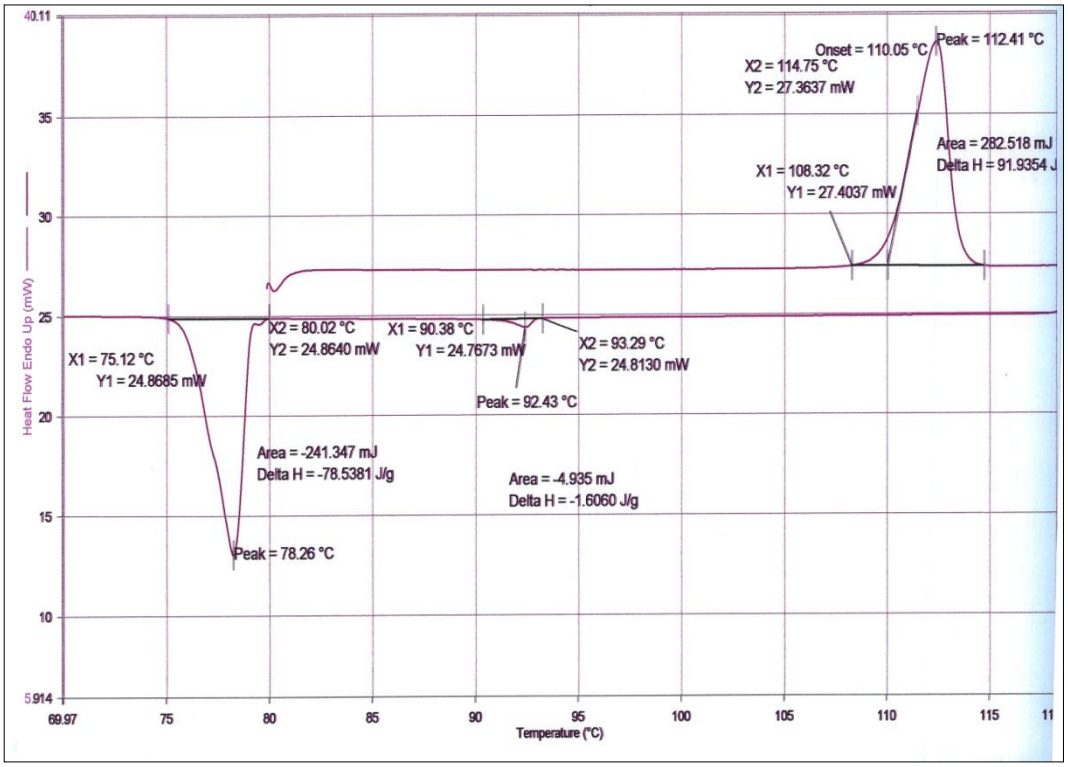

DSC thermogram of compound 35f

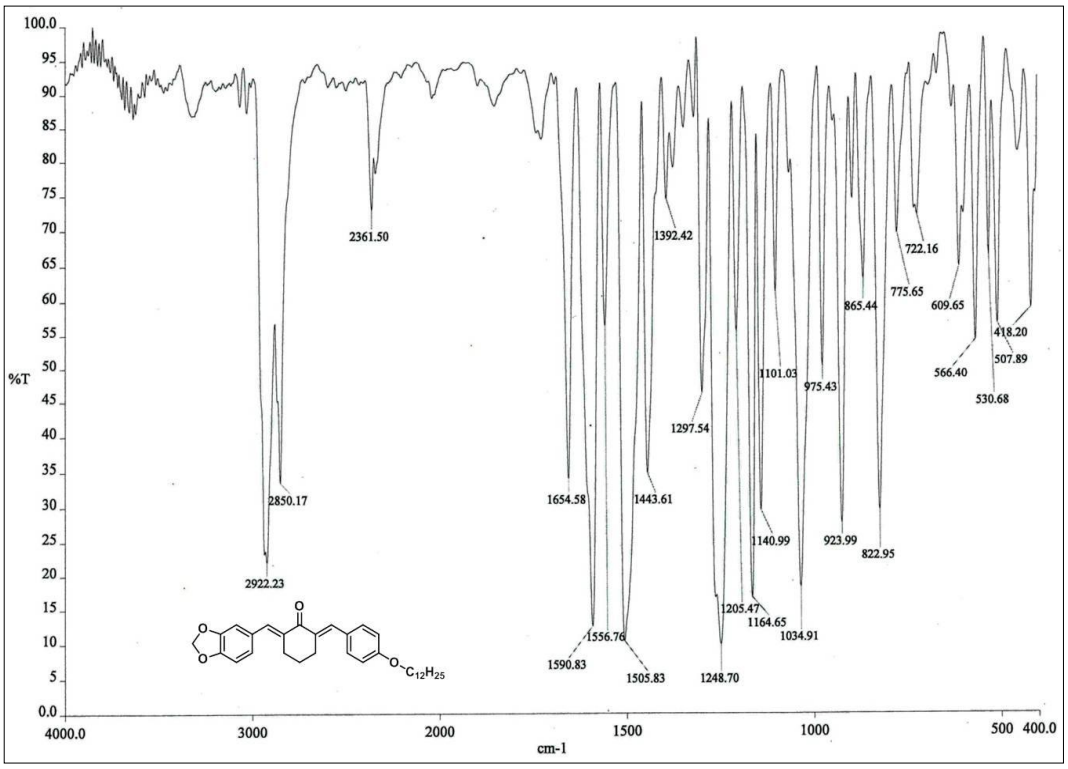

IR spectra of compound 35f

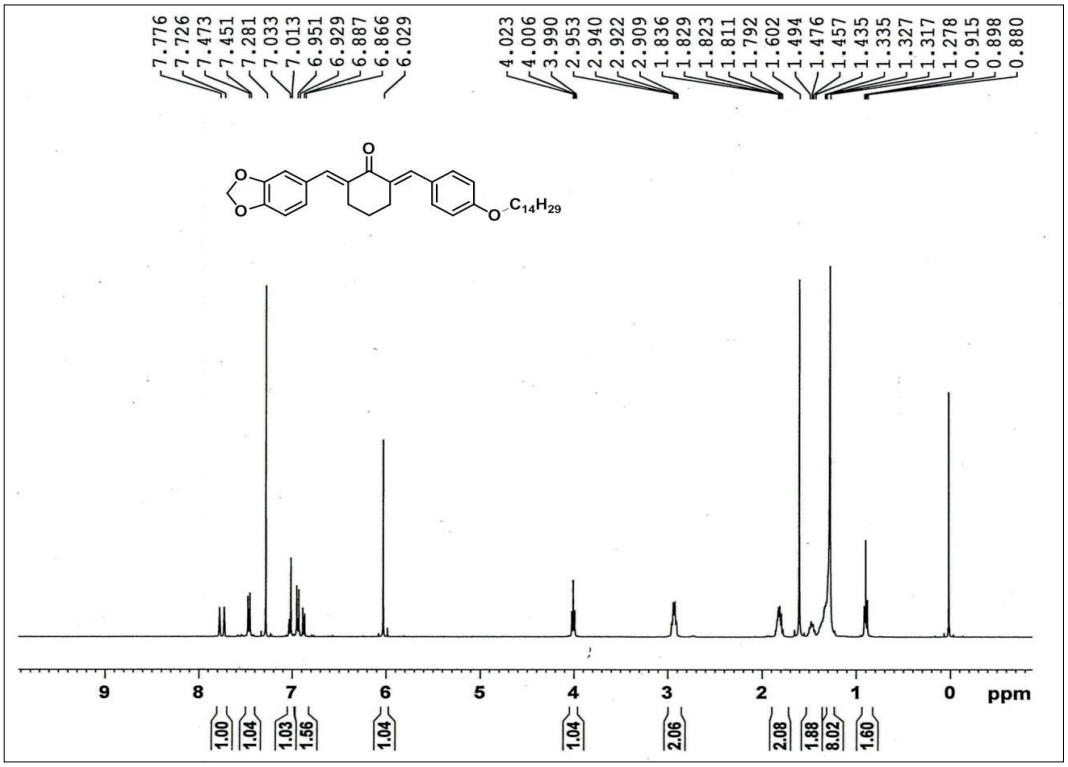

^{1}H-NMR of compound 35g

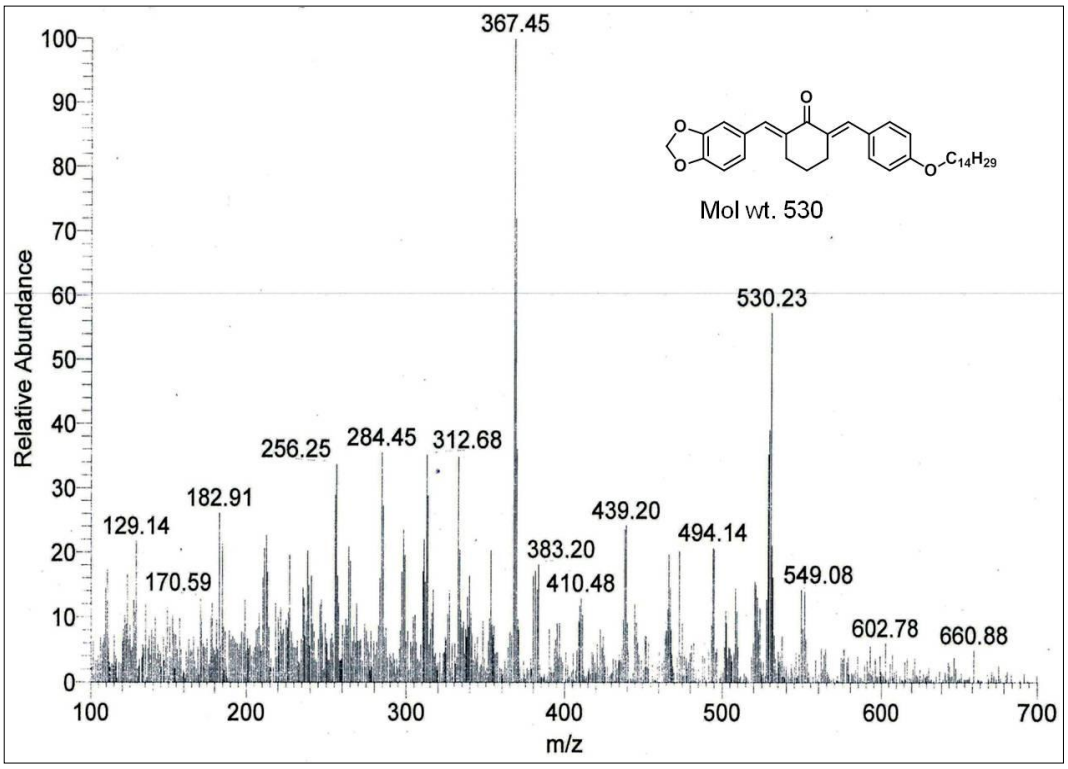

Mass spectra of compound 35g

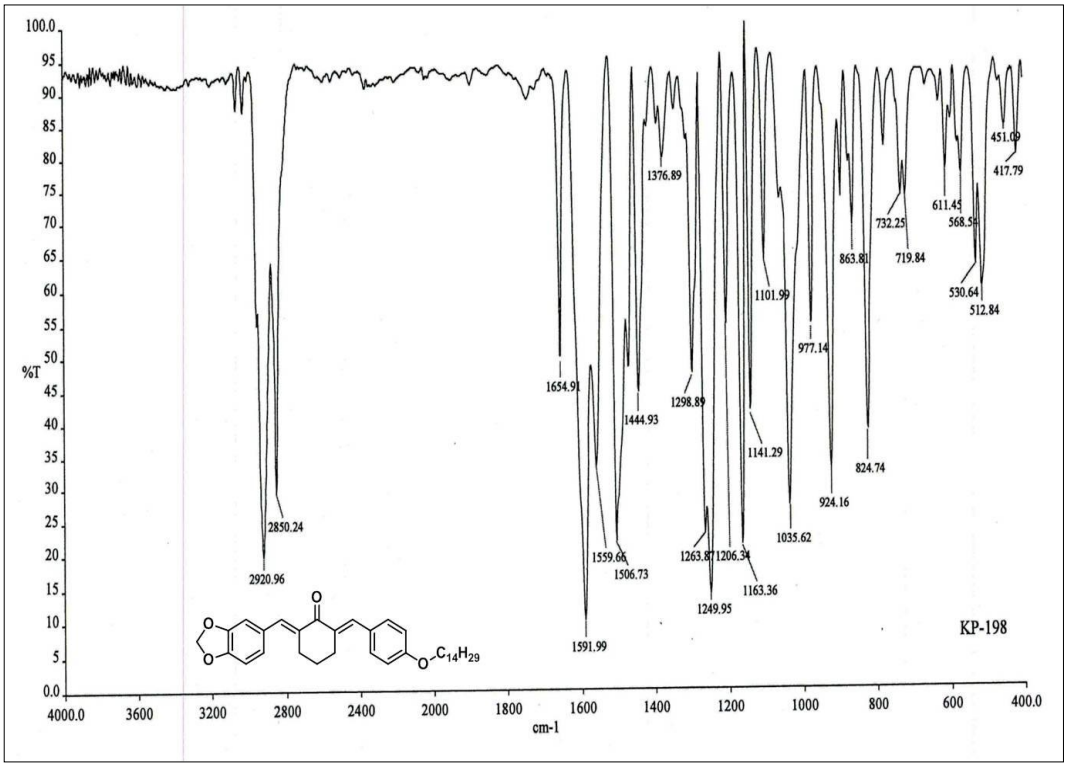

IR spectra of compound 35g

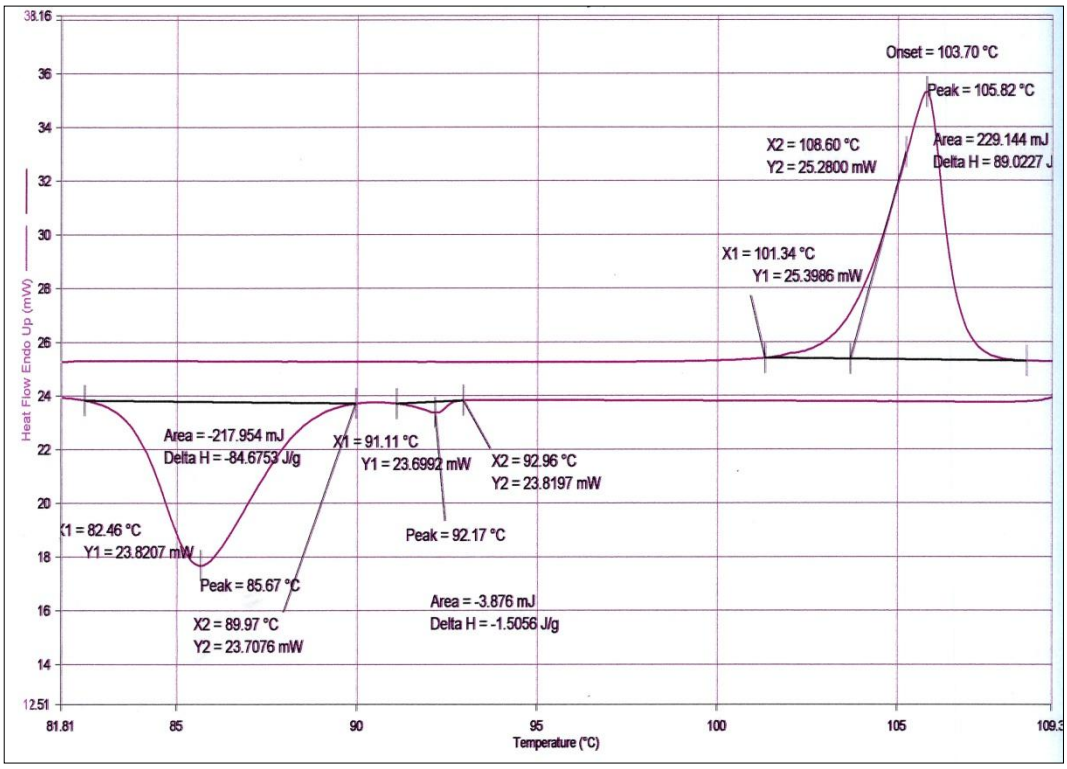

DSC thermogram of compound 35g

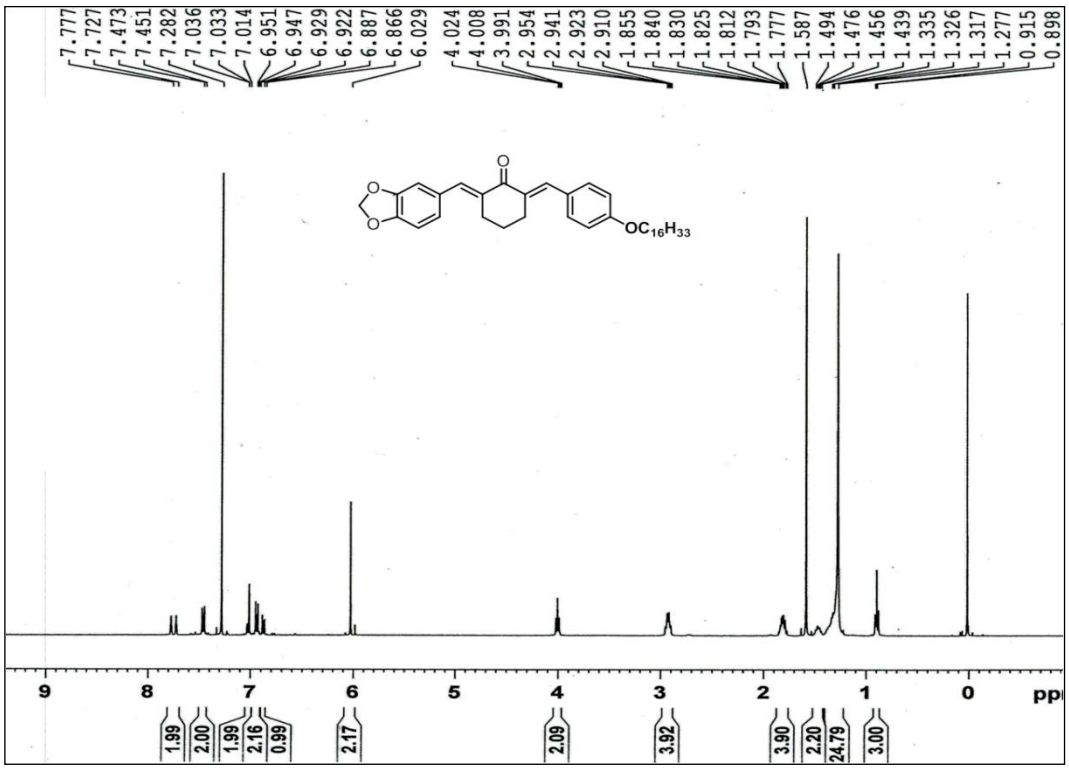

^{1}H-NMR of compound 35h

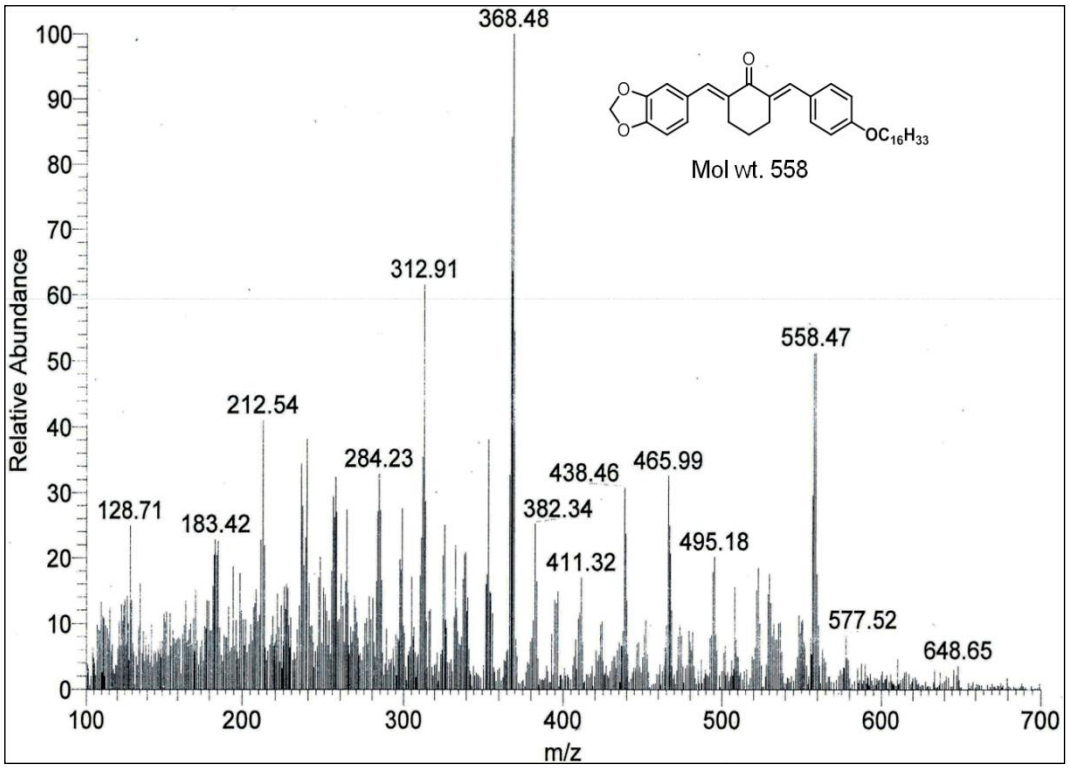

Mass spectra of compound 35h

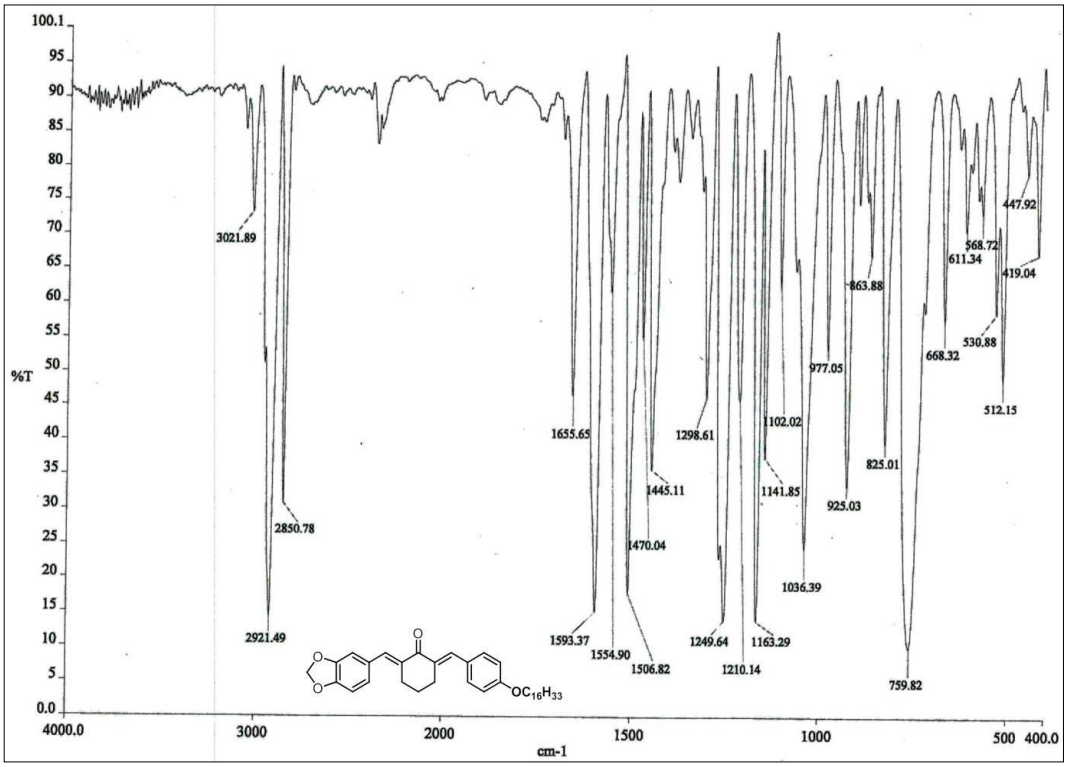

IR spectra of compound 35h

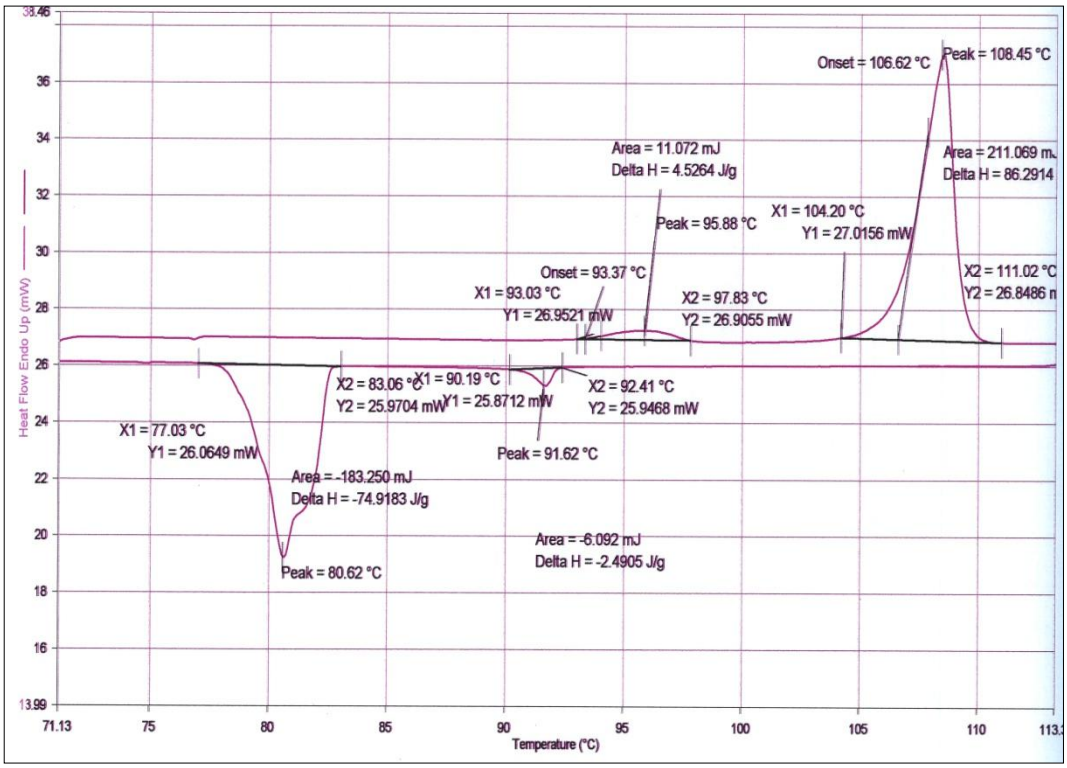

DSC thermogram of compound 35h

3.3 Conclusion

In conclusion to this chapter, we have shown the applications of different conjugated molecules. In first section, we have synthesized OPVs using previously developed one-pot methodology and studied its absorbance and fluorescence properties. Also, pyridine terminated OPVs displayed acidochromic behavior which was systematically studied. In second section, symmetrical bis-chalcone derivatives were synthesized by mechanochemistry and studied their properties as chromic compounds. Internal charge transfer was proposed to be responsible for its acidochromicity in both the cases. In last section, unsymmetrical bis-chalcone derivatives with alkyloxy chain were synthesized and characterized. Amongst the synthesized derivatives, compound with heptyloxy chain and so on showed liquid crystalline-nematic phase which was studied by polarizing microscope. Hence, variety of conjugated molecules were synthesized and studied for its applications.

3.4 References

1. Saiyed, A. S.; Bedekar, A. V. *Tetrahedron Lett.* **2010**, *51*, 6227.
2. Jacobs, S.; Eevers, W.; Verreyt, G.; Geise, H. J.; Degroot, A.; Dommisse, R. In Symposium on Molecular Electronics: Doping and Recognition in Nanostructured Materials of the E-MRS Spring Conference, 19930504−19930507, Strasbourg, France, 1−2 ed.; Elsevier Science: Lausanne, Switzerland; *61*, 189.
3. Park, Y.; Kuo, C-Y.; Martinez, J. S.; Park, Y. S.; Postupna, O.; Zhugayevych, A.; Kim, S.; Park, J.; Tretiak, S.; Wang, H-L *Appl. Mater. Interfaces* **2013**, *5*, 4685
4. Nakaya, T.; Imoto, M. *Bull. Chem. Soc. Jap*. **1966**, *39*, 1547.
5. Caruso, U.; Casalboni, M.; Fort, A.; Fusco, M.; Panunzi, B.; Quatela, A.; Roviello, A.; Sarcinelli, F. *Optical Materials* **2005**, *27*,1800.
6. Chen, C.; Liu, K. Y.; Sudhakar, S.; Lim, T-S.; Fann, W.; Hsu, C-P.; Luh, T-Y. *J. Phys. Chem. B* **2005**, *109*, 17887.
7. Stilz, Walter; DE 1112072, 1959.
8. Yan, Y-X.; Tao, X-T.; Sun, Y-H.; Wang, C-K.; Xu, G-B.; Yu, W-T.; Zhao, H-P.; Yang, J-X.; Yu, X-Q.; Wu, Y-Z. *New Journal of Chemistry* **2005**, *29*, 479.
9. Siegrist, A. *Helvetica Chimica Acta* **1980**, *63*, 1311.
10. Ciorba, S.; Galiazzo, G.; Mazzucato, U.; Spalletti, A. *J. Phys. Chem. A.* **2010**, *114*, 10761.

11. Chang, M-J.; Ai, Y.; Zhang, L.; Gao, F.; Zhang, H. L. *J. Mater. Chem.* **2012**, *22*, 7704.
12. Asiri, A.M.; Khan, S.A. *J. Heterocylic Chem.* **2012**, *49*, 1434.
13. El-Daly, S.A.; Gaber, M.; Al-Shihry, S.S.; El Sayed, Y.S. *J. Photochem. Photobiol A: Chem*. **2008**, *195*, 89.
14. Sharma, A.; Chakravarti, B.; Gupta, M.P.; Siddiqui, J.A.; Konwar, R.; Tripathi, R.P. *Bioorg. Med. Chem*. **2010**, *18*, 4711.
15. Abonia, R.; Insuasty, D.; Castillo, J.; Insuasty, B.; Quiroga, J.; Nogueras, M.; Cobo, J. *Eur. J. Med. Chem.* **2012**, *57*, 29.
16. El-Daly, S.A.; Asiri, A.M.; Khan, S.A.; Alamry, K.A.; Hussein, M.A. *Chin. J. Chem*. **2011**, *29*, 2557.
17. Perozo-Rondon, E.; Martin-Aranda, R.M.; Casal, B.; Duran-Valle, C.J.; Lau, W.N.; Zhang, X.F.; Yeung, K.L. *Catal. Today* **2006**, *114*, 183.
18. Li, J.; Yang, W.; Wang, S.; Li, S.; Li, T. *Ultrasonics Sonochemistry*, **2002**, *9*, 237.
19. Yesuthangam, Y.; Pandian, S.; Venkatesan, K.; Gandhidasan, R.; Murugesan, R. *J. Photochem. Photobiol B: Biol.* **2011**, *102*, 200.
20. (a) Zhang, L.; Wang, S.; Sheng, E.; Zhou, S. *Green Chem*. **2005**, *7*, 683. (b) Khan, S.A.; Asiri, A.M.; Alamry, K.A.; El-daly, S.A.; Zayed, M.A.M. *Russ. J. Bioorg. Chem*. **2013**, *39*, 312.
21. Shan, Y.; Liu, Z.; Cao, D.; Sun, Y.; Wang, Y.; Chen, H. *Sensors and Actuators B* **2014**, *198*, 15.
22. Kamal, A.; Kumar, K.; Kumar, V.; Mahajan, R. *Electrochimica Acta*, **2014**, *145*, 307–313.
23. Motiur Rahman, A.F.M.; Ali, R.; Jahng, Y.; Kadi, A. *Molecules* **2012**, *17*, 571.
24. Wang, G.-W. *Chem. Soc. Rev*. **2013**, *42*, 7668.
25. Yadav, J.; Subba Reddy, B.; Nagaraju, A.; Sharma, J. *Synth. Commun*. **2002**, *32*, 893.
26. Pal, R.; Mandal, T.K.; Mallik, A.K. *J. Ind. Chem. Soc*. **2009**, *86*, 402.
27. Motiur Rahman, A.F.M.; Jeong, B.; Kim, D.H.; Ki Park, J.; Lee, E.S.; Jahng, Y. *Tetrahedron* **2007**, *63*, 2426.
28. Lin, P.; Li, B.; Li, J.; Wang, H.; Bian, X.; Wang, X. *Catal. Lett.* **2011**, *141*, 459.
29. Wen-Bin, Y.; Cai, C. *J. Fluorine Chem.* **2005**, *126*, 1553.
30. Liang, G.; Li, X.; Li, C.; Yang, S.; Wu, X.; Studer, E.; Gurley, E.; Hylemon, P.B.; Ye, F.; Li, Y.; Zhou, H. *Bioorg. Med. Chem. Lett*. **2008**, *18*, 1525.

31. Bhalla, V.; Singh, G.; Kumar, M.; Singh, C.; Rawat, M.; Anand, R.S. *RSC Advances* **2013**, *3*, 14722.
32. (a) Chandrasekar, S. in *Liquid crystals*, 2nd Ed.; Cambridge University Press: New York, 1994. (b) De Gennes, P.G.; Prost, J. in *The physics of liquid crystals*; Oxford Science Publications, Oxford, 1993.
33. (a) Renitzer, F. *Monatsh. Chem*. **1988**, *9*, 421. (b) Kitzerow, H.-S. *Chem. Phys. Chem*. **2006**, *7*, 63. (c) Crooker, P.P. *Mol. Cryst. Liq. Cryst*. **1983**, *98*, 31.
34. Gray, G.W. in *Molecular structure and the properties of liquid crystals*, Academic Press, London and New York, 1962.
35. Kelkar, H. in *Handbook of liquid crystals*, Kelkar, H.; Hatz, R. (Ed.), VCH, Weinheim, 1980.
36. Collings, P.J.; Hird, M. in *Introduction to liquid crystal chemistry and physics*, Taylor and Francis, New York, 1997.
37. Demus, D. Zaschke, H. in *Flüssige kristaale in Tabellen*, Vol II, VEB Deutscher Verlag für Grundstoffindustrie, Leipzig, Germany 1984.
38. Vill, V. in *Liquid Crystal 2.0 Database of liquid crystalline compounds for personal computers*, Fijitsu Kyushu system (KOS) Ltd., Fukuoka, LCI, Hamburg, 1996.
39. (a) Vorländer, D.; *Ber*. **1907**, *40*, 1415. (b) Vorländer, D.; *Ber*. **1907**, *40*, 4527.
40. Vorländer, D.; *Ber*. **1921**, *54*, 2261.
41. Matsunaga, Y.; Miyamoto, S. *Mol. Cryst. Liq. Cryst*. **1993**, *237*, 311.
42. Aly, K.I.; Sayed, M.M. *Liq. Cryst*. **2014**, *41*, 67.
43. Alkskas, I.A.; El-Gnidi, B.A. *J. Macromol. Sci. A: Pure and Appl. Chem*. **2006**, *43*, 1435.
44. Details of crystallographic analysis of **35d** have been deposited with the Cambridge Crystallographic Data Centre (CCDC 1036816). Copies of the data can be obtained from http://www.ccdc.cam.ac.uk/conts/retrieving.html or from the Cambridge Crystallographic Data Centre, 12 Union Road, Cambridge CD21EZ, UK (fax: +44-1223-336-033; e-mail: deposit@ccdc.cam.ac.uk).
45. (a) Hatakeyama T.; Zhenhai, L. J. Hand Book of Thermal Analysis, Wiley and Sons Ltd., Chichester, West Sussex, England, **1998**. (b) Marzotko, D.; Demus, D. Pramana Suppl., **1975**, *1*, 189.
46. Emerson, W.S.; Birum, G.H.; Longley Jr., R.I. *J. Am. Chem. Soc*. **1953**, *75*, 1312.